May 2018

Low-Light Collision Scene Reconstruction Using Unmanned Aerial Systems

Final Report

Prepared by:

Joe Eyerman, Bradley Mooring, and Maureen Catlow
RTI International
3040 E. Cornwallis Road
Research Triangle Park, NC 27709

Sayantan Datta and Srinivas Akella
Department of Computer Science
University of North Carolina at Charlotte
9201 University City Blvd
Charlotte, NC 28223

Prepared for:

North Carolina Department of Transportation (NCDOT)
Transportation Building
1 S. Wilmington St.
Raleigh, NC 27601

ACKNOWLEDGMENTS

Suggested Citation:

Eyerman, J., Mooring, B., Catlow, M., Datta, S., & Akella, S. (2018). *Low-light collision scene reconstruction using unmanned aerial systems*. Research Triangle Park, NC: RTI International; Charlotte, NC: University of North Carolina at Charlotte. https://www.rti.org/publication/low-light-collision-scene-reconstruction-using-unmanned-aerial-systems

CONTENTS

FIGURES

TABLES

EXECUTIVE SUMMARY

The North Carolina Department of Transportation (NCDOT) maintains nearly 80,000 miles of roadway and works closely with multiple state and local agencies to respond to emergencies that impact road systems. When collisions occur, the NCDOT Traffic Management Unit partners with the North Carolina State Highway Patrol (NCSHP) to investigate the incident and clear roads as quickly as possible. Collision scene investigation and reconstruction is a time-sensitive process focused on gathering and recording critical evidence in a safe, fast, and efficient manner.

In 2017, NCDOT and NCSHP conducted research on utilizing an unmanned aerial system (UAS) for collision reconstruction. The study found significant benefits and advantages that UAS technology offers the NCSHP, as well as other government agencies, for daylight collision reconstruction. Using a UAS can cut the time to perform a collision reconstruction from over 90 minutes to less than half an hour and save thousands of dollars. However, the research identified that low light conditions posed a unique hurdle. NCDOT and NCSHP partnered again to study how UAS could be used in low light conditions with lighting supplements. The NCDOT and NCSHP contracted RTI International and The University of North Carolina at Charlotte (UNC Charlotte) for this research effort.

The goal of this project is to evaluate the suitability of using unmanned aerial systems (UAS) to perform low-light collision scene reconstructions. Prior work by the NCDOT and NCSHP has shown that UAS are suitable for replacing 3-D scans by the FARO Focus3D X330 laser scanner for daytime collision scenes. The RTI and UNC Charlotte teams were tasked by NCDOT (sponsor) and NCSHP (client) with understanding whether, and if so, under what conditions UASs are suitable for producing low-light collision reconstructions.

RTI and UNC Charlotte collaborated, with the support of NCDOT and NCSHP, to address low-light collision scene reconstruction (LLCSR). RTI developed a study design and performed a data usefulness assessment, while UNC Charlotte performed analysis of the images and the impact of UAS trajectories, sensors, and lighting on reconstructions. As a result, two reports were written as standalone documents. They are combined here as two parts within a single document for the convenience of the reader; hence there may be some duplication across the two parts.

Key Findings:

- Data collected using UAS can provide evidence-grade images in some low-light conditions when supplemented with appropriate external lighting equipment.

- Data collected using UAS can provide report-grade images that will add value to collision scene reports in most low-light conditions, even if the data are not of sufficient quality to be used as evidence in court.

- Two UAS, the DJI Phantom 4 Pro and the DJI Mavic Pro, were compared for LLCSR. The DJI Phantom 4 Pro was found to be more suitable, because its larger camera sensor is sufficiently sensitive for use in low light situations, and the UAS is more stable in windy conditions.

- The quality of reconstructions in twilight conditions, when there is sufficient ambient light to view the car features and Ground Control Points, is better than for nighttime conditions with artificial lights.

- The external lighting systems had the greatest impact on data quality, suggesting that research into lighting systems may add the most value to the usability of data collected from off-the-shelf UAS for LLCSR.

- Mobile light towers are more effective than inflatable light towers for illuminating the scene, as they have a higher luminous intensity.

- Grid trajectories provide better orthomosaics; whereas, orbit trajectories provide 3-D reconstructions with better lateral feature reconstructions. Using both double grid and orbit trajectories to record image datasets is recommended, because they can be combined to generate both orthomosaics and 3-D reconstructions without compromising much on quality.

- Rigorous assessments of UAS and lighting systems for law enforcement applications can inform policy and practice if conducted using scientific standards; however, appropriate evaluation methods and quantitative measure of quality must be developed and validated by the research community.

Additional Findings:

- Whereas automatic camera settings work well for daytime scenes, manually selecting camera settings is important for twilight and nighttime scenes. Extra initial flights should be carried out to calibrate the camera settings, based on the lighting conditions of the scene. Multiple flights are recommended for low light scenarios if possible, to provide redundancy in the event of image blur.

- Using Ground Control Points (GCPs) reduces the standard deviation of lengths measured in the scene reconstruction to about 0.5 inch. However, the differences between reconstructions with and without GCPs are not visually apparent.

- Reconstruction with the Pix4D Model software is faster than reconstruction with the Agisoft Photoscan software.

- 3-D reconstructions enable viewing the scene from different angles and make terrain features more apparent. Artefacts not visible in the orthomosaics also become apparent in the 3-D reconstructions.

- Orbit trajectories with 8-degree image sampling take half the time of orbit trajectories with 4-degree sampling, and they provide reconstructions that are visually comparable.

PART 1:

LOW-LIGHT COLLISION SCENE RECONSTRUCTION: STUDY DESIGN AND DATA USEFULNESS ASSESSMENT

by Joe Eyerman, Bradley Mooring, and Maureen Catlow
RTI International

1.   INTRODUCTION

There were nearly 35,000 fatal automobile accidents on U.S. roads in 2016 (NHTSA, 2017). In addition to the tragic loss of life, these accidents required lane closures for evidence collection that caused delays and increased traffic congestion. These accidents also caused secondary accidents in the queue, increased the risk to public safety officers, and created economic costs to society.

Recent work by the North Carolina Department of Transportation (NCDOT) and the North Carolina State Highway Patrol (NCSHP) demonstrates that unmanned aircraft systems (UAS) can reduce the time required to clear a collision scene during daylight hours by nearly 77 percent when used to supplement current collision scene investigation techniques (NCDOT Division of Aviation, 2017). If these efficiencies can be replicated during low-light collision events—about half of fatal accidents occur at night (NHTSA, 2017)—integration of UAS into the collision scene reconstruction will reduce the total amount of time that lanes are closed, potentially saving nearly $424 million a year in congestion costs (NHTSA, 2015; Bureau of Labor Statistics, n.d.).

NCDOT and NCSHP collaborated with RTI International, the University of North Carolina at Charlotte (UNC Charlotte), and Remote-Intelligence to replicate and extend their 2017 study to examine the usability of collision data collected with an unmanned aerial system (UAS) at night. RTI was tasked with conducting interviews with NCSHP to define the use case and inform the research questions, designing and managing the field trials, and assessing the value of the UAS data for use by the NCSHP for collision scene reconstruction. All components of the study were completed between December 2017 and April 2018.

RTI extended on the NCDOT (2017) research to determine the potential value of the data collected by UAS, considering additional variables. Most importantly, they examined the effect that low-light environments have on processed data. Other considerations were the UAS type, value of additional lighting options, and data processing techniques.

Overall, the objectives for this study were to assess the following:

- Which lighting sources and conditions are appropriate for data collection from UAS?
- How should the lighting equipment be adjusted for collecting UAS data and imagery in twilight and low-light settings?
- What are the differences in usability of processed UAS data for evidence analysis and collision reports?

- Can a method for quantifying or coding data quality be developed for measuring the quality of the processed data (orthomosaics and 3-D models) for evidence and reports?

This report summarizes the methods and findings from the study. The key findings from the study are as follows:

- Data collected using UAS can provide *evidence-grade* images in some low-light conditions, when supplemented with appropriate external lighting equipment.

- Data collected using UAS can provide *report-grade* images that will add value to collision scene reports in most low-light conditions, even if the data are not of sufficient quality to be used as evidence in court.

- Although there was a noticeable difference in the quality of the data across the two tested aircraft systems (DJI Mavic Pro and DJI Phantom 4 Pro), there was little difference in the usefulness of the images created. That is, both aircrafts and sensor sets produced about the same number of *evidence-grade* and *report-grade* images under the different low-light conditions.

- The external lighting systems had the greatest impact on data quality, suggesting that research into lighting systems may add the most value to the usability of data collected from off-the-shelf UAS for low-light collision scene reconstruction (LLCSR).

- Rigorous assessments of UAS and lighting systems for law enforcement applications can inform policy and practice, if conducted using scientific standards. However, appropriate evaluation methods and quantitative measure of quality must be developed and validated by the research community.

2. METHODS

RTI combined stakeholder interviews and controlled flight trials to evaluate the potential of UAS for gathering *evidence-grade* and *report-grade* data to support collision scene reconstruction in low-light conditions. The data collected from the controlled flight trials were processed into 2-D orthomosaics and 3-D models and then shared with NCSHP. A Data Quality Assessment was held with NCSHP to score the data quality of each processed orthomosaic and 3-D model.

This section describes the methods for the User Needs Assessment, flight trials, and the assessment and coding of the data gathered with UAS.

2.1 User Needs Assessment and Background Data Gathering

RTI gathered user requirements, data needs, data quality specifications, likely use cases for LLCSR, and other technical specifications through a review of background materials and during project planning meetings with staff from NCDOT and NCSHP. The purpose of these meetings was to understand the near-term and long-term research needs of the stakeholders to clarify and prioritize research objectives and to identify any data, expertise, or other resources that can be used to design efficient and expeditious trials (***Table 2-1***).

Table 2-1.   Background Materials Provided by the Study Sponsor

ITEM
▪ NCDOT report on 2017 daytime UAS flight trials at a controlled collision event (NCDOT, 2017)
▪ UAS data collected from 2017 daytime flight trials
▪ Example of NCSHP collision scene reconstruction report
▪ Example data from the current system used for collision scene reconstruction—FARO scanner: portable coordinate measuring machine

Additional information was needed to design the controlled flight trials. The RTI team organized a User Needs Assessment with three members of NCSHP's Collision Scene Reconstruction (CSR) team and a member of NCDOT's geographic information system (GIS) analytics group on December 28, 2018, at the RTI offices in Research Triangle Park, NC. Questions were distributed in advance, and the meeting was facilitated around the following topics:

- Known data specifications, tolerances, and requirements
- Likely use cases
- Current data capture methods (e.g., ground, airborne manned, airborne unmanned)
- Availability and access to existing data
- Availability and access to existing analyses and reports
- Evidence requirements for courts
- Known or suspected barriers to UAS use
- Previous experience with LLCSR, including hardware and software tools

The primary outcome of this meeting was a more detailed understanding for the RTI team about the current CSR data-collection processes using the terrestrial FARO scanner at the collision scene, the data management and processing techniques used by NCSHP for evidence analysis, and the reporting process for court cases.

> **USE CASE**
>
> NCSHP reported that the most frequent LLCSR event is a single car on a two-lane road with trees on at least one side of the road. They also reported that the events with the biggest impact on traffic and related safety issues are multicar accidents on major, multilane highways.

A secondary outcome was the refinement of the use case that would be tested in the controlled flight trials. The officers noted that the most frequently investigated collision scenes are single-car accidents on rural highways. According to the officers, these incidents can be investigated without excessive traffic delays and lane closures and without the associated risk to officer safety. However, they also noted that multicar accidents on busy highways are more difficult, increase the risk to the safety of the investigation team, and create greater delays to motorists. The officers noted that the time savings from using UAS for CSR would have a greater benefit to all concerned, if they were used on multicar accidents on major highways. From this research, we selected multicar accidents on a major highway as our use case.

A third outcome of the User Needs Assessment was a better understanding of variability of the lighting conditions at different collision scenes. The officers reported that although they have access to some lighting equipment, they generally rely on other supporting first-responder organizations to provide scene lighting. The other organizations use lighting systems mounted on the response vehicles and portable systems that can be placed strategically around the scene. The type and placement of the lighting system can have a large impact on the quality of data collected at collision scenes that have debris distributed over a large area that may not be covered by the standard lighting options. However, the lighting systems are generally positioned to support rescue operations and not to optimize image quality.

> **OUTCOME MEASURE**
>
> 1. Do the data collected from UAS meet the officer's minimum threshold for use as evidence in a CSR report?
>
> 2. Do the data collected from UAS meet the officer's minimum threshold for use as context or explanation in the CSR report but *not* for use as evidence?

A fourth important finding from the User Needs Assessment addressed the types of data collected at the scene and the typical use of the portable, coordinate measurement scanning machine known as FARO. As noted in the NCDOT 2017 report, FARO collects high-quality data, but it requires a long time to complete a data-collection session. Officers reported that the quality of the FARO data is exceptional and that FARO provides high-resolution images that are essential for analyzing the vehicles in the collision. The officers also stated that the data far exceeds the threshold required for locating debris, mapping the location of the vehicles for scene reconstruction, and providing context to inform the overall scene report. The officers noted that UAS could be used in coordination with FARO to capture both high-quality and acceptable-quality data in a reduced amount of time. This discussion allowed the RTI team to refine the outcome measure of the study as a threshold of usability for evidence analysis and reporting.

2.2 Controlled Flight Trials

The RTI team prepared a study design with a trial schedule, flight parameters, research questions, and hypotheses to guide the implementation of the field work. The study design was vetted with NCDOT, NCSHP, and UNC Charlotte, and it was revised based on their feedback. The RTI team visited the North Carolina Highway Patrol Driving Track before the trials to select the best location for the use case and to collect preliminary data about the tire marks and debris field.

We designed the flight schedule for a 2-arm study with 10 factors (2 aircraft; 5 lighting conditions) to test the impact of the aircraft and lighting conditions on the usefulness of the data.

- DJI Phantom 4 Pro
- DJI Mavic Pro
- ambient,
- twilight 1 mobile light tower (MLT),

- twilight 2 MLT,
- full dark 1 MLT,
- full dark 2 MLT

This required 10 flights. We included 8 additional orbit flights to support 3-D model construction, and 6 camera setting tests for a total of 24 flights on Day 1 (***Table 2-2***).

Table 2-2.   Day 1 Flight Trials

UAS	Trajectory	15:00	17:30	19:30
DJI Phantom 4 Pro		Camera setting check and light meter check	Camera setting check and light meter check	Camera setting check and light meter check
	Grid	Ambient	1 MLT	1 MLT
	Grid		2 MLTs	2 MLTs
	Orbit	Ambient	2 MLTs	2 MLTs
	Orbit		2 MLTs, manual camera settings: see table 5-1	
	Orbit		2 MLTs, manual camera settings	
DJI Mavic Pro		Camera setting check	Camera setting check	Camera setting check
	Grid	Ambient	1 MLT	1 MLT
	Grid		2 MLTs	2 MLTs
	Orbit	Ambient	2 MLTs	2 MLTs

Lessons learned for Day 2:

- MLTs were moved farther away from the collision scene to avoid "washing out" important scene markers.

- Flights scheduled for 17:30 were flown earlier (17:00) to better leverage twilight lighting conditions.

- Flights scheduled for 19:30 were flown earlier (19:00) due to no change in full-dark lighting conditions.

We tested two different lighting conditions on Day 2 by adding an inflatable light tower (ILT).

- DJI Phantom 4 Pro
- DJI Mavic Pro
- twilight ILT,
- twilight 2 MLT and 1 ILT,
- full dark 1 ILT,
- full dark 2 MLT and 1 ILT

Although this is eight factors (2x4), we only flew seven trials because the DJI Mavic Pro produced unusable data at twilight with one ILT; we did not feel it was necessary to test the full dark 1 ILT condition. We also flew seven orbits for 3-D modeling under the same lighting conditions and flew four flights with the DJI Inspire Thermal for exploratory purposes. We flew a total of 18 flights on Day 2 (***Table 2-3***).

Table 2-3.   Day 2 Flight Trials

UAS	Trajectory	15:00	17:00	19:00
DJI Phantom 4 Pro	Grid		2 MLTs + ILT	2 MLTs + ILT
	Grid		ILT	ILT
	Orbit		2 MLTs + ILT	2 MLTs + ILT
	Orbit		ILT	ILT
DJI Mavic Pro	Grid		2 MLTs + ILT	2 MLTs + ILT
	Grid		ILT	
	Orbit		2 MLTs + ILT	2 MLTs + ILT
	Orbit		ILT	
DJI Inspire Thermal	Grid	Ambient light		Ambient light
	Orbit	Ambient light		Ambient light

2.2.1 Time and Location

The flight trials occurred from 13:00 to 21:00 on January 20, 2018, and from 15:00 to 21:00 on January 21, 2018. Members from NCDOT, NCSHP, and UNC Charlotte were present on both days for the trials. The weather conditions were favorable for the experiment:

- The maximum wind speed was 8 mph.
- The temperature ranged from 46°F to 67°F.
- The skies were mildly cloudy with no rain.

2.2.2 The Scene

The scene was created with two undamaged, police-issued 2013–2015 Dodge Chargers placed in a "T" formation *(Figures 2-1* and *2-2*). NCSHP created the scene for the study. The officers simulated tire marks before staging the scene, and the track was well marked from previous activity. The research team distributed simulated debris around the accident. The officers painted the scene using the same process they would use at a CSR on the highway. The research team painted additional markings, as needed, to provide measurements for analysis. The team also placed five ground-control points around the cars.

Figure 2-1.   Simulated Collision Scene from DJI Phantom 4 Pro, 15:00

Figure 2-2.   Simulated Collision Scene from DJI Phantom 4 Pro, 19:00 2 MLTs

2.2.3 Lighting Conditions

Two MLTs and one ILT were used to illuminate the simulated collision scene during low-light conditions (*Figures 2-3, 2-4, 2-5*, and *2-6*). The ILT light is a lamp with an inflated covering that tempers lighting to a "glow," adjusting for glare and reducing any washing out of important scene elements, including markers, tire tracks, and debris.

Lighting conditions for this experiment included the following:

- **Ambient lighting.** No additional light sources were used for Day 1 flights at 15:00 for the DJI Mavic Pro and DJI Phantom 4 Pro. Thermal flights with the DJI Inspire did not require additional lighting.

- **1 MLT.** Day 1 flights at 17:00 and 19:00 used a single MLT: Allmand Night-Lite Pro II Towable Diesel Light Plant , Metal Halide SHO HD, 1,250-watt lamp, 135,500 lumens.[1]

- **2 MLTs.** Day 1 and Day 2 flights used two MLTs for the flights at 17:00 and 19:00 for the DJI Mavic Pro and DJI Phantom 4 Pro.

- **1 ILT.** Day 2 trials included an ILT: Prism PIL Nitelite, Metal Halide 250-watt lamp, 22,000 lumens.[2]

- **2 MLTs and ILT.** Day 2 trials included two MLTs and an ILT.

---

[1] The MLT used can be seen here:
https://www.allmand.com/na/en_us/product-catalog/light-towers/nightlite-pro-ii-ldseries.html#Specifications.

[2] The ILT used can be seen here: https://prismlighting.net/2016/03/03/pil-nitelite/.

Figure 2-3.   MLT Used for Test Flights

Figure 2-4.   ILT Used for Day 2 Test Flights

Figure 2-5.   **Sample Image of ILT Used for Day 2 Test Flights, retrieved from prismlighting.net**

Figure 2-6.   **Sample Image of MLT Used for Day 1 and 2 Test Flights, retrieved from allmand.com**

2.2.4 UAS and Flights

The DJI Mavic Pro (**Figure 2-7**) and DJI Phantom 4 Pro (P4P) (**Figure 2-8**) were the primary UAS used for the flight trials, with the DJI Inspire (**Figure 2-9**) used only to collect thermal scans on the second day. No special modifications were made to the aircraft, and we used the DJI integrated flight-planning software.

Figure 2-7. **DJI Mavic Pro, image from dji.com (©DJI)**

Figure 2-8. **DJI Phantom 4 Pro, image from dji.com (©DJI)**

Figure 2-9. **DJI Inspire, image from dji.com (©DJI)**

A grid and orbit flight pattern were flown for most time and lighting combinations (***Tables 2-2*** and ***2-3***). The grid flight pattern collected about 44 images for every run and completed a grid pattern over the mock scene. The orbit flight pattern collected 90 images while circling over the mock scene. The orbit pattern did not fly over any elements of the scene. Instead, it recorded from the outside of the scene perimeter.

2.2.5 Camera Settings

Camera settings for each UAS were set to automatic, unless otherwise noted. The flight team conducted a pre-check on Day 1 to determine the optimal settings. Manual settings were used, because the pre-check showed that automatic settings produced poor image quality in low light conditions.

Tables 2-4 and ***2-5*** include the flight patterns, settings, and parameters used for Day 1 and Day 2.

Table 2-4.   Day 1 Flight Information

Flight parameters for Day 1 were as follows:	
▪ DJI Phantom 4 Pro, DJI Mavic Pro	▪ Camera settings:
▪ 100-foot flight elevation for all flights	– Set to automatic for trials at 15:00
▪ Grid flight pattern: about 44 images recorded per flight	– Set to manual settings for trials at 17:30 and 19:30
▪ Orbit flight pattern: 90 images recorded per flight	▪ 80% overlap with an 80-degree camera angle for all flights
▪ Safe mode for all flights	

Table 2-5.   Day 2 Flight Information

Flight parameters for Day 2 were as follows:	
▪ DJI Phantom 4 Pro, DJI Mavic Pro, DJI Inspire with thermal sensor	▪ Camera settings:
▪ 100-foot flight elevation for all flights	– Set to automatic for trials at 15:00
▪ Grid flight pattern: about 44 images recorded per flight	– Set to manual settings for trials at 17:00 and 19:00
▪ Orbit flight pattern: 90 images recorded per flight	▪ 80% overlap with an 80-degree camera angle for all flights
▪ Safe mode for all flights	

2.2.6 Data Processing

The UNC Charlotte team processed all UAS imagery data into orthomosaics and 3-D models using Pix4D. The team also measured tire track markers for each orthomosaic and created sample procedures for

pulling final outputs up in Pix4D for future analysis by NCSHP and NCDOT. A detailed description of the data processing can be found in Part 2, UNC Charlotte's report: Low-Light Collision Scene Reconstruction: Impact of UAS Trajectories, Sensors, and Lighting.

2.3 Data Quality Assessment

RTI developed an image quality assessment tool based on the requirements *for evidence-grade* and *report-grade* data, as defined during the User Needs Assessments. The tool was administered during the Data Quality Assessment meeting held at RTI offices in Research Triangle Park, NC, on March 30, 2018 (*Figure 2-10*). Five NCSHP CSR officers participated in the assessment.

Figure 2-10.   Data Quality Assessment Meeting with NCSHP and UNC Charlotte at RTI Headquarters

Each officer was provided all the processed orthomosaics and 3-D models in advance, along with the quality assessment tool. Officers were asked to review the images before the meeting and to be prepared to identify which images could be used for evidence, for reporting, or not at all. The images were viewed during the Data Quality Assessment meeting on the NCSHP issued laptops used for CSR, and on large high-resolution monitors, using the Windows Preview tool. The RTI team facilitated the discussion and asked the officers to consider the quality of the images and to note any problems that reduced the value of the image for evidence or reports. The officers reached a consensus on each image. RTI captured notes on the discussion and scored the images as follows:

- Usable for evidence analysis (UEA): Usable for evidence analysis in court
- Usable, not for evidence analysis (UNEA): Usable for a collision report but not for evidence analysis
- Not usable (NU): Not usable for evidence analysis or collision reporting

The review lasted for 3.5 hours and covered 35 orthomosaics and seven 3-D models. We assessed the quality of orthomosaics and 3-D models constructed using data only from the grid flights, only from the orbit flights, and from both the grid and orbit flights (grid+orbit). UNC Charlotte was available through video conferencing to answer questions. The coded results can be seen in *Tables 2-6, 2-7*, and *2-8*.

Table 2-6. **Coded Results for Day 1 Flight Orthomosaics**

UEA = ☐ (white)
UNEA = ▨ (gray)
NU = ▦ (hatched)

	Day 1 Mavic Pro	Day 1 P4P	Day 1 P4P grid+orbit
	15:00 grid ambient UEA	15:00 grid ambient UEA	15:00 grid+orbit ambient UEA
	15:00 orbit ambient UEA	15:00 orbit ambient UEA	(NU)
	17:30 grid 1 MLT UNEA	17:30 grid 1 MLT UEA	(NU)
	17:30 grid 2 MLTs UNEA	17:30 grid 2 MLTs UNEA	17:30 grid+orbit 2 MLTs UNEA
	17:30 orbit 2 MLTs UNEA	17:30 orbit 2 MLTs UNEA	(NU)
	19:30 grid 1 MLT UNEA	19:30 grid 1 MLT UNEA	(NU)
	19:30 grid 2 MLTs UNEA	19:30 grid 2 MLTs UNEA	19:30 grid+orbit 2 MLTs UNEA
	19:30 orbit 2 MLTs UNEA	19:30 orbit 2 MLTs UNEA	(NU)

Table 2-7. **Coded Results for Day 2 Flight Orthomosaics**

UEA = ☐ (white)
UNEA = ▨ (gray)
NU = ▦ (hatched)

	Day 2 Mavic Pro	Day 2 P4P	Day 2 P4P grid+orbit
	(NU)	17:00 grid ILT UEA	17:00 grid+orbit ILT UEA
	(NU)	17:00 orbit ILT UEA	(NU)
	17:00 grid 2 MLTs & ILT UEA	17:00 grid 2 MLTs & ILT UEA	17:00 grid+orbit 2 MLTs & ILT UEA
	17:00 orbit 2 MLTs & ILT UEA	17:00 orbit 2 MLTs & ILT UEA	(NU)
	(NU)	19:00 grid ILT UNEA	19:00 grid+orbit ILT UNEA
	(NU)	19:00 orbit ILT UNEA	(NU)
	19:00 grid 2 MLTs & ILT UEA	19:00 grid 2 MLTs & ILT UEA	19:00 grid+orbit 2 MLTs & ILT UEA
	19:00 orbit 2 MLTs & ILT UEA	19:00 orbit 2 MLTs & ILT UEA	(NU)

Table 2-8. **Coded Results for Day 1 & Day 2 3-D Models**

	Day 1 Mavic Pro	Day 1 P4P	Day 2 P4P
UEA = ☐ UNEA = ▨ NU = ▨	15:00 grid ambient lighting NU	15:00 grid+orbit ambient lighting UNEA	19:00 grid+orbit 2 MLTs & ILT UNEA
	19:30 grid 1 MLT NU	19:30 grid+orbit 2 MLTs UNEA	19:00 grid+orbit ILT NU
		19:30 grid 1 MLT NU	

Some key findings from the Data Quality Assessment are as follows:

- Most of the images were useful to illustrate the crash environment and identify debris and tire marks in a large viewing field. This is valuable information for describing the accident within context.

- The scene lighting set up by other first responders (fire department generally) has a large impact on the data quality and should be considered as part of any UAS-enabled CSR policy or training program.

- None of the 3-D models were scored as *evidence-grade*. However, most of them were considered *report-grade* or at least sufficient for descriptive purposes for court proceedings and visual "walk-throughs" for juries.

- Scene artefacts and distortions from shadows and low-light conditions caused reticence among the officers to use the models as supplementary visuals in a report. The inclusion of these models could cause confusion among juries and create doubts on the integrity of the evidence analysis data results.

- NCSHP members were impressed with the level of detail that could be pulled from their models, but the distortion due to low light conditions made it difficult to validate accuracy, especially in comparison with FARO scans.

- ILT provides tempered lighting to address areas of extreme shadow contrasting; however, two MLTs and ILT were preferred for image analysis.

- MLTs were too close to the scene for Day 1, washing out important scene markers. This was adjusted for Day 2.

- Orthomosaics created from the grid flight pattern were preferred over the orbit pattern. Grid+orbit orthomosaics were preferred over stand-alone grid or orbit orthomosaics for full-scene aerial photos.

3. CONCLUSIONS

The LLCSR study provided some useful insight into the challenges and benefits of using UASs to support CSR. The study also highlighted the need for better design and analytic tools for conducting rigorous evaluations of UAS-enabled field practices for law enforcement and all first responders. Some of the key findings appear below:

- Lighting conditions are crucial to the quality of processed data.

  – The daytime flights are generally accurate and have little distortion, so continued research should focus on low-light environments and the lighting options that could help to build a scene.

  – Well-lit areas tend to produce better images, but excessively bright lights or a light placement too close to the scene can cause important scene markers, debris, or tire tracks to be washed out.

  – Day 2 lighting was adjusted to account for washed-out evidence, and the resulting orthomosaics demonstrate that the distance between light sources and the collision scene evidence affected whether or not the image would be coded as usable for forensic analysis.

  – The Day 2 lighting condition changed to include ILTs, which seemed to help create a softer glow by not washing out important markers and by creating softer contrasts for shaded elements.

- FARO reconstructions are far more accurate than UAS reconstructions and will not be replaced for forensic analysis for off-site reconstructions without significant innovation to UAS data collection systems.

  – The UAS data meets the threshold for collecting and producing valuable data for on-site collision data collection and can create valuable visuals for both a report and for measurements. However, the FARO reconstructions and the FARO software (*Reality*) have a higher level of detail and software modules that are ideal for forensic analysis at an off-site location.

- Additional research is needed to improve image quality and to test different lighting solutions. Some considerations for future studies include:

  – Limiting the research to the nighttime flights. Nighttime flights offer the most value to the research objective. All the daytime flights and most of the twilight flights produce *evidence-grade* results. The nighttime flights are the most problematic and will benefit the most from continued study. This will also allow more time to vary lighting systems.

  – Testing more lighting conditions to understand how to select and place different light sources on the scene to account for shadows, distortions to the scene, and washed-out scene markers.

  – Marking and painting the scene before the flight trials with the appropriate and preferred measurements. This allows for adjustments after an initial setting check to move lighting to a different distance, if needed, without having to measure the scene again. This also provides more opportunities for forensic analysis techniques.

– Limiting the number of UAS platforms to streamline the testing and reduce variable changes.

– Adding images collected at ground level to data collected via UAS to determine whether the additional ground level images can adjust for shadow contrasts and increase accuracy.

– Flying simultaneous trials over multiple simulated accidents in the same test field. This could be used to increase the number of trials without increasing the number of days in the field.

– Inviting collaborative first-responders, like firefighters and city police officers, to the scene construction and flight trials for input on lighting layout.

– Developing a quantitative method for coding data that reflects the qualitative components of the Data Quality Assessment from this study. This would be a valuable tool for measuring and identifying patterns in large datasets.

– Standardizing the Data Quality Assessment process so the coding can be completed remotely at the convenience of the CSR teams (in addition to the Data Quality Assessment meetings, which produced valuable discussion).

4. REFERENCES FOR LLCSR: STUDY DESIGN AND DATA USEFULNESS ASSESSMENT

Blincoe, L. J., Miller, T. R., Zaloshnja, E., & Lawrence, B. A. (2015, May). *The economic and societal impact of motor vehicle crashes, 2010 (Revised).* (Report No. DOT HS 812 013). Washington, DC: National Highway Traffic Safety Administration. https://crashstats.nhtsa.dot.gov/Api/Public/ViewPublication/812013

Bureau of Labor Statistics. (2013). *CPI inflation calculator*. Retrieved from https://www.bls.gov/data/inflation_calculator.htm

National Highway Traffic Safety Administration (NHTSA). (2017, October 6). *USDOT releases 2016 fatal traffic crash data*. Retrieved from https://www.nhtsa.gov/press-releases/usdot-releases-2016-fatal-traffic-crash-data

North Carolina Department of Transportation Division of Aviation, UAS Program Office. (2017, August). *Collision scene reconstruction & investigation: Using unmanned aircraft systems*. Retrieved from https://www.ncdot.gov/aviation/download/ncshp-uas-mapping-study.pdf

PART 2:

LOW-LIGHT COLLISION SCENE RECONSTRUCTION: IMPACT OF UAS TRAJECTORIES, SENSORS, AND LIGHTING

by Sayantan Datta and Srinivas Akella
University of North Carolina at Charlotte

1.   INTRODUCTION

The goal of this project is to evaluate the suitability of using unmanned aerial systems (UAS) to perform low-light collision scene reconstructions (LLCSRs). There are around 34,000 fatal crashes annually in the United States. These lead to lengthy lane closures and traffic slowdowns. Prior work by the North Carolina Department of Transportation (NCDOT) and North Carolina State Highway Patrol (NCSHP) (North Carolina Department of Transportation, 2017) has shown that UAS are suitable for replacing 3-D scans by the FARO Focus3-D X330 laser scanner (FARO, n.d.) for daytime collision scenes, and can reduce the duration of lane closure by recording critical evidence quickly. The UNC Charlotte and RTI International teams were tasked by NCDOT (sponsor) and NCSHP (client) with understanding whether, and if so, under what conditions UASs are suitable for producing LLCSRs. This report contains results of reconstructions from the datasets collected at the NCDOT test track at Garner, NC, on January 20 and 21, 2018. We have used two commercially available Structure from Motion (SfM) software packages, Pix4D Mapper^{TM} (ver. 4.1.22; Pix4D, n.d.) and Agisoft Photoscan (ver. 1.3.4 build 5067; Agisoft, 2018), for the reconstructions.

SfM methods developed in the computer vision community (Tomasi & Kanade, 1992; Poelman & Kanade, 1997; Agarwal et al., 2011; Frahm et al., 2010) recover the 3-D structure of a stationary scene from a collection of 2-D images, via estimation of motion of the cameras corresponding to these images. SfM approaches take a large number of RGB images of a scene, identify matching features, and use these to estimate camera positions and thus obtain 3-D point clouds of the scene. Polygonal models are then fit to these point clouds to obtain a 3-D representation of the scene. Texture mapping of relevant images onto the polygonal models yields 3-D models that can be viewed from arbitrary camera viewpoints. SfM has also been paired with geolocation information through Ground Control Points (GCPs) (Westoby, Brasington, Glasser, Hambrey, & Reynolds, 2010; Turner, Lucieer, & Watson, 2010) to not only increase the accuracy of the reconstructions, but also make them geographically accurate.

Pix4D Mapper is available as a standalone SfM software for Windows. It generates reconstructions considerably faster than Agisoft Photoscan. The software even allows for reconstruction of thermal images. The Pix4D Mapper trial version does not allow the generation of orthomosaics or Digital Elevation Models. The commercial version however also allows reconstructions over the cloud.

Agisoft Photoscan is available as a similar standalone software for Mac OS X, Windows, and Linux. It does not feature reconstructions in the cloud and requires considerably more time than Pix4D to perform reconstructions. Agisoft offers an image quality metric that quantifies the usability of an image in a reconstruction.

1.1   Datasets

The flight test plan was developed by RTI in consultation with NCSHP. Flights were planned at three times—15:00, 17:30, and 19:30—to record data corresponding to daytime, twilight, and nighttime conditions. The twilight datasets exhibit a wide range of ambient lighting conditions due to the rapid change in light levels in a relatively short period of time. The datasets used in the reconstructions were captured using the DJI Phantom 4 Pro and Mavic Pro drones. Both these drones were flown at an altitude of 100 feet above the ground plane either in a 2-D grid trajectory (also referred to as a NADIR trajectory) or an orbital (or oblique) trajectory. The height of 100 feet was selected in consultation with NCSHP because it ensures the UAS are above trees, power lines, streetlights, and other objects in typical usage scenarios.

In our report, the orthomosaics and 3-D reconstructions have been generated using Pix4D; a few orthomosaics have been generated using Agisoft Photoscan.

Note: The names Pix4D Mapper and Pix4D have been used interchangeably and refer to the desktop application for Pix4D Mapper. Similarly, Agisoft Photoscan and Agisoft have been used to refer to the desktop application for Agisoft Photoscan. We also use the terms UAS and drone interchangeably.

2.   CAMERA SETTINGS

Correct camera settings calibrated to the amount of light present in the scene lead to clear and sharp images being captured. As the reconstruction is made from image data, it is important that the images recorded are in focus, and that they are not underexposed or overexposed.

In the presence of uniform ambient light (e.g., sunlight), the automatic camera settings are sufficient, as the camera metering provides uniform exposure over all images. However, in the presence of artificial lights and no sunlight, the drone camera selects different camera parameters for each location and orientation of the drone. This results in images with widely varying exposures. In practice, this generates images with varying levels of exposure for an object in the scene. This adversely affects the quality of reconstruction.

2.1   Manual and Automatic Camera Settings

The camera settings for the drones can be set to either automatic or manual. Depending on the ambient light, we have to choose whether to go for automatic or manual settings.

- **Automatic camera settings:** The automatic camera settings can be used whenever there is daylight. Based on our experiments, using automatic camera settings works even at twilight with a light meter reading of 400 lux.

- **Manual camera settings:** The manual camera settings are ideal when the artificial light sources (e.g., mobile light tower [MLT], inflatable light tower [ILT]) overpower the ambient light. This usually happens when the effect of sunlight is no longer visible. The manual camera settings ensure that all the images captured in a dataset have minimal exposure variance.

2.2   Procedure to Change Camera Settings

Setting the manual camera settings for a scene involves flying the drone to a height of 100 feet above ground, over the area of interest (e.g., the crash scene). While in flight, the drone operator has to select the best settings for the current scene.

Changing the camera settings to manual involves:

1. Starting off the Pix4D Capture mobile application on an iOS device,
2. Sending the Pix4D Capture application to the background,
3. Opening the DJI GO application,
4. Changing the camera settings to manual and adjusting the settings, and
5. Going back to the Pix4D capture application and starting the data gathering.

2.3   Recommended Camera Settings

Based on our experiments, the set of recommended camera settings for the DJI Phantom 4 Pro for the given lighting scenarios are presented in ***Table 2-1***.

Table 2-1.   Camera Settings for Different Lighting Conditions

Lighting Scenario	Illuminance Lux (Max, Min)	Camera ISO	Aperture, Shutter Speed
Two mobile light towers (MLTs)	138, 61[a]	400	F2.8, 1/20
One MLT	61, 0	800	F2.8, 1/20
Inflatable Light Tower (ILT)	41, 0	1600	F2.8, 1/6
Two MLTs + ILT	69, 32	400	F2.8, 1/25

[a]   Note that the two MLTs scenario has a higher illuminance than the two MLTs + ILT scenario, because both MLTs were moved farther away from the cars in the latter scenario.

We used two types of portable lighting sources, a MLT and an ILT. Both these lighting solutions are powered by a generator and are therefore portable. The MLT has four spotlights mounted on a metal mast. The MLT used was the Allmand Night-Lite Pro II Towable Diesel Light Plant Portable Light Tower (Allmand Brothers, n.d.), Metal Halide SHO HD, 1,250-watt lamp, 135,500 lumens. The MLT serves as a directed light source, which provides higher illuminance on the region of the scene where it is directed. The higher illuminance can cause specular reflections on the road surface, where the light gets reflected off the road to the drone camera. Such reflections are disadvantageous, as they wash out scene elements such as tire marks and paint markings up to 20 ft in the direction in which the MLT is incident. The ILT has a lamp covered by an inflatable covering, which not only acts as a diffuser but also allows the light to spread 360 degrees around the point of the light source. The ILT used was the Prism PIL Nitelite (Prism Lighting Services, n.d.), Metal Halide 250-watt lamp, 22,000 lumens.

The Phantom 4 Pro's camera can increase the ISO up to 6400. A higher ISO means a more sensitive camera photo sensor. A high sensitivity would allow for images being captured using a faster shutter speed but would also result in greater image noise. Furthermore, our settings were recorded when flying the drone in "safe mode" in the Pix4D Capture iOS™ application, during which the drone stops at a position, clicks the image, and then moves on to the next location. The safe mode is available in the iOS™ application, but not available in the Android™ application.

3.   EFFECT OF UAS TRAJECTORY

The drone trajectory affects the number of images recorded in the dataset. It also affects the percentage of images that cover the object of interest, and the surrounding area. The following subsections show the effects of different drone trajectories on the final reconstruction.

3.1   Grid Trajectory

A grid trajectory is created by the drone making a 2-D grid pattern over the scene. The grid pattern can be a single grid or a double grid trajectory. The single "to and fro" grid is along one direction, for example east to west. The double grid, as the name suggests, consists of two grid trajectories along two perpendicular directions, for example east to west and north to south. The single grid is a minimum requirement for constructing the orthomosaic, while the double grid can be used for reconstructing the 3-D model of the scene. One of the biggest advantages of the grid is the relatively short time to record the dataset and to compute a 3-D reconstruction or an orthomosaic. On average, the double grid trajectory takes around 6 minutes[3] to record, and a 3-D reconstruction can be performed in under 10 minutes[4]. In this report, the only grid trajectory we have used is the double grid; hence by "grid trajectory" we mean a double grid trajectory unless otherwise stated. See *Figure 3-1* for an example grid trajectory.

Figure 3-1.   **Double Grid Trajectory: The path is marked in green, the red circles denote the geolocation of the images captured and the blue "+"signs denote the position of the Ground Control Points.**
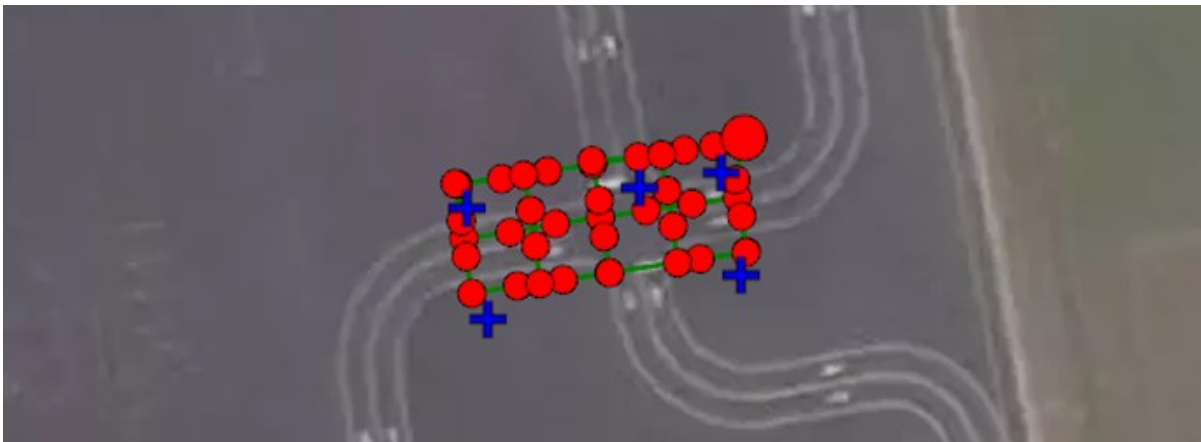
The grid trajectory is best suited for just generating the orthomosaic of the scene without much detail in the 3-D reconstruction.

---

[3] On a DJI Phantom 4 Pro under normal wind conditions.

[4] Using Pix4D Mapper using 3D Model settings.

3.2   Orbital Trajectory

An orbital trajectory is characterized by the drone taking a circular or elliptical path around the scene (*Figure 3-2*). This ensures that all the images taken include the objects within the scene. An orbital trajectory in Pix4D Capture can be deployed to capture images with a sampling frequency of 4 degrees. This provides around 90 images for a scene. On average, the trajectory takes around 10 minutes to record[5] and 70 minutes[6] to reconstruct. Even though the time consumed is much higher than that of the double grid trajectory, the 3-D reconstruction generated is visually of a much better quality and has significantly fewer artefacts.

Figure 3-2.   **Orbital Trajectory: The red circles denote the geolocation of the images captured and the blue '+'signs denote the position of the Ground Control Points.**
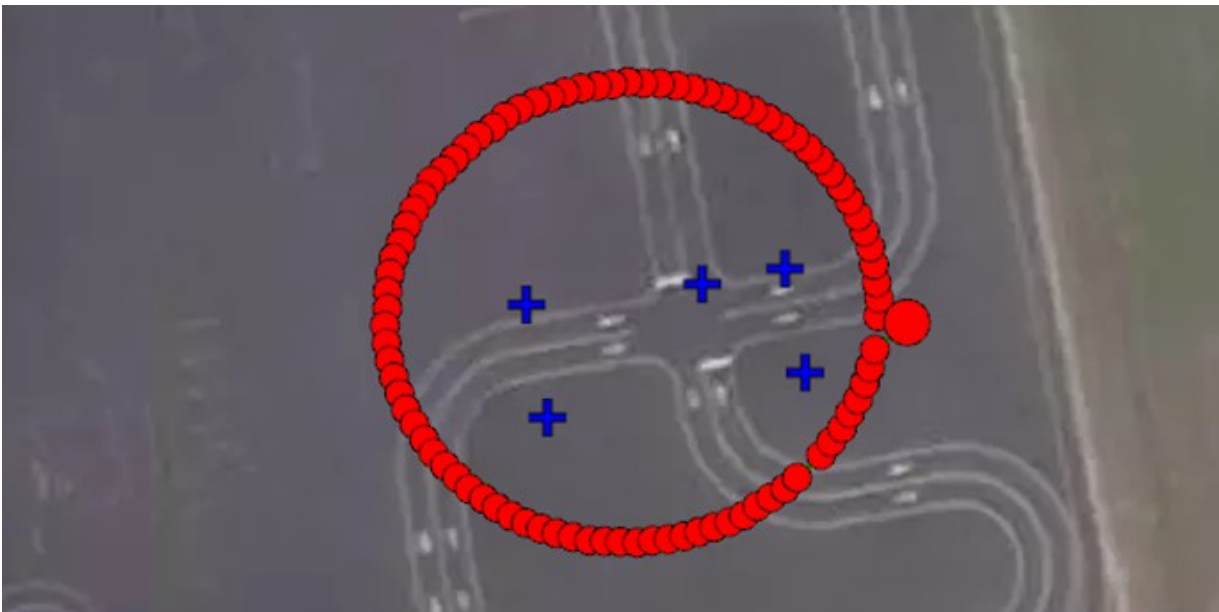
When using an orbital trajectory, the camera angle is oblique toward the center of the orbit, rather than pointing straight down toward the ground. This is the reason orbit trajectory images are also referred to as oblique imagery. The camera is at an angle with respect to the ground plane, and this causes the light from the MLT to reflect off the road to the camera. If the road is wet after precipitation, this reflection can be quite prominent and can cause overexposed patches on the road. It is recommended that when using the orbit trajectory, the MLTs should be placed at least 40 feet away from the skid marks.

---

[5] On a DJI Phantom 4 Pro under normal wind conditions.

[6] Using Pix4D Mapper using 3D Model settings.

3.3   Grid + Orbital Trajectory

When we have the data from the grid trajectory and the orbital trajectory, we can create a virtual grid-plus-orbital trajectory that uses both the grid and orbital trajectories (***Figure 3-3***). For brevity, we will refer to such trajectories as "grid+orbit" trajectories. This helps us ensure that the overhead and oblique images are both present in the dataset, and the reconstruction provides a better result than an individual reconstruction. The 3-D reconstruction time is around 1 hour 20 minutes.

Figure 3-3.   **A virtual Grid + Orbit Trajectory: The path is marked in green, the red circles denote the geolocation of the images captured and the blue '+' signs denote the positions of the Ground Control Points.**
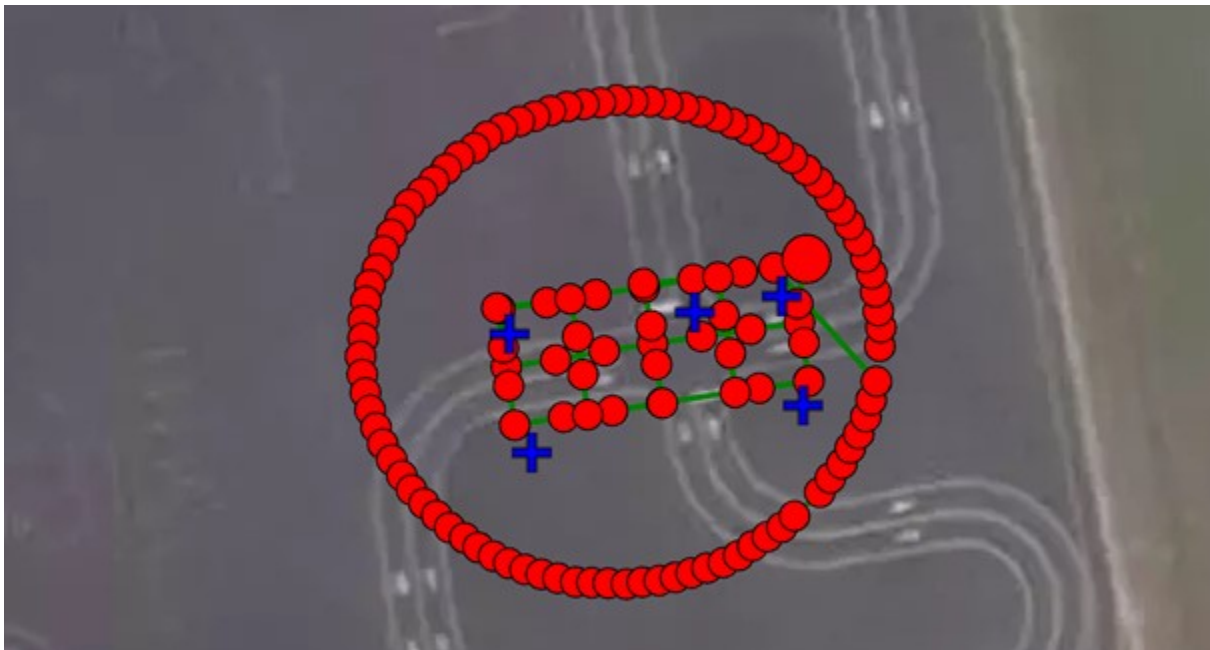
3.4   Comparisons

For a visual comparison of the quality of reconstructions, we now provide three views: an overhead view, a close-up, and a lateral view. The comparisons are between grid, orbital and grid + orbital trajectories.

In ***Figures 3-4, 3-5***, and ***3-6***, we see the overhead view of the daytime reconstructions from the grid, orbit, and grid+orbit trajectories respectively. As the grid trajectory has overhead images, we notice that the geometry on the roof of the car in ***Figure 3-4*** appears well formed and has less distortions when compared to ***Figure 3-5***. In the Grid + Orbit trajectory as in ***Figure 3-6***, due to both overhead and oblique images, the texture on the car surface has fewer artefacts when compared to the orbit trajectory but is not as accurate as that from the grid trajectory.

Figure 3-4. **Overhead View: Grid Trajectory Daytime Reconstruction from DJI Phantom 4 Pro**

Figure 3-5. **Overhead View: Orbit Trajectory Daytime Reconstruction from DJI Phantom 4 Pro**

Figure 3-6.   **Overhead View: Grid + Orbit Trajectory Daytime Reconstruction from DJI Phantom 4 Pro**

Figures 3-7 through *3-12* illustrate through close-up and lateral views the differences in the 3-D reconstructions obtained using the grid, orbit, and grid+orbit trajectories.

Figure 3-7.   **Close-Up View: Grid Trajectory Daytime Reconstruction from DJI Phantom 4 Pro. Note the black scene artefacts on the far side of the gray car caused by the shadows.**

Figure 3-8.   **Close-Up View: Orbit Trajectory Daytime Reconstruction from DJI Phantom 4 Pro**

Figure 3-9.   **Close-Up View: Grid + Orbit Trajectory Daytime Reconstruction from DJI Phantom 4 Pro**

Figure 3-10.   Lateral View: Grid Trajectory Daytime Reconstruction from DJI Phantom 4 Pro
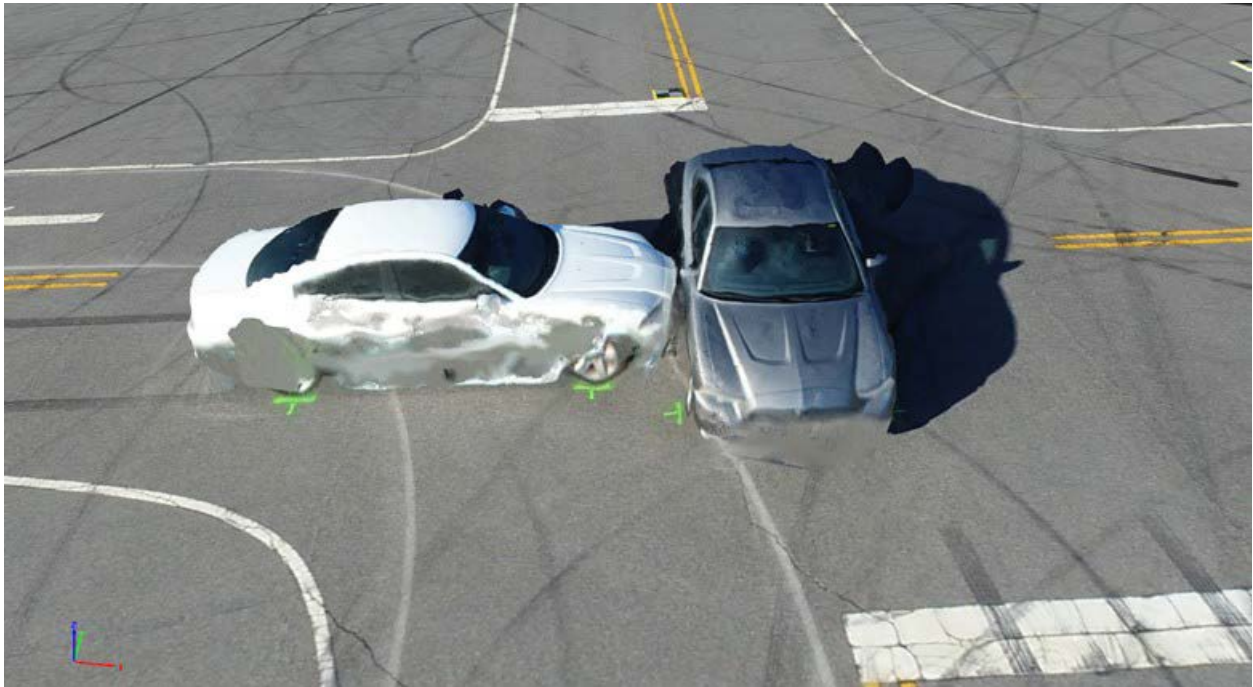
Figure 3-11.   Lateral View: Orbit Trajectory Daytime Reconstruction from DJI Phantom 4 Pro
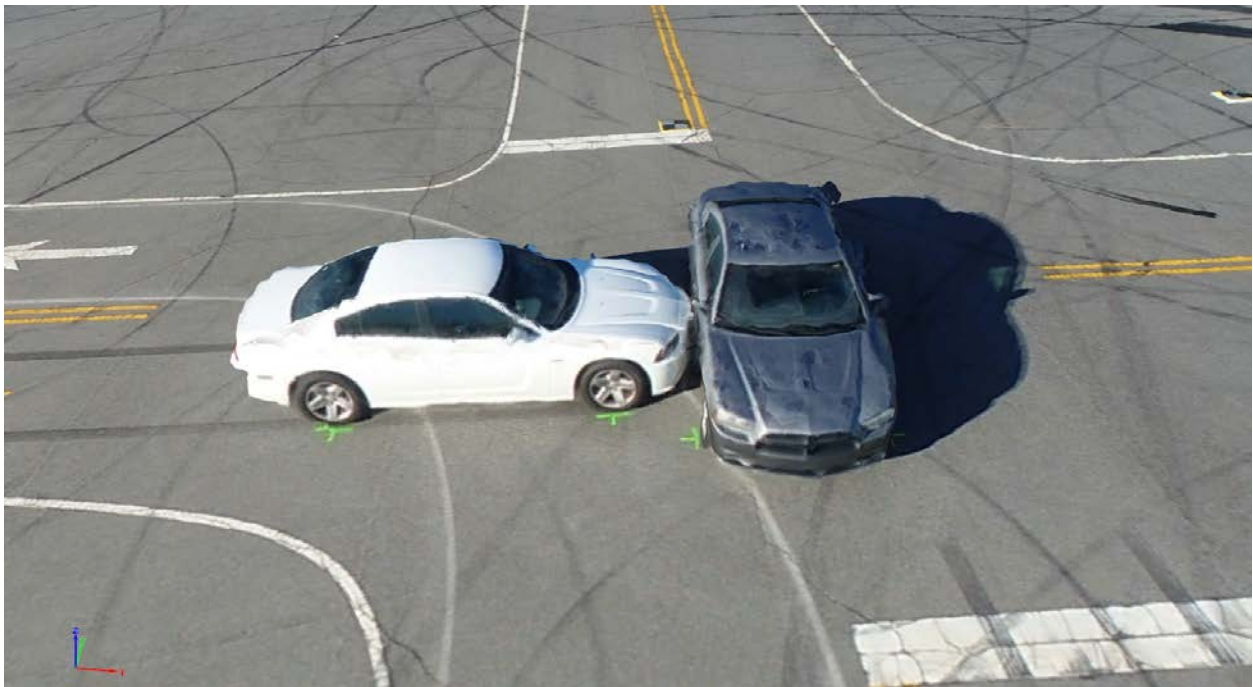
Figure 3-12.   Lateral View: Grid + Orbit Trajectory Daytime Reconstruction from DJI Phantom 4 Pro

We can observe the shortcomings of a grid trajectory in *Figure 3-10*, where the side of the car has several artefacts and the texture of the doors is severely distorted. The front of the gray car in *Figure 3-10* illustrates the "waterfall effect" where the lower part of the car appears to merge with the road surface in the 3-D reconstruction; this is due to a lack of images capturing the lower portions of the cars. From the above images, we can conclude that top surfaces are best reconstructed with a grid trajectory, side surfaces are best reconstructed with an orbit trajectory, and there is a good compromise with a grid + orbit trajectory.

The next set of figures illustrate the effect of the trajectory on the quality of reconstruction in nighttime reconstruction. *Figures 3-13* through *3-21* are images taken after 15:30, ensuring that the only two sources of light were the two MLTs in the scene. The dataset used in this test was the Day 1 evening dataset from the DJI Phantom 4 Pro, recorded at 19:30 hours.

Figure 3-13.   Overhead View: Grid Trajectory Nighttime Reconstruction from DJI Phantom 4 Pro
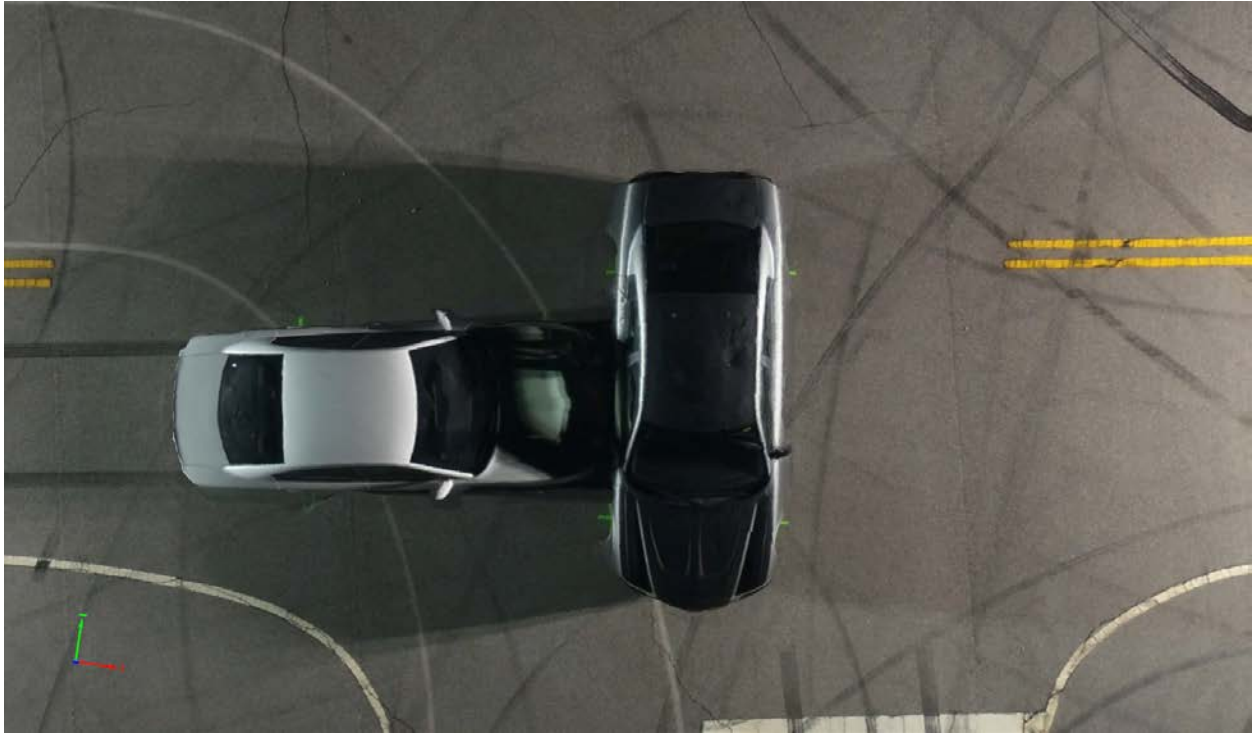
Figure 3-14.   Overhead View: Orbit Trajectory Nighttime Reconstruction from DJI Phantom 4 Pro
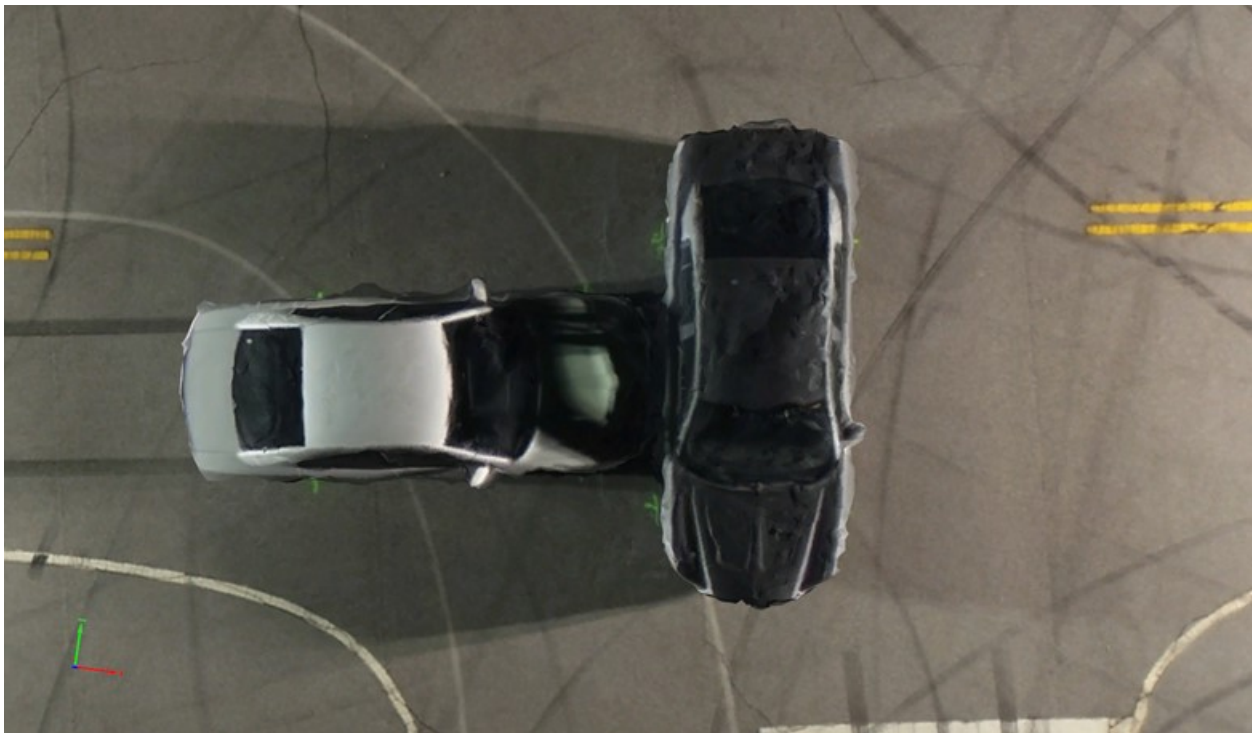
Figure 3-15. **Overhead View: Grid + Orbit Trajectory Nighttime Reconstruction from DJI Phantom 4 Pro**

Figure 3-16. **Close-Up View: Grid Trajectory Nighttime Reconstruction from DJI Phantom 4 Pro**
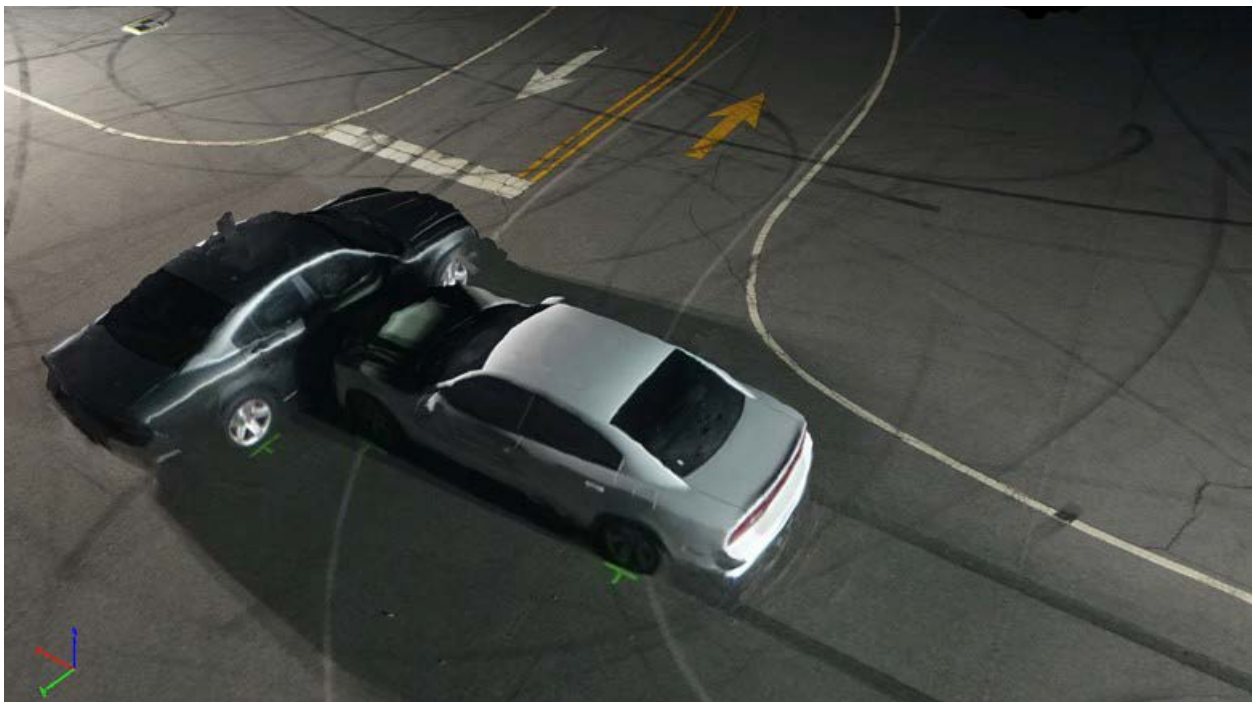
Figure 3-17. **Close-Up View: Orbit Trajectory Nighttime Reconstruction from DJI Phantom 4 Pro**

Figure 3-18. **Close-Up View: Grid + Orbit Trajectory Nighttime Reconstruction from DJI Phantom 4 Pro**
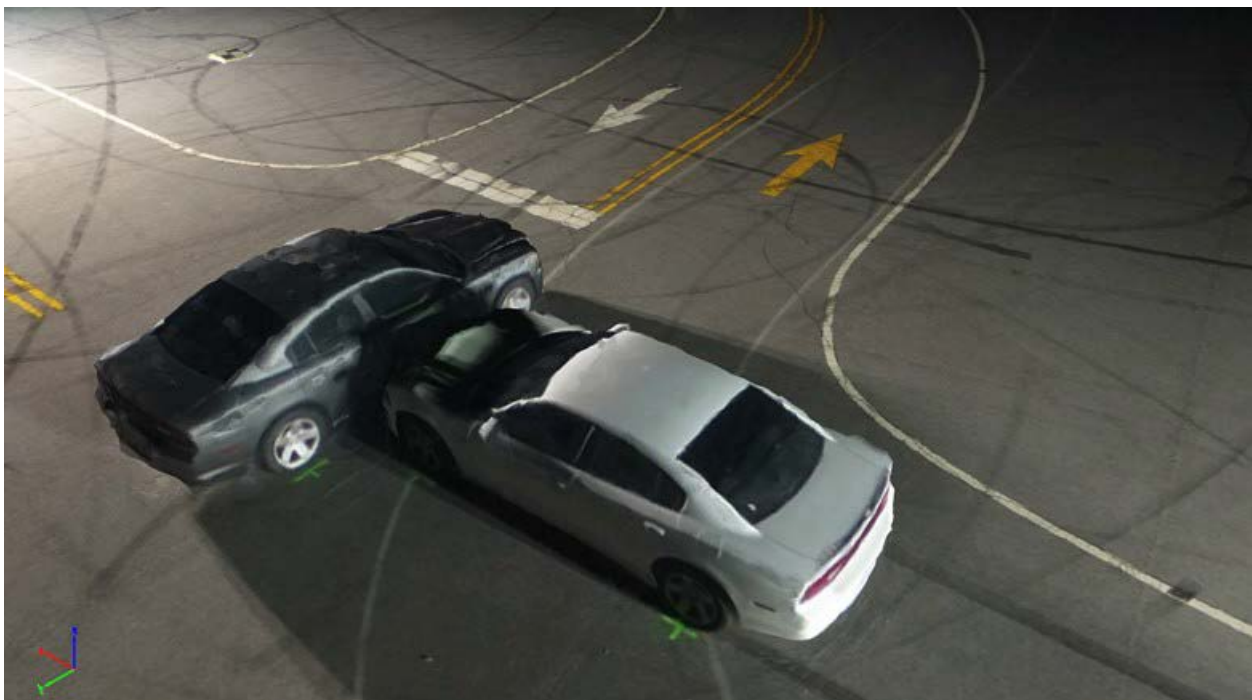
Figure 3-19. **Lateral View: Grid Trajectory Nighttime Reconstruction from DJI Phantom 4 Pro**

Figure 3-20. **Lateral View: Orbit Trajectory Nighttime Reconstruction from DJI Phantom 4 Pro**
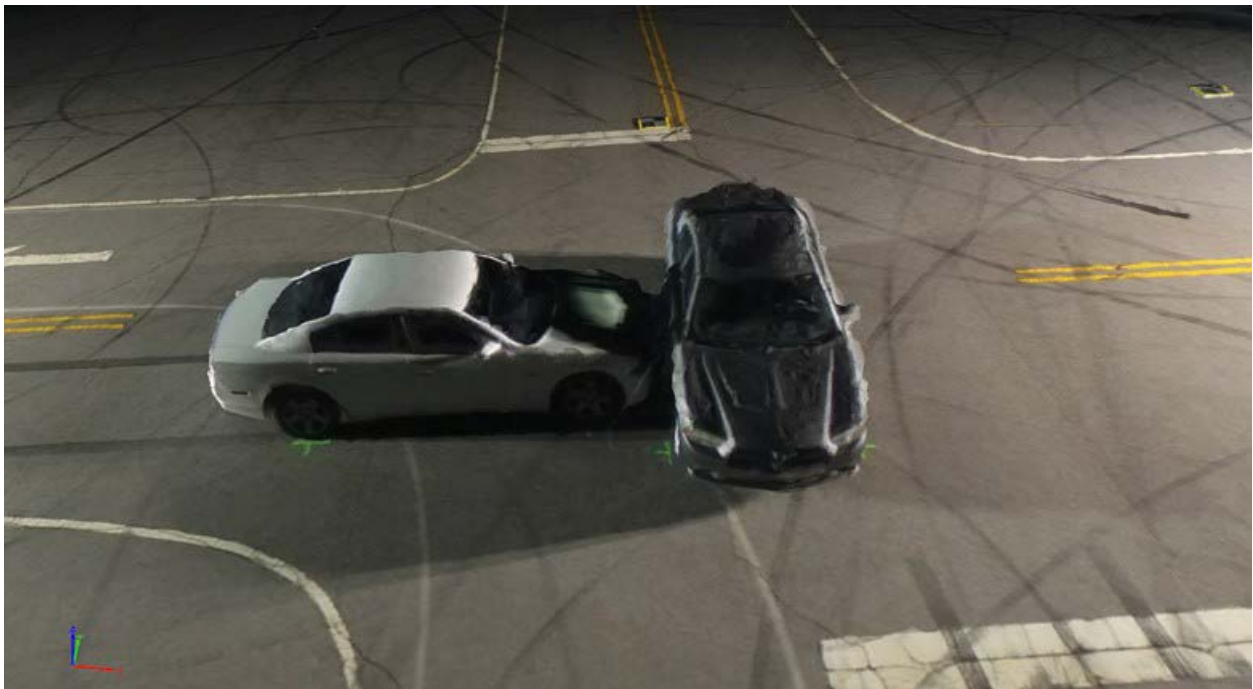
Figure 3-21.   Lateral View: Grid + Orbit Trajectory Nighttime Reconstruction from DJI Phantom 4 Pro

From the above reconstructions, we can conclude that the Orbit trajectory performs better than the Grid trajectory for the reconstruction of the side surfaces, and Grid trajectory performs better for overhead views. Consequently, the Grid + Orbit trajectory is a good tradeoff between the Grid and Orbit trajectories.

4. EFFECT OF UAS CAMERA SENSOR

The DJI Phantom 4 Pro has a better camera than the DJI Mavic Pro. The DJI Phantom 4 Pro's camera has a larger 1-inch CMOS sensor with 20 megapixel (MP) resolution, whereas the DJI Mavic Pro's camera has a 1/2.3-inch CMOS sensor with a 12MP resolution. This greatly affects the reconstruction as the number of 3-D points generated for the DJI Phantom 4 Pro is far greater than the number of points generated by the Mavic Pro.

Structurally, the DJI Phantom 4 Pro is more robust compared to the DJI Mavic Pro. In windy conditions, the DJI Phantom 4 Pro is less affected and still produces clear images. The DJI Mavic Pro, being a smaller drone, is more prone to be affected by wind gusts. Given the additional factor that the DJI Mavic Pro has a lower quality camera, images from the DJI Mavic Pro can be blurry (due to motion blur and focus blur).

The effect of the sensor quality is less prominent in daytime reconstructions and becomes more pronounced as the number of artificial lights reduces during the night reconstructions. If the scene is not properly illuminated, annotating the Aeropoints™ Ground Control Points during the reconstruction becomes more challenging. In some cases (e.g., Day 2 reconstructions with just the ILT), it was impossible to annotate the ground control points from the images captured by the DJI Mavic Pro.

The following images illustrate the differences in reconstructions from grid and orbital trajectories of the DJI Phantom 4 Pro and DJI Mavic Pro. *Figures 4-1, 4-3*, and *4-5* are images from a reconstruction from an orbital trajectory using a Mavic Pro, while *Figures 4-2, 4-4* and *4-6* are the images from a reconstruction from an orbital trajectory using the Phantom 4 Pro. Both the drones were flown at approximately the same time of the day ensuring that there was an equal amount of ambient light and the same set of artificial lights. The next six images (*Figures 4-7* to *4-12*) depict reconstructions from comparable grid trajectories.

We notice that in the reconstructions from the Mavic Pro, the textures have much less detail and sharpness than those for the Phantom 4 Pro. The surfaces of the road and those on the car, especially near the door handles in the close-up views, appear blurred. We also notice that that Phantom 4 Pro's camera sensor is able to capture a much higher amount of light, compared with the Mavic Pro's sensor.

The images in *Figures 4-1, 4-3*, and *4-5* illustrate the reconstruction of a grid trajectory of the DJI Mavic Pro in a scene illuminated only by an ILT. In each of these figures, the images captured had inadequate illumination for us to annotate the ground control points manually. The images in *Figures 4-2, 4-4*, and *4-6* illustrate the reconstruction of the same scene and same lighting conditions with the DJI Phantom 4 Pro. We notice that the reconstruction by the DJI Phantom 4 Pro is significantly brighter than the reconstruction by DJI Mavic Pro. Notice the extent of shadows and the quality of textures in the DJI Mavic Pro reconstructions. Even though the DJI Phantom 4 Pro's reconstruction is poor, because it is a challenging scene with just one source of light, the quality of its textures—especially near the door handles and on the road—is much better than that of the DJI Mavic Pro.

In the three pairs of images in *Figures 4-7* through *4-12*, we compare the reconstruction quality of a scene illuminated by two MLTs and an ILT. In this case, we see that the geometry of the reconstruction by the Mavic Pro is as accurate as that from the Phantom 4 Pro. On close observation, we notice the

lower resolution textures in the Mavic Pro reconstruction. For example, the texture on door handles is blurred, and edges of the car doors lack sharpness.

Figure 4-1. **Overhead View: 17:00 ILT Orbit Trajectory from DJI Mavic Pro (Day 2). Note: Caption format specifies view type, time of day, lighting type, trajectory type, and UAS type.**

Figure 4-2. **Overhead View: 17:00 ILT Orbit Trajectory from DJI Phantom 4 Pro (Day 2)**

Figure 4-3. **Close-Up View: 17:00 ILT Orbit Trajectory from DJI Mavic Pro (Day 2)**

Figure 4-4. **Close-Up View: 17:00 ILT Orbit Trajectory from DJI Phantom 4 Pro (Day 2)**
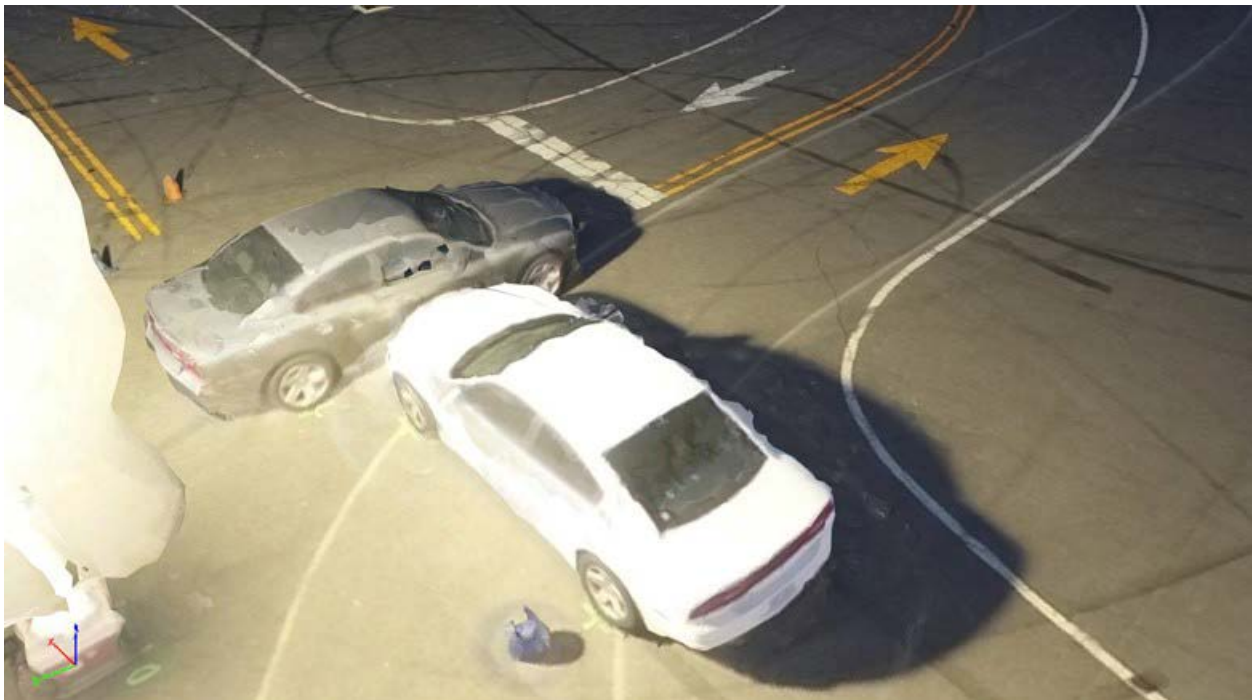
Figure 4-5. **Lateral View: 17:00 ILT Orbit trajectory from DJI Mavic Pro (Day 2)**

Figure 4-6. **Lateral View: 17:00 ILT Orbit trajectory from DJI Phantom 4 Pro (Day 2)**

Figure 4-7. **Overhead View: 19:30 Two MLTs + ILT Grid Trajectory from DJI Mavic Pro (Day 2)**

Figure 4-8. **Overhead View: 19:30 Two MLTs + ILT Grid Trajectory from DJI Phantom 4 Pro (Day 2)**

Figure 4-9.   Close-Up View: 19:30 Two MLTs + ILT Grid Trajectory from DJI Mavic Pro (Day 2)

Figure 4-10.   Close-Up View: 19:30 Two MLTs + ILT Grid Trajectory from DJI Phantom 4 Pro (Day 2)

Figure 4-11.   Lateral View: 19:30 Two MLTs + ILT Grid trajectory from DJI Mavic Pro (Day 2)

Figure 4-12.   Lateral View: 19:30 Two MLTs + ILT Grid Trajectory from DJI Phantom 4 Pro (Day 2)
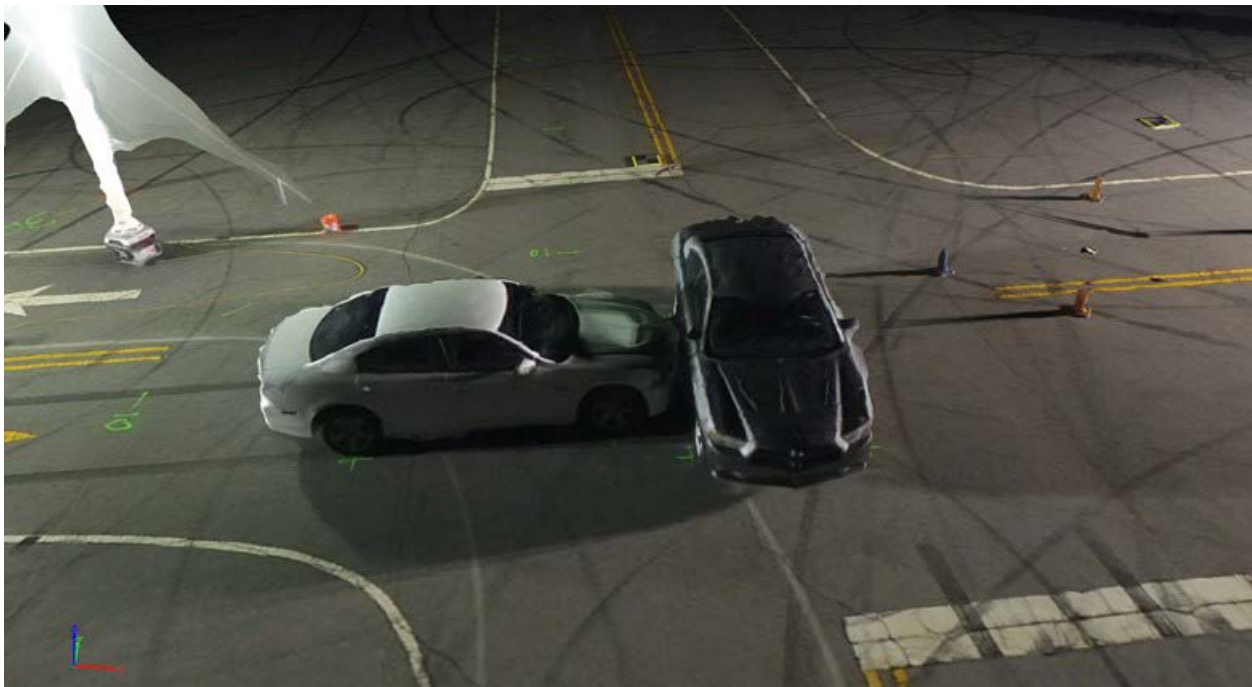
Table 4-1 outlines the conditions under which we were able to obtain sufficiently good images for 3-D reconstruction using the two different cameras.

Table 4-1. **Lighting and Weather Conditions to Obtain Sufficiently Good Images for 3-D Reconstruction**

Dataset Time	Trajectory	Conditions	DJI	
			Phantom 4 Pro	Mavic Pro
15:00 Day 1	Grid Orbit	Sunlight	✓	✓
17:00 Day 2	Grid Orbit	Twilight, 2 Mobile Light Towers (MLTs) Inflatable Light Tower (ILT)	✓	✓
17:30 Day 1	Grid	Twilight, 2 MLTs	✓	✓
17:30 Day 1	Grid	Twilight 1 MLT	✓	✓
17:30 Day 2	Grid Orbit	Twilight ILT	✓	✗
17:30 Day 1	Grid Orbit	Twilight	✓	✗
19:30 Day 2	Grid Orbit	2 MLTs ILT	✓	✓
19:30 Day 2	Grid Orbit	2 MLTs	✓	✓
19:30 Day 1	Orbit	1 MLT	✓	✓
19:30 Day 1	Grid	1 MLT	✓	✗
19:30 Day 2	Grid Orbit	ILT	✓	✗
19:30	Grid Orbit	No light source	✗	✗
17:30 19:30	Grid Orbit	Weather: Windy	✓	✗

5.   EFFECT OF AMBIENT LIGHT ON RECONSTRUCTION

The presence of ambient light significantly improves the quality of the 3-D reconstruction. The following images illustrate the impact of decreasing amounts of ambient light on the quality of reconstructions.

Overhead views of the 3-D reconstructions are illustrated in *Figures 5-1, 5-2*, and *5-3*. In *Figure 5-6*, we can see that the artefact on the roof of the car is quite significant when compared to *Figures 5-4* and *5-5*. A similar observation can also be made in *Figure 5-9*, where we notice that the artefact near the rear wheel of the white car is larger than in the other two reconstructions at a brighter ambient light in *Figures 5-7* and *5-8*. As these reconstructions are made from a grid trajectory using only overhead images, the lateral view of the reconstruction of the car is generally distorted.

Figure 5-1.   Overhead View: 17:00 Two MLTs + ILT Grid Trajectory from DJI Phantom 4 Pro (Day 2)

Figure 5-2. **Overhead View: 17:30 One MLT Grid Trajectory from DJI Phantom 4 Pro (Day 1)**

Figure 5-3. **Overhead View: 17:30 Two MLTs Grid Trajectory from DJI Phantom 4 Pro (Day 1)**
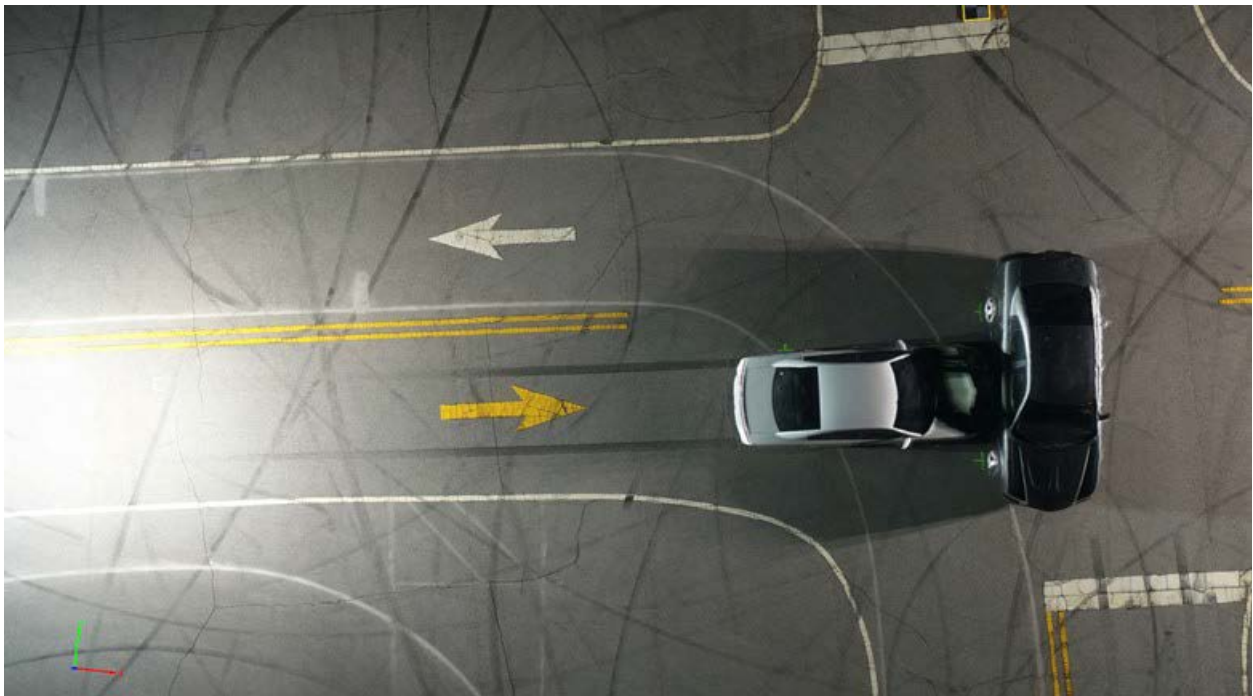
Figure 5-4. **Close-Up View: 17:00 Two MLTs + ILT Grid Trajectory from DJI Phantom 4 Pro (Day 2)**

Figure 5-5. **Close-Up View: 17:30 One MLT Grid Trajectory from DJI Phantom 4 Pro (Day 1)**
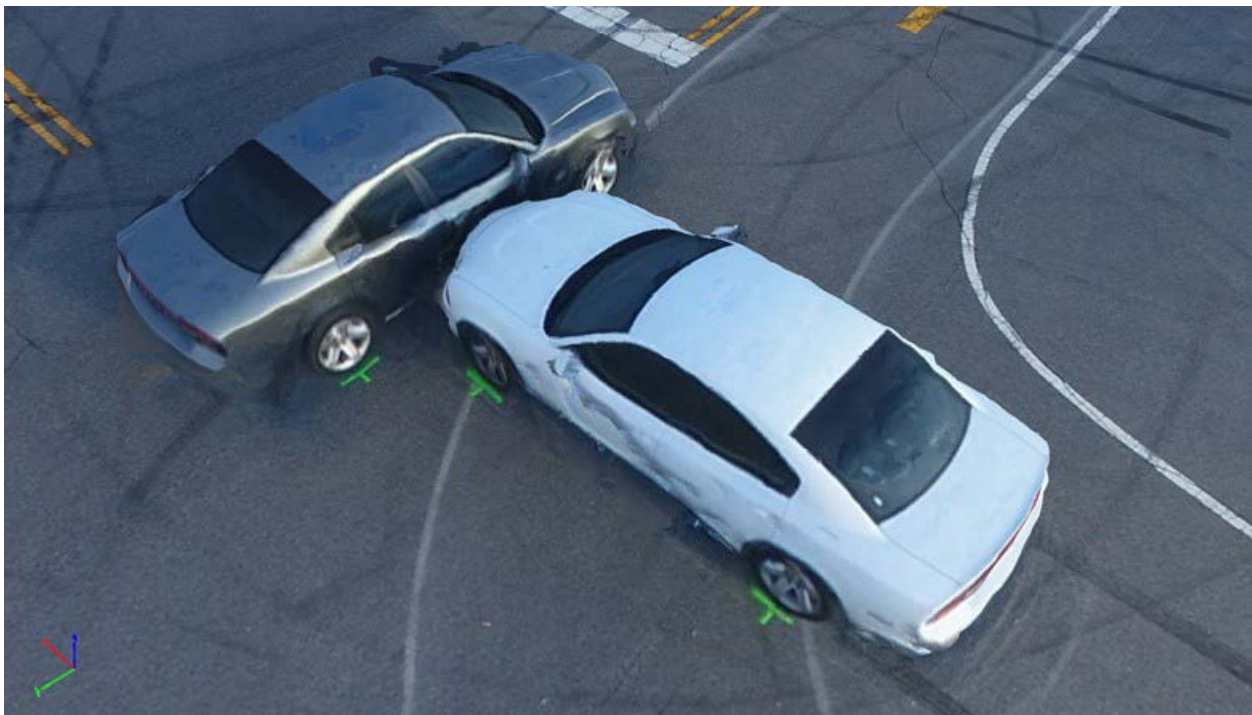
Figure 5-6. **Close-Up View: 17:30 Two MLTs Grid Trajectory DJI Phantom 4 Pro (Day 1)**

Figure 5-7. **Lateral View: 17:00 Two MLTs + ILT Grid Trajectory DJI Phantom 4 Pro (Day 2)**

Figure 5-8. **Lateral View: 17:30 One MLT Grid Trajectory DJI Phantom 4 Pro (Day 1)**

Figure 5-9. **Lateral View: 17:30 Two MLTs Grid Trajectory DJI Phantom 4 Pro (Day 1)**

6. COMPARISON OF ARTIFICIAL LIGHTING SCENARIOS FOR RECONSTRUCTION

In this section we discuss the different lighting conditions tested out during our experiments. We tested out the lighting conditions with:

- Two MLTs + one ILT

- Two MLTs

- One MLT

- ILT

The list above is arranged in decreasing order of luminous intensity in the scene. Uniform illumination of the scene ensures even brightness across all the captured images. This ensures that the reconstruction generated has all the road marks perfectly observable. If the light sources are reduced to a single point source (e.g., a single ILT or a single MLT), the reconstruction quality degrades due to the following reasons:

- Single light sources cast large shadows of the cars on the ground. The dark shadows lead to erroneous reconstructions, thereby generating more artefacts.

- The camera on the drone cannot focus on the ground plane accurately in low-light conditions. This results in the images captured being blurry. Although reconstruction from blurred images is possible, the quality of the reconstruction cannot maintain sharp edges in the geometry, and the textures are blurred as well.

By observing the reconstructions in the different lighting scenarios listed above (as illustrated in *Figures 6-1* through *6-12*), we have noticed that MLTs adequately illuminate any object placed in the scene (e.g., cars, traffic cones). The luminous intensity of MLTs being considerably higher than that of the ILT, reconstructions with multiple MLTs are more accurate in terms of geometry and texture. When one MLT is used, the part of the road near the light source gets overexposed in the images captured by the drone, when compared to the rest of the scene. This results in a bright patch on the road at which the road marks get washed out.

The ILT is good for illuminating skid marks and road features. It acts best as a filler light, illuminating the part of the scene which is left dark after using the MLTs. Using only the ILT is insufficient, as it casts large shadows behind the car. These shadows eventually result in scene artefacts in the reconstruction. While reconstruction artefacts on the cars in the scene can be addressed by offsite reconstruction of the cars using the FARO scanner, scene reconstruction artefacts caused by shadows (see *Figures 6-11* and *6-12* for examples) cannot be similarly addressed.

Figure 6-1. **Overhead View: 19:30 Two MLTs + ILT Grid trajectory from DJI Phantom 4 Pro (Day 2)**

**Figure 6-2.** **Overhead View: 19:30 Two MLTs Grid Trajectory from DJI Phantom 4 Pro (Day 1)**
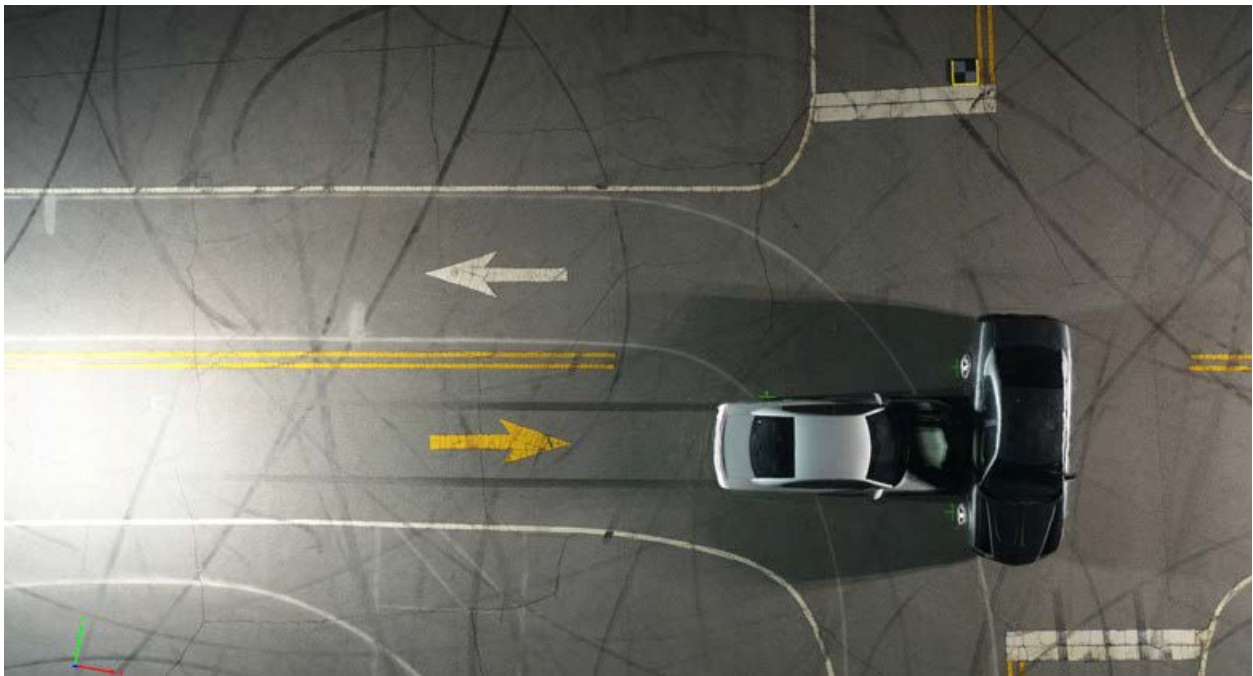
Figure 6-3. **Overhead View: 19:30 One MLT Grid Trajectory from DJI Phantom 4 Pro (Day 1)**
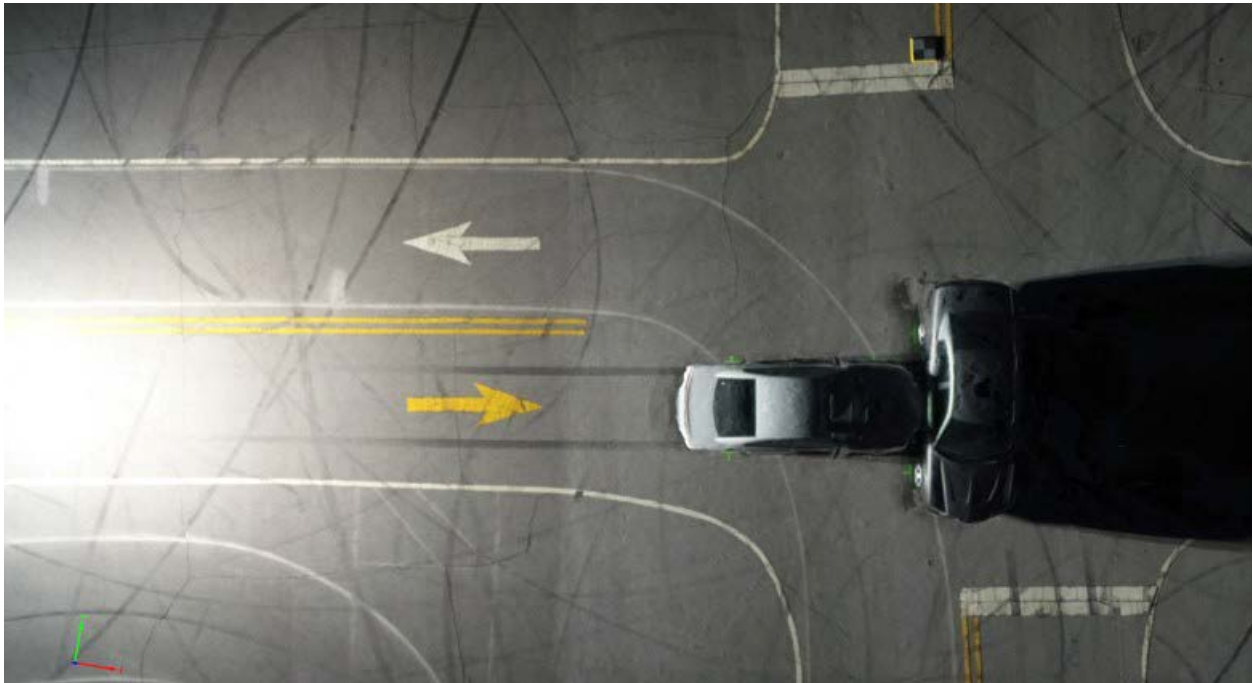
Figure 6-4. **Overhead View: 19:30 ILT Grid Trajectory from DJI Phantom 4 Pro (Day 2)**

Figure 6-5. **Close-Up View: 19:30 Two MLTs + ILT Grid trajectory from DJI Phantom 4 Pro (Day 2)**

Figure 6-6. **Close-Up View: 19:30 Two MLTs Grid trajectory from DJI Phantom 4 Pro (Day 1)**
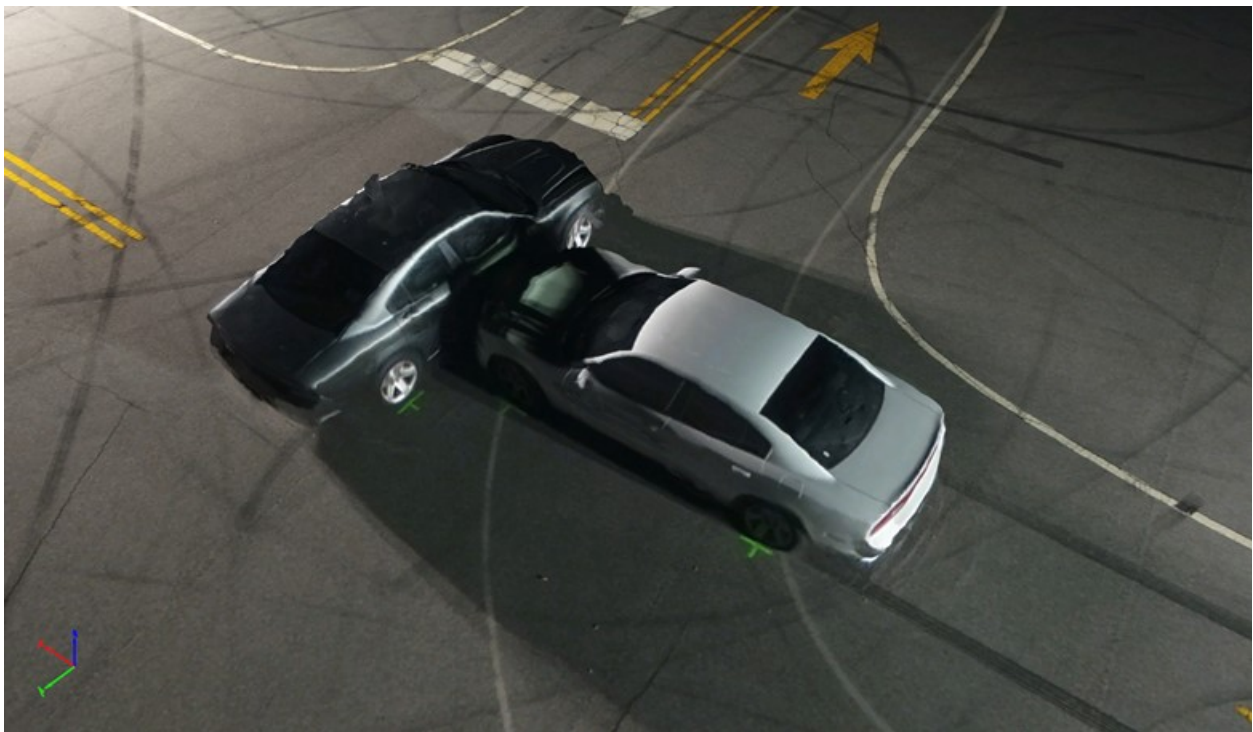
Figure 6-7. **Close-Up View: 19:30 One MLT Grid trajectory from DJI Phantom 4 Pro (Day 1). Note the significant scene artefacts in the shadow regions in the upper left part of the reconstruction.**

Figure 6-8. **Close-Up View: 19:30 ILT Grid Trajectory from DJI Phantom 4 Pro (Day 2). Note the significant scene artefacts in the shadow regions of the reconstruction.**

Figure 6-9. **Lateral View: 19:30 Two MLTs + ILT Grid trajectory using DJI Phantom 4 Pro (Day 2)**

Figure 6-10. **Lateral View: 19:30 Two MLTs Grid Trajectory using DJI Phantom 4 Pro (Day 1)**
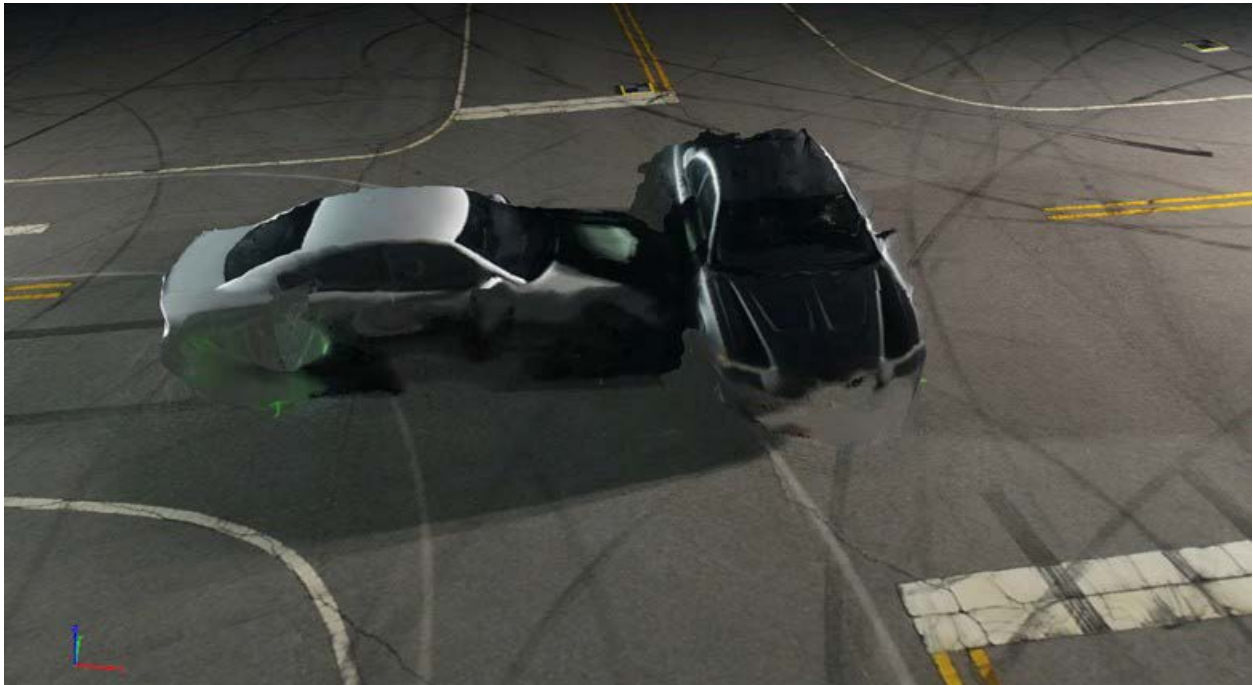
Figure 6-11. **Lateral View: 19:30 One MLT Grid Trajectory from DJI Phantom 4 Pro (Day 1)**

**Figure 6-12.** **Lateral View: 19:30 ILT Grid Trajectory from DJI Phantom 4 Pro (Day 2). Note the significant artefacts in the shadow regions on the right side of the reconstruction.**

7. RECONSTRUCTION TIME

The reconstruction time in Pix4D is typically considerably lower than in Agisoft. The Pix4D 3-D reconstructions were performed on a single computer using the reconstruction preset 3-D Model. To calculate the time taken to generate orthomosaics, we used a different reconstruction preset 3-D Map. However, some of the Agisoft reconstructions were performed on a laptop computer and some were done on a desktop computer. *Table 7-1* compares the 3-D and orthomosaic reconstruction times for selected datasets gathered at different times and with different trajectories. The laptop reconstructions have been marked with (L) and the desktop reconstructions have been marked with (D). The specific configurations of the computers have been provided in detail in *Appendix A*. A few of the Agisoft reconstructions involved color correction as a step in the reconstruction pipeline. The following table ignores the time duration for color correction in the reconstruction. This is because color correction is an optional parameter, and second, color correction has not been performed on all the reconstructions.

Figure 7-1 is a plot of the 3-D reconstruction and orthomosaic generation times of all Phantom 4 Pro datasets, using Pix4D. The processing times for two different templates of Pix4D (3d Model and 3D Map) have been represented separately. *Table 7-1* compares reconstruction times using Pix4D and Agisoft for selected datasets. Comprehensive reconstruction time data for all Phantom 4 Pro and Mavic Pro datasets are presented in *Appendix B*.

Figure 7-1.   **Box and Whisker Plot Showing the Reconstruction Times for All Phantom 4 Pro Grid, Orbit, and Grid+Orbit Trajectories Using Pix4D. Pix4D 3d Model gives 3-D reconstructions, and Pix4D 3D Map gives orthomosaics.**
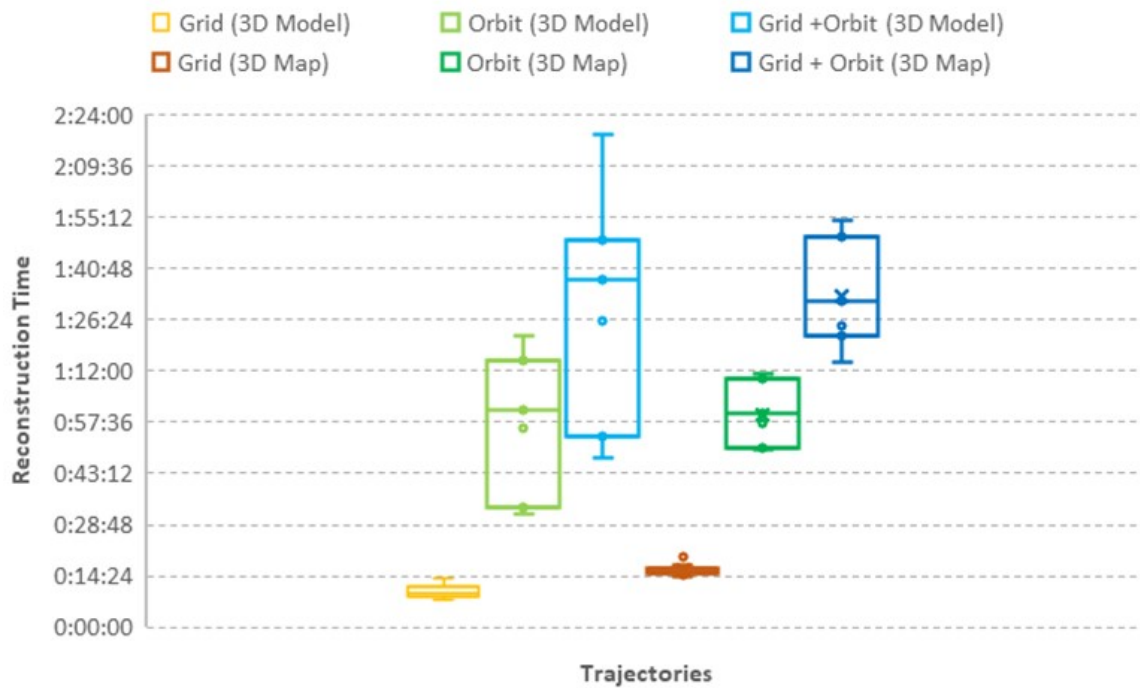
Table 7-1. **Reconstruction Time Comparison of Selected Datasets of DJI Phantom 4 Pro Using Pix4D and Agisoft Photoscan**

	Reconstruction Time (HH:MM:SS)	
Dataset	**Pix4D** **3-D Reconst. Time** **Orthomosaic Time**	**Agisoft** **3-D Reconst. Time** **Orth mosaic Time**
DJI Phantom 4 Pro Saturday 15:00 Grid (Ambient Light)	0:08:43 0:17:12	00:24:34 (D) 00:36:16 (D)
DJI Phantom 4 Pro Saturday 17:30 Grid (2 Mobile Light Tower (MLTs))	0:09:44 0:16:15	00:24:43 (L) 00:33:39 (L)
DJI Phantom 4 Pro Saturday 19:30 Grid (2 MLTs)	0:09:03 0:15:27	01:18:11 (L) 01:26:49 (L)
Mean Time for Grid (DJI Phantom 4 Pro)	**0:09:10** **0:16:18**	
DJI Phantom 4 Pro Saturday 15:00 Orbit (Ambient Light)	0:33:42 0:52:53	06:43:32 (L) 07:30:45 (L)
DJI Phantom 4 Pro Saturday 17:30 Orbit (2 MLTs)	1:01:08 1:02:20	26:16:37 (L) 26:55:54 (L)
DJI Phantom 4 Pro Saturday 19:30 Orbit (2 MLTs)	1:01:09 1:01:51	01:13:13 (L)[7] 01:47:05 (L)[5]
Mean Time for Orbit (DJI Phantom 4 Pro)	**0:52:00** **0:59:01**	
DJI Phantom 4 Pro Saturday 15:00 Grid + Orbit	00:53:19 01:24:41	—
DJI Phantom 4 Pro Saturday 17:30 Grid + Orbit	01:38:22 01:37:30	—
DJI Phantom 4 Pro Saturday 19:30 Grid + Orbit	01:37:52 01:35:17	—
Mean Time for Grid + Orbit (DJI Phantom 4 Pro)	**1:23:11** **1:32:29**	

The reconstruction time is affected by a set of intrinsic and extrinsic parameters. We label the intrinsic parameters as the reconstruction settings. For Pix4D these parameters are:

- Image Scale:
  - Initial Processing: Full, Image Scale: 1
  - Point Cloud Densification: multiscale, ½ (Half image, size)
- Point Density: Optimal
- Minimum number of matches: 3

---

[7] Reconstruction quality at low. Other reconstructions have a quality of Medium.

- 3-D Texture Resolution: Medium Resolution

Similarly, for Agisoft, the reconstruction is affected by parameters:

- Dense Cloud Quality (Ultra, High, Medium, Low)

- Depth Filtering

- Mesh Face Count (Ultra, High, Medium, Low)

- Color Correction

For our reconstruction times recorded in Pix4D, we used one of the default reconstruction templates, 3-D Model. The 3-D Model template uses full scale (1:1) image while matching features across images, and uses a scale of half (0.5:1) image size for the 3-D reconstruction. The latter is performed to alleviate memory issues, which occur at full scale reconstructions.

For the extrinsic parameters, we have noticed that a processor with better parallelism performs much faster. For the default set of parameters that we had used in Pix4D reconstruction of an orbital trajectory, we have noticed the memory usage is less than 8 GB but the processor usage goes up to 100 percent. For this reason, we recommend that all background applications like web browsers should be closed during the reconstruction. We have also noticed a general sluggishness of the computer while the reconstruction takes place.

8.   SAMPLING OF ORBITAL TRAJECTORIES

Orbital trajectories with images sampled every 4 degrees take a much longer time to reconstruct than grid trajectories with 80 percent image overlap. This section discusses the effects of lowering the sampling rates of images for the reconstruction. Because using a lower sampling rate would mean a lower number of images, it would take a much smaller time to reconstruct. *Table 8-1* presents the 3-D reconstruction times for orbital trajectory for 4-degree, 8-degree, and 16-degree sampling; the latter two datasets are obtained by uniformly sampling the 4-degree dataset.

Table 8-1.   Reconstruction Time for Changing Sampling Rates

Sampling Degree	Dataset	Reconstruction Time
4	DJI Phantom 4 Pro Saturday 19:30 Orbit (2 MLTs)	1:01:09
8	DJI Phantom 4 Pro Saturday 19:30 Orbit (2 MLTs)	19:14
16	DJI Phantom 4 Pro Saturday 19:30 Orbit (2 MLTs)	6:21

Figures 8-1 through *8-9* illustrate the reconstruction quality of orbital trajectories at different sampling rates.

Figure 8-1.   Overhead View: 19:30 Two MLTs Orbit Trajectory DJI Phantom 4 Pro (4-degree sampling) (Day 1)
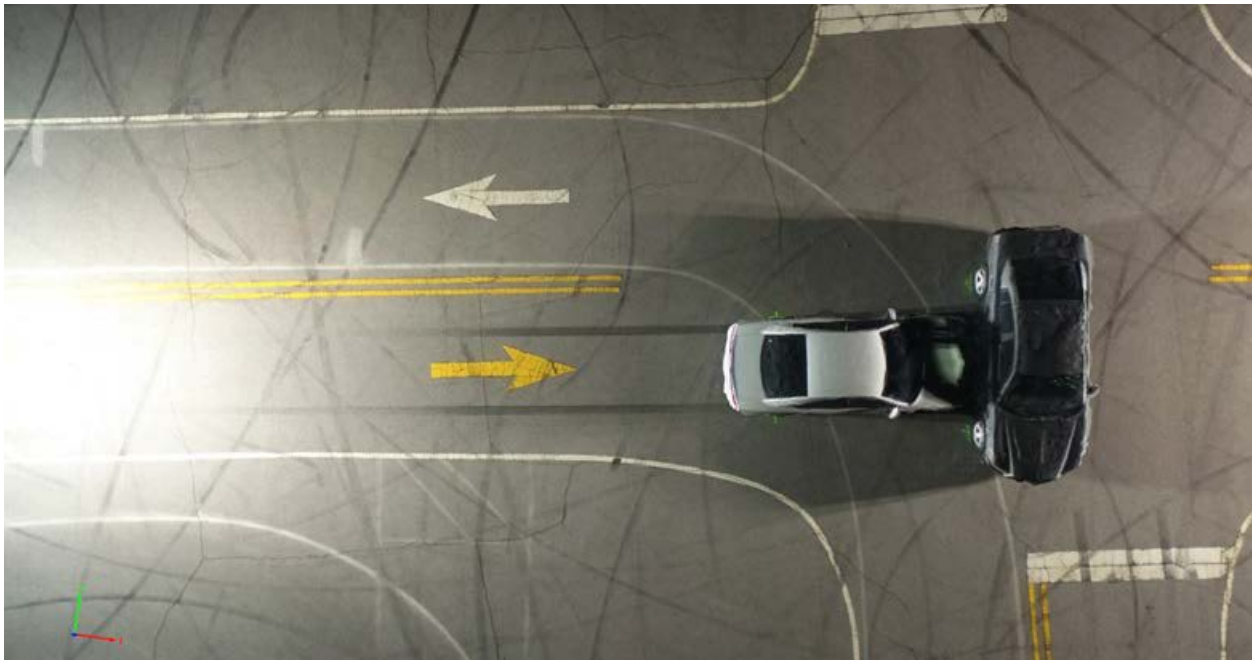
Figure 8-2. **Overhead View: 19:30 Two MLTs Orbit Trajectory DJI Phantom 4 Pro (8-degree sampling) (Day 1)**
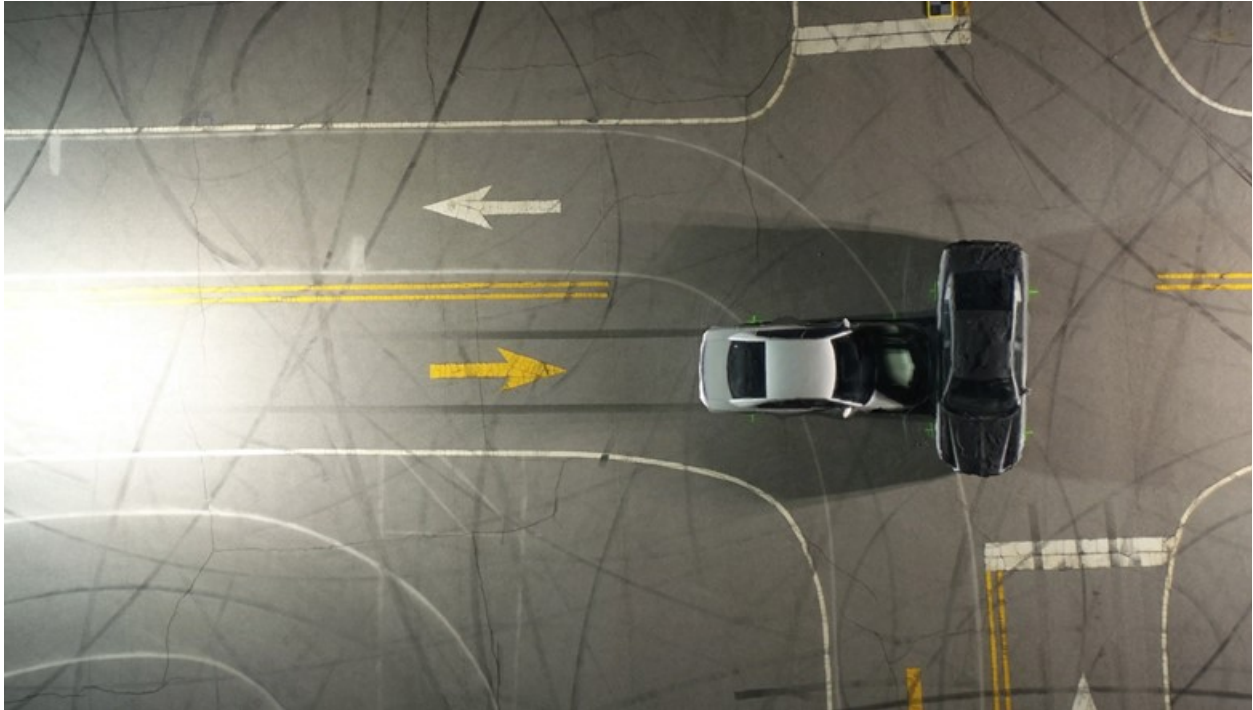
Figure 8-3. **Overhead View: 19:30 Two MLTs Orbit trajectory DJI Phantom 4 Pro (16-degree sampling) (Day 1)**

Figure 8-4. **Close-Up View: 19:30 Two MLTs Orbit Trajectory DJI Phantom 4 Pro (4-degree sampling) (Day 1)**

Figure 8-5. **Close-Up View: 19:30 Two MLTs Orbit Trajectory DJI Phantom 4 Pro (8-degree sampling) (Day 1)**
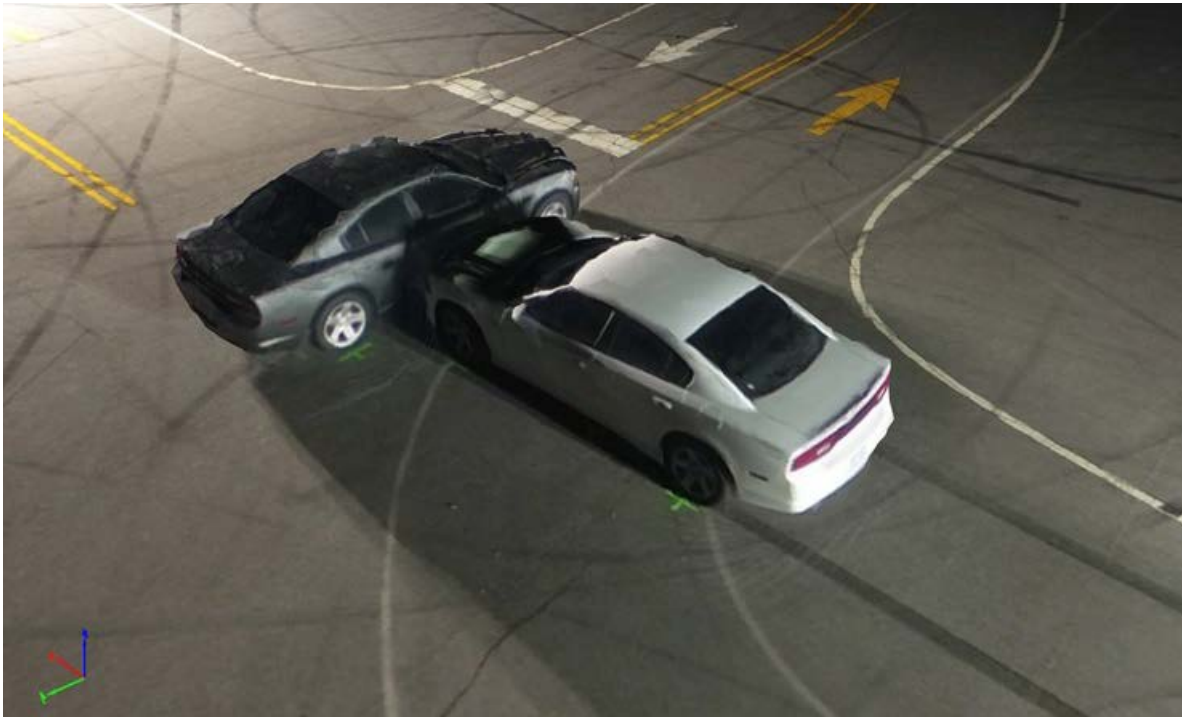
Figure 8-6.   **Close-Up View: 19:30 Two MLTs Orbit Trajectory from DJI Phantom 4 Pro (16-degree sampling) (Day 1). Note the artefacts on the roof of the gray car.**

Figure 8-7.   **Lateral View: 19:30 Two MLTs Orbit Trajectory from DJI Phantom 4 Pro (4-degree sampling) (Day 1)**
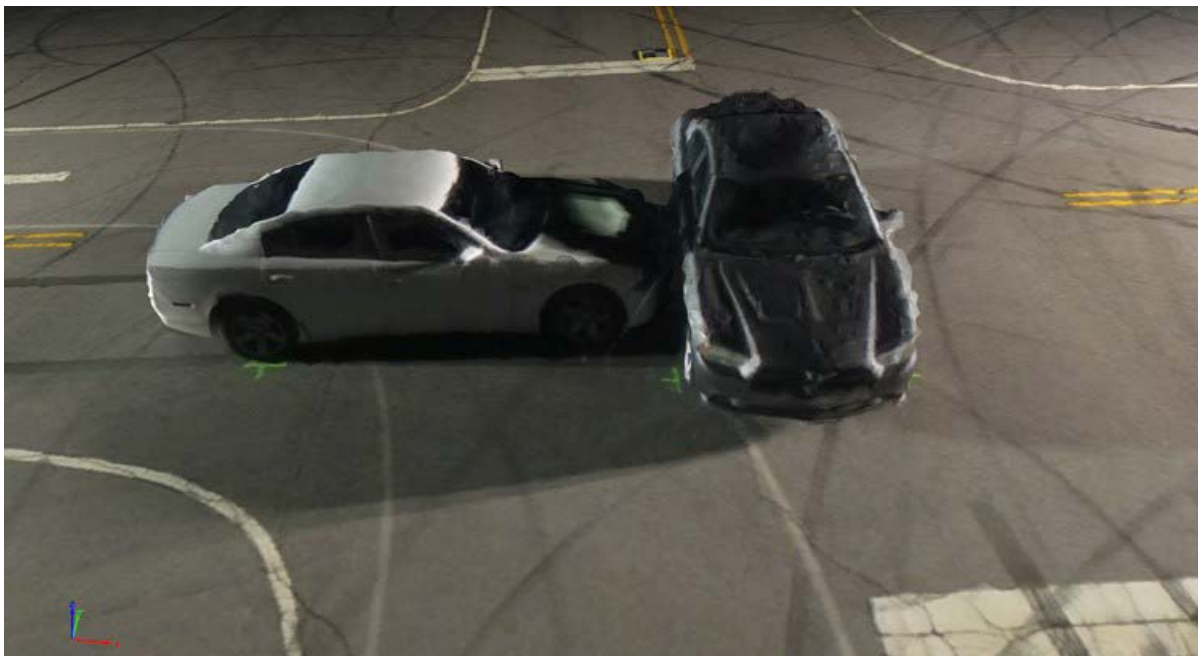
Figure 8-8.   **Lateral View: 19:30 Two MLTs Orbit Trajectory from DJI Phantom 4 Pro (8-degree sampling) (Day 1)**

Figure 8-9.   **Lateral View: 19:30 Two MLTs Orbit Trajectory from DJI Phantom 4 Pro (16-degree sampling) (Day 1)**

From the above figures, we observe that changing the sampling rate does not decrease the quality of the reconstruction much. Only in the close-up view of 16-degree sampling, **Figure 8-6**, do we observe artefacts on the roof of the car.

To calculate the quantitative difference between the 8-degree and 16-degree sampling, we measured the 3-D lengths of the yellow and white arrows in the reconstructed collision scene. **Table 8-2** shows the yellow and white arrow lengths obtained using the different sampling rates.

Table 8-2. **3-D Lengths of the Yellow and White Arrows as Measured from the Reconstruction of 19:30 Two MLTs Orbit Trajectory from DJI Phantom 4 Pro**

Sampling Degree	Feet	
	Yellow Arrow	White Arrow
4	9.97	10.08
8	9.98	10.07
16	9.99	10.07

A significant additional benefit of a lower sampling rate in the field is that it would reduce the time required for data gathering.

9. EFFECT OF GROUND CONTROL POINTS

In the experiments conducted we have used AeroPoints™ as GCPs, which add a separate georeference along with the geolocation of the images. As GCPs are significantly more accurate than geolocated drone images, using these makes the reconstruction accurate to the accuracy of the GCPs. This becomes useful when measuring distances in a reconstruction.

The GCPs should be set up with these guidelines:

- At least four GCPs should be used.

- The GCPs should not be collinear.

- The artificial lights used in the scene should illuminate the GCPs.

Manually annotating GCPs to a reconstruction requires around 2 minutes per GCP. While annotating the ground control points to the images, Pix4D makes image suggestions based on the geolocation of the GCP along with the image geolocation. Generally, these suggestions are accurate when the camera's field of view includes the GCP. Sometimes, especially in the case of an oblique (orbital) trajectory, the image suggestions based on the Global Positioning System coordinates may be incorrect even when the drone is over the GCP. This is because the drone's camera is pointing at the center of the scene, which does not include the GCP.

A general suggestion while adding GCPs is to first verify the correct order of coordinates, for example, as (X, Y, Z) or (Y, X, Z), where X refers to the easting coordinates, Y refers to the northing coordinates, and Z refers to the altitude coordinates.

Table 9-1 illustrates the lengths of the tire skid marks calculated with and without GCPs. The lengths are represented as the 3-D length and 2-D projected length. The 3-D length is the length measured between the start and end point, taking into account their three coordinates: northing, easting, and altitude. Similarly, the 2-D projected length is measured taking into account their northing and easting coordinates. The procedure to compute lengths of the tire skid marks is illustrated in *Appendix C*. The 3-D length corresponds to the tape-measured length between the two points. The tape-measured lengths of the skid marks as measured at the site were 47 feet 11 inches (47.92 feet) and 43 feet 2.5 inches (43.21 feet) for Skid Mark 1 and Skid Mark 2 respectively.

For reference, *Tables 9-1* and *9-2* present the computed lengths of the traffic arrows on the road (behind the white car) when calculated with and without GCPs. When measured on site, the lengths of the arrows were measured as 9 feet 11 inches (9.92 feet) for the yellow arrow and 10 feet (10.0 feet) for the white arrow. Note that when measuring lengths in the reconstructions, there is some subjectivity in the choice of which pixel to treat as the endpoint of a measurement. This causes some variation in the measurement values.

Table 9-1. **Skid Mark Distances Measured from 3-D Reconstruction. The 3-D length is the length measured between the start and end point, taking into account their three coordinates: northing, easting, and altitude. Similarly, the 2-D projected length is measured taking into account their northing and easting coordinates.**

Dataset (Trajectory)	3-D Length (2-D Projected Length) in feet			
	Without GCP		With GCP	
	Skid Mark 1	Skid Mark 2	Skid Mark 1	Skid Mark 2
Day1-p4pro-15:00bcd Grid-Orbit	48.23 (48.23)	43.53 (43.50)	47.98 (47.94)	43.37 (43.34)
Day2-p4pro-17:00c Orbit	48.88 (48.56)	43.99 (43.96)	48.08 (48.04)	43.26 (43.23)
Day2-p4pro-19:30c Orbit	48.69 (48.65)	43.99 (43.96)	48.01 (47.97)	43.35 (43.33)
Mean	48.6 (48.48)	43.84 (43.81)	**48.02 (47.98)**	**43.33 (43.30)**
Standard deviation	0.27 (0.18)	0.22 (0.22)	**0.04 (0.04)**	**0.05 (0.05)**

Table 9-2. **Traffic Arrow Lengths Measured from 3-D Reconstruction**

Dataset (Trajectory)	3-D Length (2-D Projected Length) in feet			
	Without GCP		With GCP	
	Yellow Arrow	White Arrow	Yellow Arrow	White Arrow
Day1-p4pro-15:00bcd Grid-Orbit	9.91 (9.91)	10.07 (10.07)	9.87 (9.87)	10.01 (10.00)
Day2-p4pro-17:00c Orbit	10.10 (10.07)	10.23 (10.23)	9.99 (9.98)	10.08 (10.07)
Day2-p4pro-19:30c Orbit	10.07 (10.03)	10.17 (10.17)	9.93 (9.93)	10.01 (10.01)
Mean	10.03 (10.00)	10.16 (10.16)	**9.93 (9.93)**	**10.03 (10.03)**
Standard deviation	0.08 (0.07)	0.07 (0.07)	**0.05 (0.04)**	**0.03 (0.03)**

Figures 9-1 through *9-12* illustrate the reconstruction quality with and without using GCPs. Looking at the images, we see that using GCPs does not appear to detectably improve the visual quality of 3-D reconstructions.

Figure 9-1. **Overhead View: 19:30 Two MLTs + ILT Grid trajectory from DJI Phantom 4 Pro Without GCPs (Day 2)**

Figure 9-2. **Overhead View: 19:30 Two MLTs + ILT Grid Trajectory from DJI Phantom 4 Pro with GCPs (Day 2)**
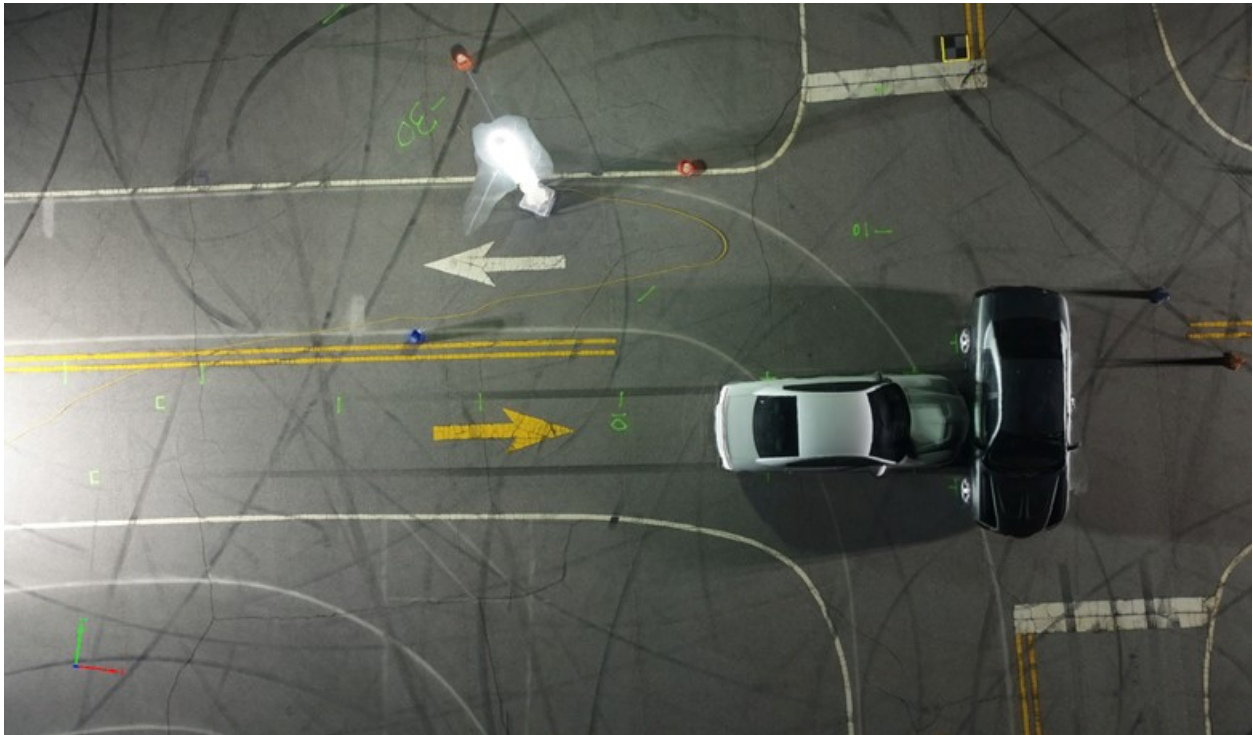
Figure 9-3. **Overhead View: 19:30 Two MLTs + ILT Orbit Trajectory from DJI Phantom 4 Pro Without GCPs (Day 2)**
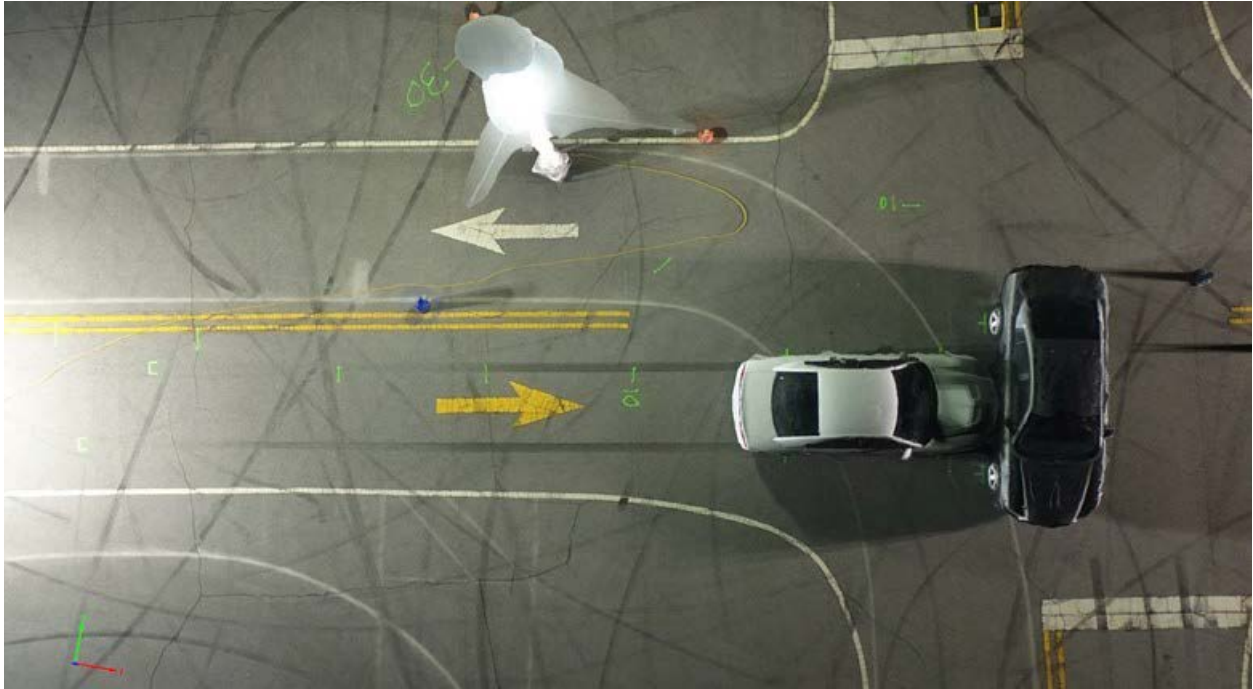
Figure 9-4. **Overhead View: 19:30 Two MLTs + ILT Orbit Trajectory from DJI Phantom 4 Pro with GCPs (Day 2)**
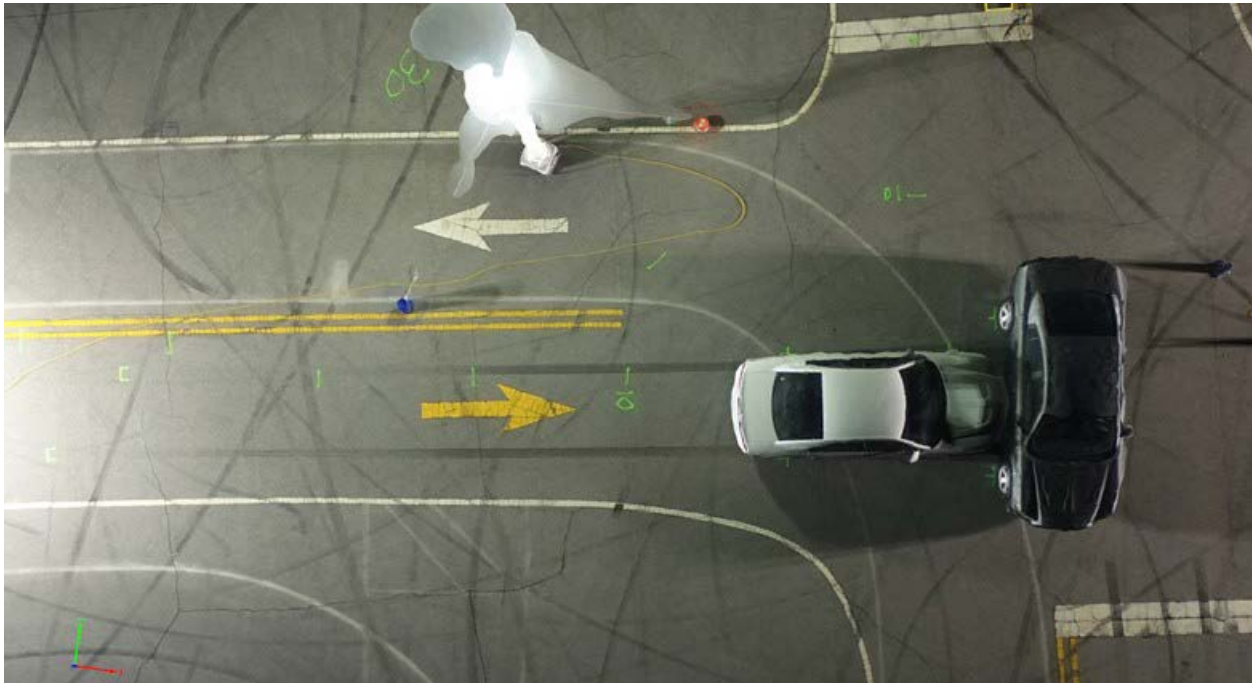
Figure 9-5. **Close-Up View: 19:30 Two MLTs + ILT Grid Trajectory from DJI Phantom 4 Pro Without GCPs (Day 2)**

Figure 9-6. **Close-Up View: 19:30 Two MLTs + ILT Grid Trajectory from DJI Phantom 4 Pro with GCPs (Day 2)**

Figure 9-7. **Close-Up View: 19:30 Two MLTs + ILT Orbit trajectory from DJI Phantom 4 Pro Without GCPs (Day 2)**

Figure 9-8. **Close-Up View: 19:30 Two MLTs + ILT Orbit trajectory from DJI Phantom 4 Pro with GCPs (Day 2)**
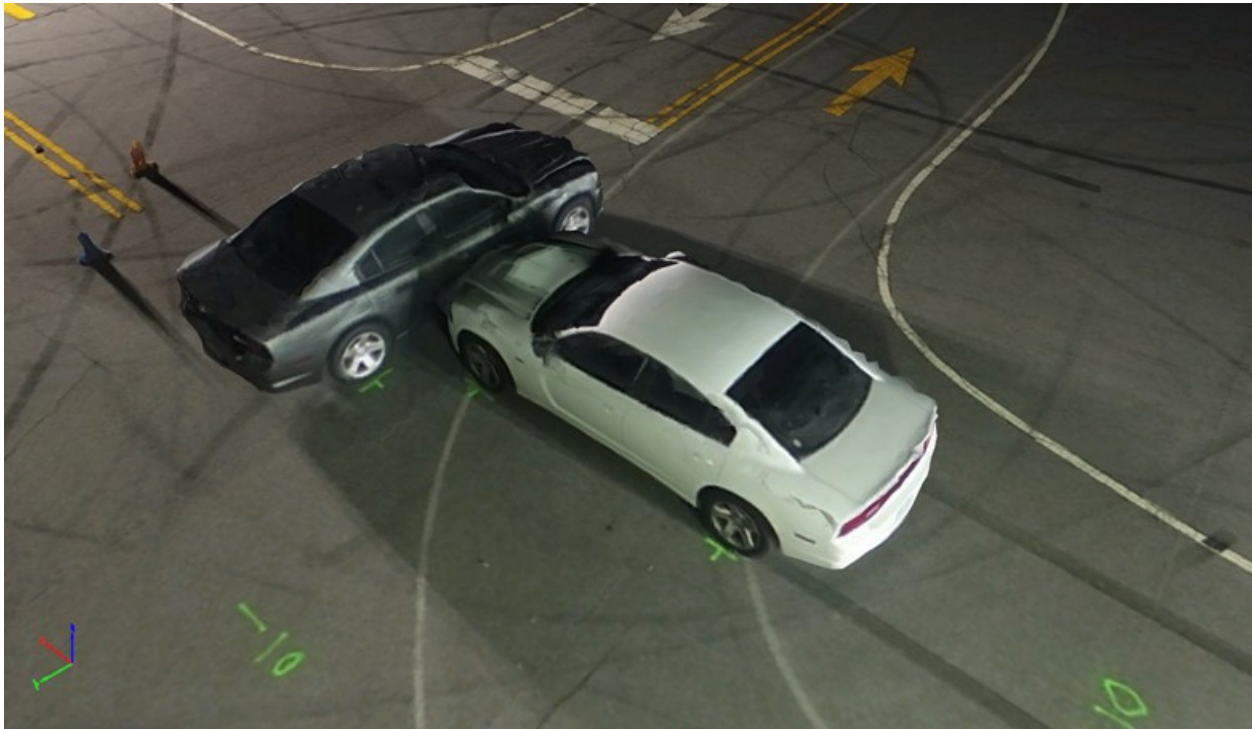
Figure 9-9. **Lateral View: 19:30 Two MLTs + ILT Grid Trajectory from DJI Phantom 4 Pro Without GCPs (Day 2.**

Figure 9-10. **Lateral View: 19:30 Two MLTs + ILT Grid Trajectory from DJI Phantom 4 Pro with GCPs (Day 2)**
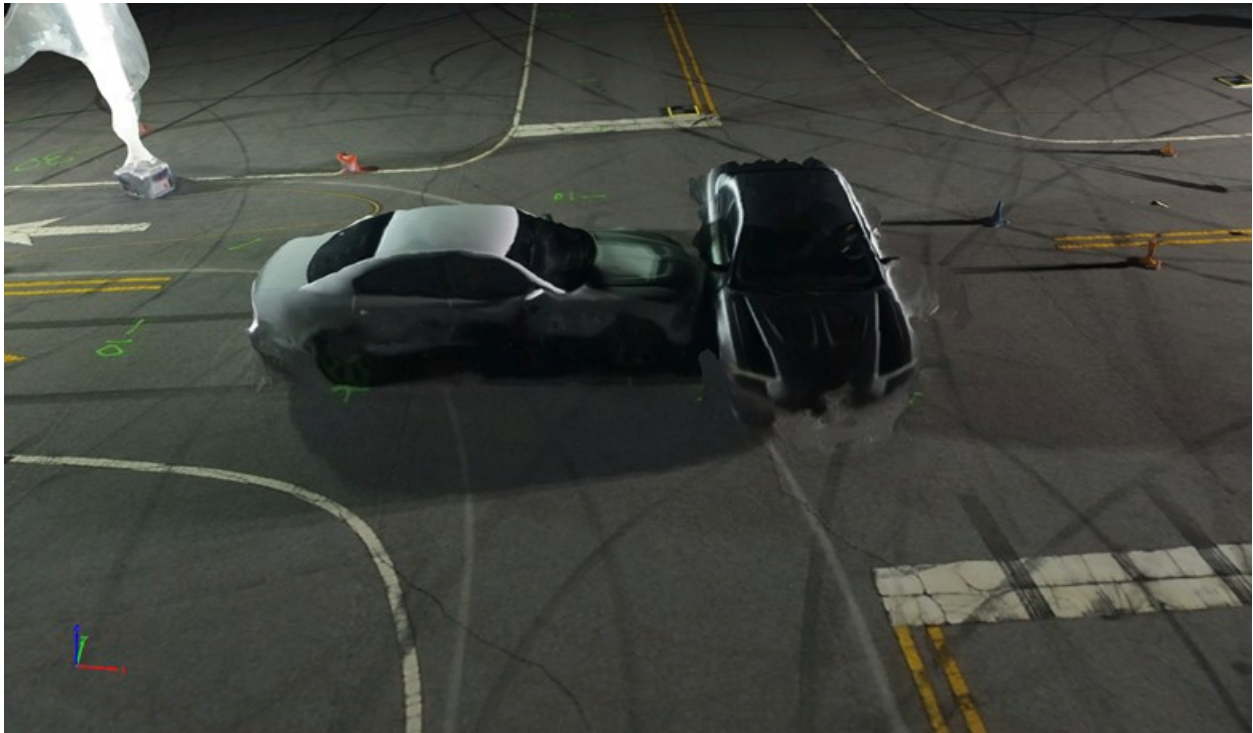
Figure 9-11.   **Lateral View: 19:30 Two MLTs + ILT Orbit Trajectory from DJI Phantom 4 Pro Without GCPs (Day 2)**
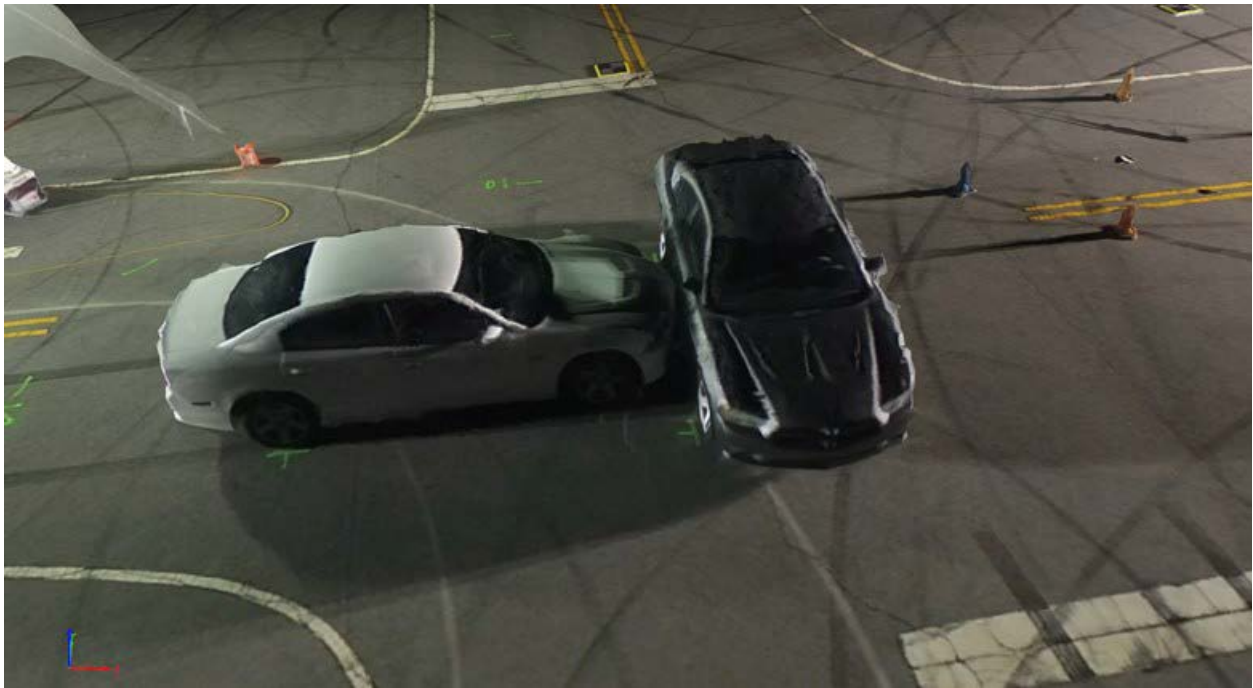
Figure 9-12.   **Lateral View: 19:30 Two MLTs + ILT Orbit Trajectory from DJI Phantom 4 Pro with GCPs (Day 2)**
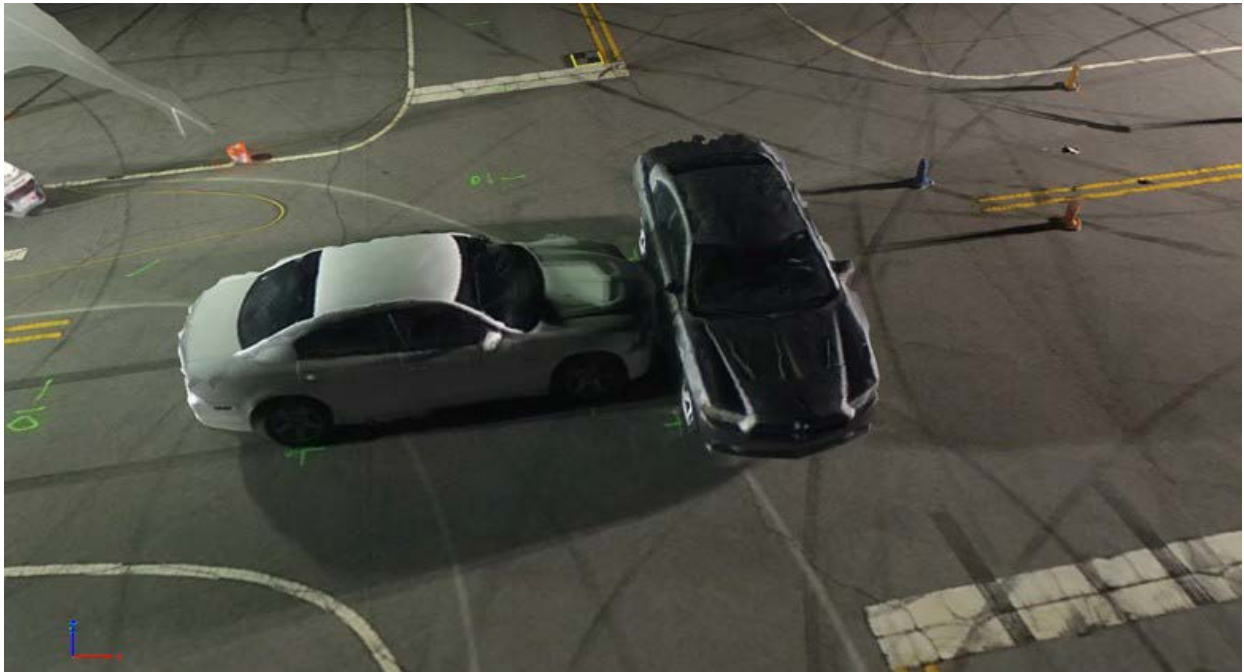
The miniscule changes in the reconstruction geometry that are visually observable are general reconstruction errors in Pix4D, which are even observed between two successive reconstructions of the same scene. To quantify the reconstruction error over successive reconstructions in Pix4D, we conducted the following experiment. We selected a single dataset (Grid trajectory at 17:00 hours using two MLTs + ILT from Phantom 4 Pro [Day 2]) and annotated the GCPs. Then we created five identical copies of this annotated dataset. Each of these datasets was reconstructed separately, and the 3-D measurements of the yellow and white arrows on the road were recorded. The variations in lengths could be due to differences in the reconstructions or due to variability in selection of measurement end points by the user. *Table 9-3* shows the data for the computed lengths of the yellow and white arrows.

Table 9-3. **Lengths of Yellow and White Arrows Using GCPs in Independent Reconstructions of the Same Dataset: Grid Trajectory At 17:00 Hours Using two MLTs + ILT from Phantom 4 Pro (Day 2)**

	Arrow Length (in feet)	
	Yellow	**White**
Reconstruction 1	9.93	10.04
Reconstruction 2	9.84	9.94
Reconstruction 3	9.91	10.02
Reconstruction 4	9.89	10.02
Reconstruction 5	9.90	10.04
Mean	**9.89**	**10.01**
Standard Deviation	**0.03**	**0.037**

10. ORTHOMOSAICS

Orthomosaics are generated after the 3-D reconstruction to provide an overhead view of the scene. They are generated as TIFF files, both in Pix4D and in Agisoft Photoscan. In our reconstructions, we have found that the size of the orthomosaic file depends on the Ground Sampling Distance (GSD), which is the distance in the real world represented by a single pixel length. The GSD depends on the 3-D reconstruction of the scene, which in turn depends on the quality and sharpness of the input images. For example, the grid dataset recorded at 15:00 hours from a Phantom 4 Pro generated a GSD of 0.7 centimeter per pixel, whereas a dataset recorded at 17:00 hours from a Mavic Pro generated a GSD of 1.8 centimeters per pixel.

Figures 10-1 and *10-2* are orthomosaics of datasets with ambient light. Due to the presence of ambient light, we notice that the entire scene is illuminated. In *Figure 10-3*, the lack of ambient light makes only the portion of the scene covered by the artificial light illuminated. The geometrical aberrations on the sides of the car surfaces are not visible in orthomosaics.

Figure 10-1.   Orthomosaic of Grid Trajectory at 15:00 from DJI Phantom 4 Pro with GCPs (Day 1)
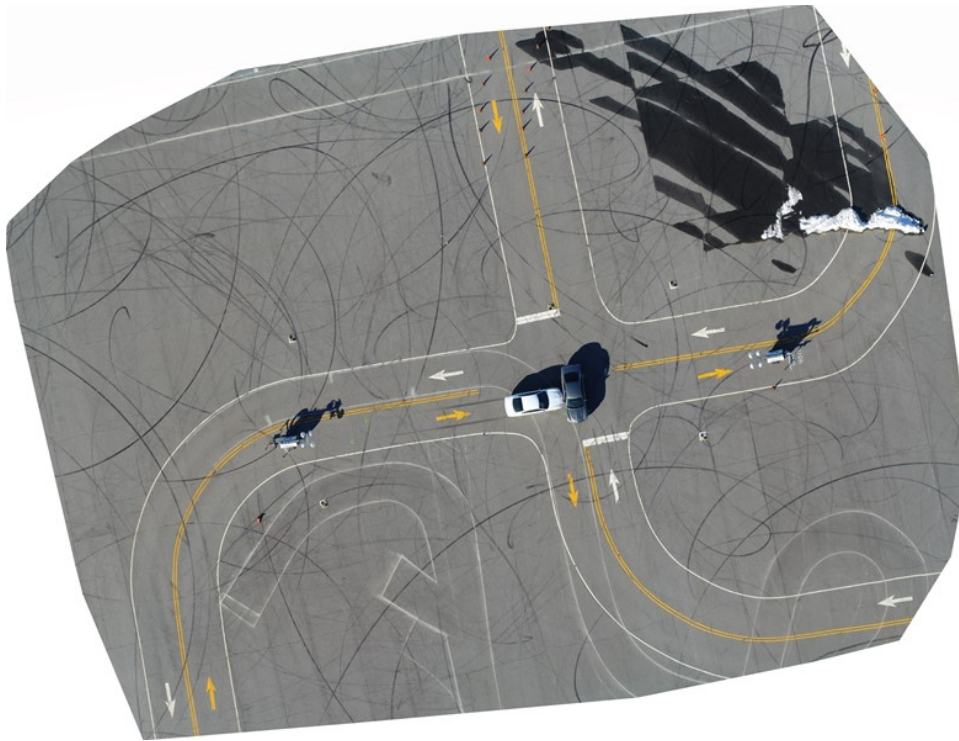
Figure 10-2. **Orthomosaic of Grid Trajectory at 17:30 from DJI Phantom 4 Pro with GCPs (Day 1)**
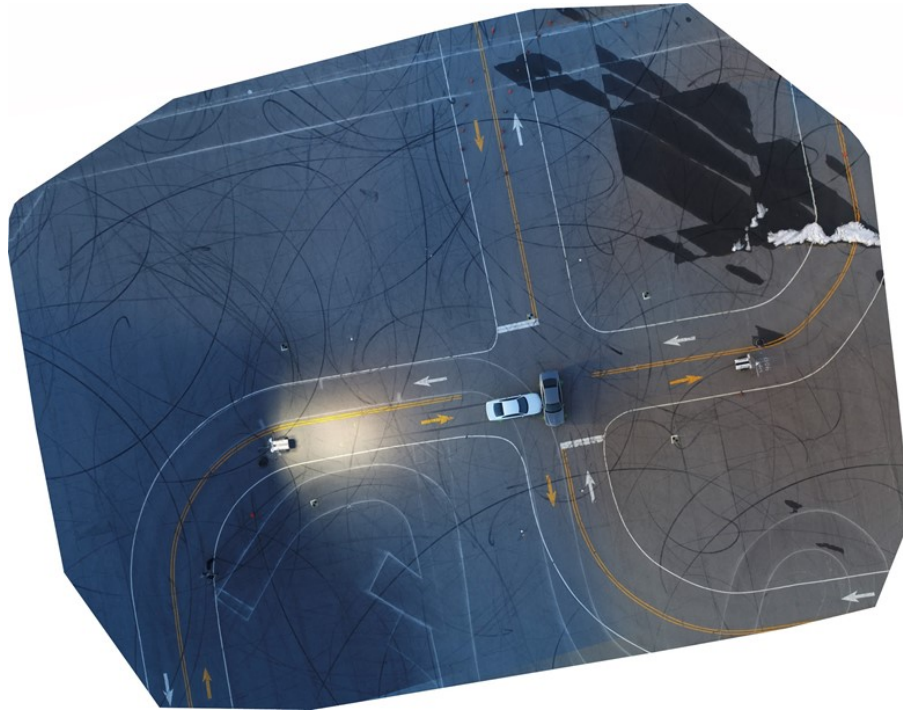
Figure 10-3. **Orthomosaic of Grid Trajectory at 19:00 from DJI Phantom 4 Pro with GCPs[8] (Day 1)**

---
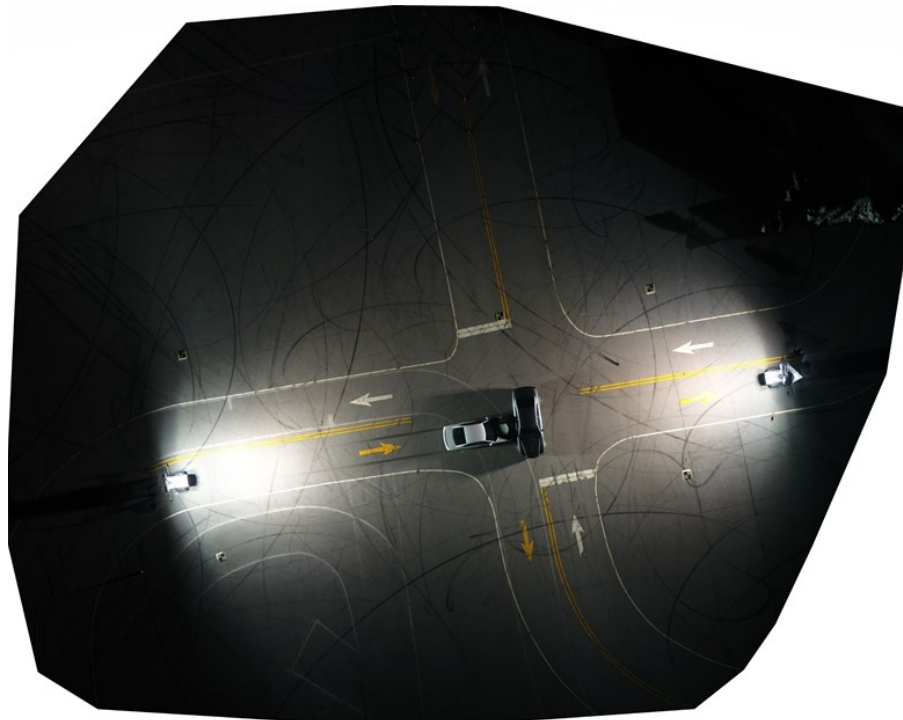
[8] The recorded name of the dataset is Day 1, DJI Phantom 4 Pro 1730f 2 Mobile Light Towers with GCP.

Figures 10-4 and *10-5* illustrate the size of the orthomosaic being affected when changing from the daytime to nighttime dataset. The nighttime orthomosaic is significantly smaller than the daytime orthomosaic.

Figure 10-4.   **Cropped View: Orthomosaic of Grid Trajectory at 15:00 from DJI Phantom 4 Pro with GCPs (Day 1)**

Figure 10-5.   **Cropped View: Orthomosaic of Orbit Trajectory at 19:30 from DJI Phantom 4 Pro with GCPs (Day 1)**
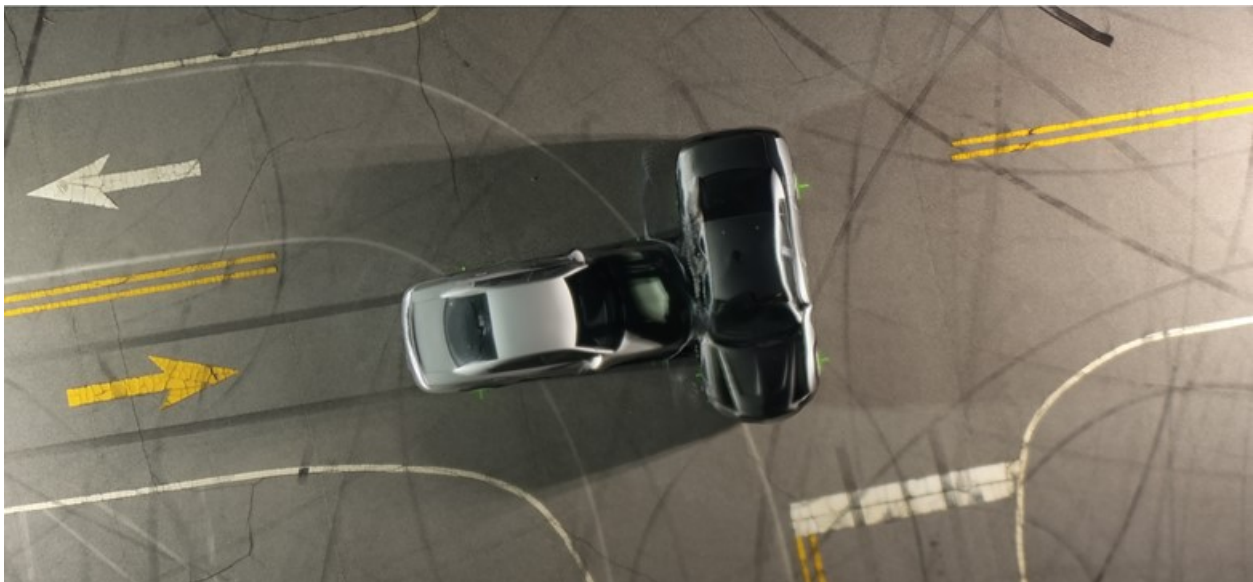
The Orbit reconstruction of Daytime datasets results in an orthomosaic with a much wider field of view, one which covers a lot more than the collision scene itself. In such a case, the orthomosaic at its periphery can have a significant amount of noise and artefacts. See **Figure 10-6** for an example.

Figure 10-6. **Orthomosaic of Orbit Trajectory at 15:00 from DJI Phantom 4 Pro with GCPs (Day 1). Note the distortions at the periphery of the scene.**
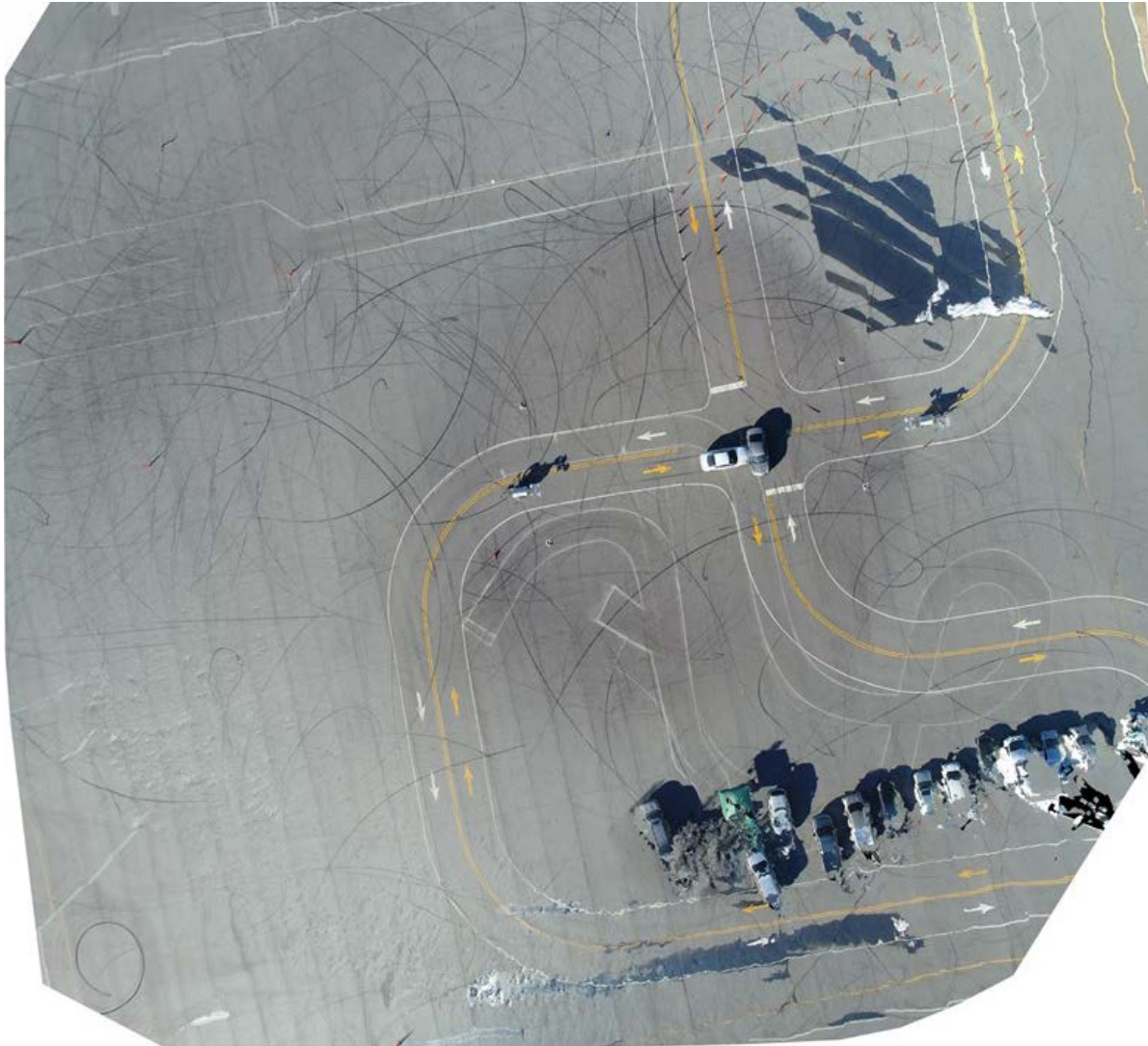
The orthomosaics generated by Agisoft Photoscan differ slightly from the orthomosaics generated by Pix4D. For example, in Agisoft, the orthomosaic has patches of blurry and sharp segments (see *Figure 10-7*), whereas in Pix4D, the mosaic generated has a seamless output (see *Figure 10-8*). In *Figure 10-7*, portions of the thick white road marks are sharp at one end and blurred at the other end. Even the yellow arrow is blurred near its head but sharp near its tail. These differences are more prominent when viewed full screen. The dataset used for this experiment was a grid trajectory recorded at 19:30 hours, using the DJI Phantom 4 Pro.

Figure 10-7. **Orthomosaic Generated Using Agisoft. Observe the white double line at the top of the image. The left portion is blurry, while the right portion is in focus. Similar variations can be observed in other parts of the image, such as the white double lines at the bottom right of the image.**

Figure 10-8. **Orthomosaic Generated Using Pix4D**
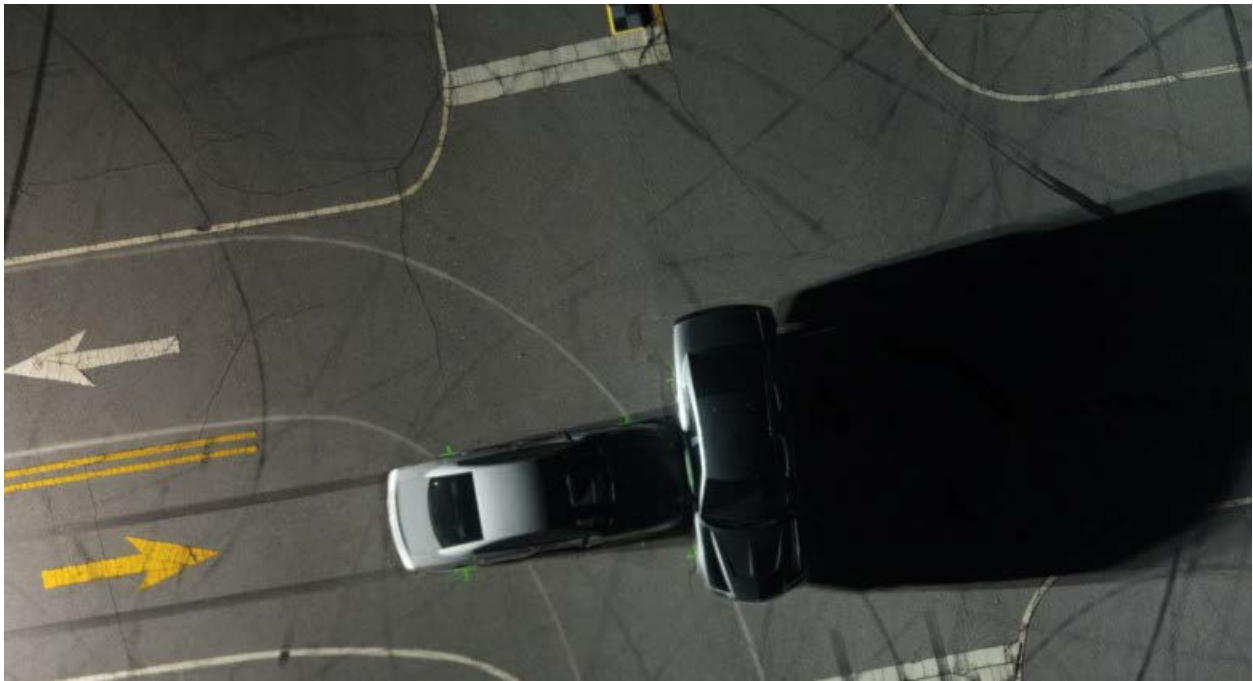
10.1 Benefits of 3-D Reconstruction over Orthomosaics

The 3-D reconstruction provides information similar to the reconstruction provided by the FARO 3-D laser scanner (FARO Technologies, n.d.). The 3-D reconstruction time for SfM is typically lower than that for the FARO reconstruction (which is about 2 hours). Even though the 3-D model reconstructed from SfM is not as accurate as a 3-D model from the FARO laser scanner, the combined data collection plus reconstruction time for SfM is usually much lower than that for the FARO. The 3-D model provides an additional dimension when compared to the orthomosaic. Details such as volumes of objects in the scene, and the relative positions of vehicles in the collision scene are more apparent in the 3-D reconstruction. Road curvature and banking are perceivable, making the scene more realistic. Moreover, the 3-D reconstruction of a scene is an intermediate step in computing the orthomosaic. It does not require any extra computation.

The 3-D reconstruction provides the user with the following advantages:

- Ability to view the scene in 3-D from any arbitrary viewpoint, as illustrated in **Figures 10-9** and **10-10**, and perform walkthroughs.

Figure 10-9. Sample 3-D Viewpoint. Note the "waterfall effect" where the rear part of the white car appears to be connected to the road.

Figure 10-10.   Sample 3-D Viewpoint Illustrating Overall Scene

- ▪ **Digital Surface Model**: The Digital Surface Model (DSM) illustrates the terrain features on the surface, such as curvature, tilt, and banking of road surfaces. Here in *Figure 10-11(b)*, we can see in the DSM heatmap, that the left of the image has a lower altitude than the right of the image.

Figure 10-11.   (a): Orthomosaic of the Scene. (b) The DSM.

| (a) | (b) |
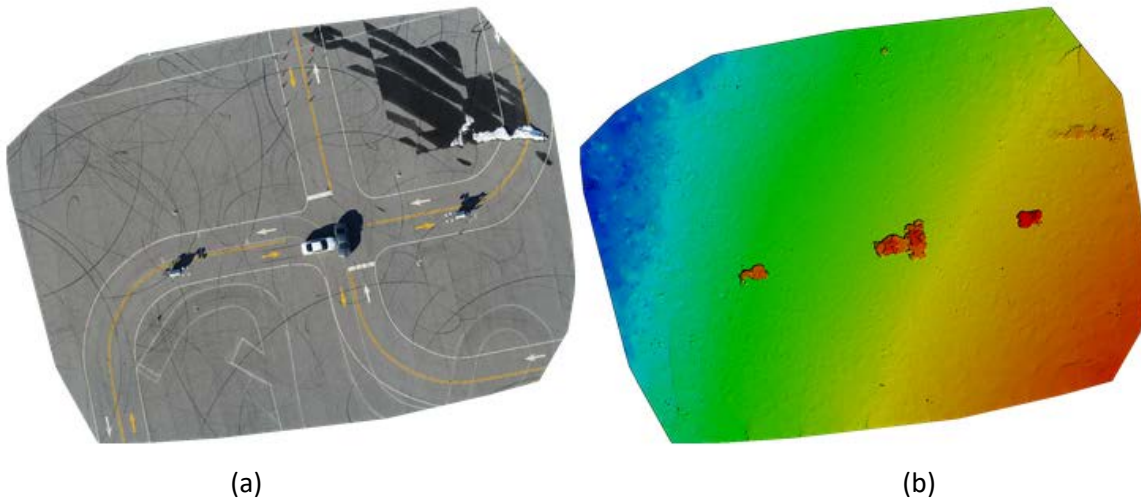
Our results suggest that although these 3-D reconstructions might not always be sufficiently accurate to replace the detailed 3-D models of the cars that can be obtained from a Faro sensor, they provide a clear idea of the overall scene in 3-D.

10.2   Thermal Imagery

Thermal image datasets were recorded using the DJI FLIR Zenmuse XT 640x512 9 mm thermal camera attached to the DJI Inspire 1. A total of four datasets were recorded: one grid trajectory, one orbit trajectory at 15:00 hours, and the same two at 19:30 hours. Out of these datasets, only one could be reconstructed successfully by Pix4D, and the rest of the datasets had error of "no calibrated cameras." The only successful reconstruction was the dataset recorded at 15:00 hours using an orbit trajectory.

Thermal cameras generally have much lower resolution than RGB cameras. The thermal camera used for our datasets had an image pixel resolution of 640×512. Due to this low resolution, the 3-D reconstruction generated will be grainy (because it has many fewer voxels in the point cloud). Generating an orthomosaic from the reconstruction gives a thermal outline of the scene. ***Figure 10-12*** illustrates an orthomosaic generated from the thermal images.

Figure 10-12.   Orthomosaic Generated from the Orbit Trajectory of Thermal Camera Using DJI Inspire 1 and no GCP.
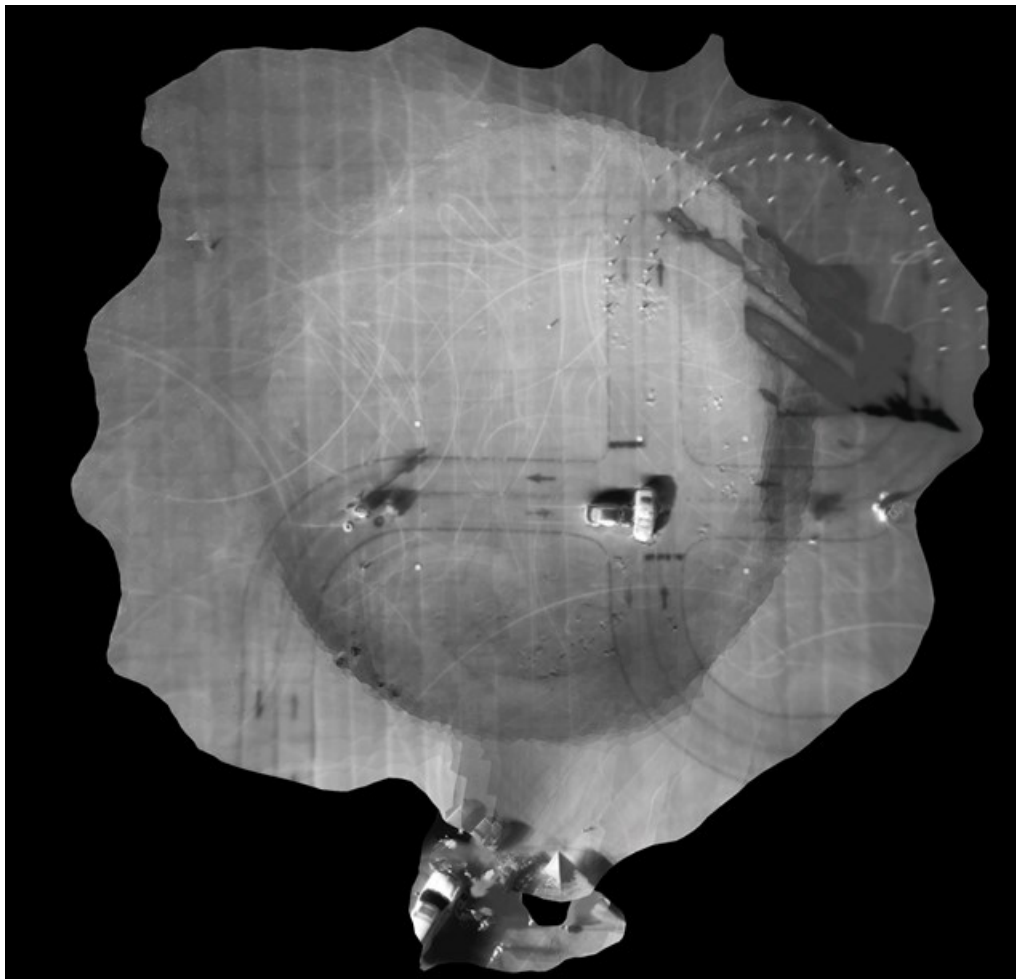
11. CONCLUSION

11.1 Observations

Our main observations are the following:

- Of the two UAS compared for LLCSR, the DJI Phantom 4 Pro was found to be more suitable than the DJI Mavic Pro, because its larger camera sensor is more sensitive for use in low-light situations, and the UAS is more stable in windy conditions. The DJI Mavic Pro can be used only for daytime scene reconstructions.

- The quality of reconstructions in twilight conditions, when there is sufficient ambient light to view the car features and GCPs, is better than for nighttime conditions with artificial lights.

- MLTs are more effective than ILTs for illuminating the scene, as they have a higher luminous intensity.

- Grid trajectories provide better orthomosaics, while orbit trajectories provide 3-D reconstructions with better lateral feature reconstructions. Using both double grid and orbit trajectories to record image datasets is recommended, because they can be combined to generate both types of reconstructions without compromising much on quality.

- Although automatic camera settings work well for daytime scenes, manually selecting camera settings is important for twilight and nighttime scenes. Extra initial flights should be carried out to calibrate the camera settings, based on the lighting conditions of the scene. Multiple flights are recommended for low-light scenarios, if possible, to provide redundancy in the event of image blur.

- Using GCPs reduces the standard deviation of lengths measured in the scene reconstruction to about 0.5 inch. However, the differences between reconstructions with and without GCPs are not visually apparent.

- Reconstruction with the Pix4D Model software is over 1.5x faster than reconstruction with the Agisoft Photoscan software.

- 3-D reconstructions enable viewing the scene from different angles, and also make terrain features more apparent. Reconstruction artefacts not visible in the orthomosaics also become apparent in the 3-D reconstructions.

- Orbit trajectories with 8-degree image sampling take half the time of orbit trajectories with 4-degree sampling and provide reconstructions that are visually comparable.

11.2 Recommendations

Based on the above observations, we make the following recommendations:

- Using a UAS that has a large image sensor to capture low-light scenes, and that is stable enough to reduce motion blur, even in windy situations, would provide the highest quality images.

- Use ambient natural lighting to the extent possible, as it is a more uniform light source than artificial lights. More uniform lighting reduces the number of scene artefacts due to shadows.

- Pix4D reconstructions are faster, and hence more practical for fast 3-D reconstruction.

- While recording datasets, use both double grid and orbit trajectories; grid trajectories provide better orthomosaics, and orbit trajectories provide better lateral views. Data from both trajectories can be combined for reconstructions that are a good compromise.

- Use the iOS Pix4D Capture application instead of the Android application, as it has the "Safe Mode" feature that permits the UAS to stop before taking an image. This reduces motion blur.

- Multiple flights are recommended for low-light scenarios. This redundancy will help to ensure at least one of the captured datasets is of sufficiently good quality to be usable for the reconstruction. Additionally, when all the datasets are of good quality, the multiple datasets can be provided as input to the SfM software to obtain more dense reconstructions.

- Additionally, extra initial flights should be carried out to manually calibrate the camera settings, based on the lighting conditions of the scene.

- MLTs are more effective than ILTs, as they have a higher luminous intensity, and illuminate the scene better.

- MLTs should be placed at least 40 feet away from skid marks and on-road spray paint marks to ensure even illumination across the scene.

11.3   Suggestions for Future Work

Suggestions for future work to improve reconstructions in low-light scenarios include the following:

- Capture images in RAW format to minimize image noise; this will enable the use of image processing techniques to enhance the images with minimal artefacts. This should be done along with keeping the UAS stationary to minimize motion blur. The Pix4D Capture and Agisoft apps currently do not permit RAW image gathering; other apps like Autopilot (Hangar Technology, 2018) provide this functionality.

- In low-light conditions, take multiple images from the same viewpoint. Through post-processing of the multiple images captured from this viewpoint, a composite image that is brighter than the individual images can be created. Using these composite images would likely result in a better 3-D reconstruction.

- Investigate techniques to reduce the size of false artefacts generated in 3-D reconstructions. Whereas artefacts on the reconstructed cars can be addressed by instead using offsite FARO reconstructions of the cars, scene artefacts caused by dark shadows or other scene lighting conditions are harder to eliminate.

- Perform experiments taking images of the cars in the collision scene from ground level and investigate whether providing these additional images to the SfM software can help eliminate the "waterfall effect" in the 3-D reconstructions.

12. REFERENCES FOR LLCSR: IMPACT OF UAS TRAJECTORIES, SENSORS, AND LIGHTING

Agarwal, S., Furukawa, Y., Snavely, N., Simon, I., Curless, B., Seitz, S. M., & Szeliski, R. (2011). Building Rome in a day. *Communications of the ACM, 54*(10), 105–112. doi:10.1145/2001269.2001293

Agisoft. (2018). *Downloads: User manuals (Agisoft PhotoScan).* Retrieved from http://www.agisoft.com/downloads/user-manuals

Allmand Brothers Inc. (n.d.). *Night-Lite Pro II LD-Series.* Retrieved from https://www.allmand.com/na/en_us/product-catalog/light-towers/nightlite-pro-ii-ldseries.html

FARO Technologies. (n.d.). *Products.* Retrieved from https://www.faro.com/products

Frahm, J. M., Fite-Georgel, P., Gallup, D., Johnson, T., Raguram, R., Wu, C., Jen, Y.H., Dunn, E., Clipp, B., Lazebnik, S., & Pollefeys, M. (2010). Building Rome on a cloudless day. In K. Daniilidis, P. Maragos, & N. Paragios (Eds.), *Computer Vision–ECCV 2010. Lecture notes in computer science* (pp. 368–381). Berlin, Heidelberg, Germany: Springer. doi:10.1007/978-3-642-15561-1_27
Hangar Technology. (2018). *Autopilot.* Retrieved from http://autoflight.hangar.com

North Carolina Department of Transportation, Division of Aviation, UAS Program Office. (2017). *Collision scene reconstruction and investigation using unmanned aircraft systems.* Retrieved from https://www.ncdot.gov/aviation/download/ncshp-uas-mapping-study.pdf

Pix4D. (n.d.). *Manual.* Retrieved from https://support.pix4d.com/hc/en-us/sections/200591059-Manual

Poelman, C. J., & Kanade, T. (1997). A paraperspective factorization method for shape and motion recovery. *IEEE Transactions on Pattern Analysis and Machine Intelligence, 19*(3), 206–218.

Prism Lighting Services, LLC. (n.d.). *PIL NITELITE.* Retrieved from https://prismlighting.net/2016/03/03/pil-nitelite

Tomasi, C., & Kanade, T. (1992). Shape and motion from image streams under orthography: A factorization method. *International Journal of Computer Vision, 9*(2), 137–154. doi:10.1007/BF00129684

Turner, D., Lucieer, A., & Watson, C. (2012). An automated technique for generating georectified mosaics from ultra-high resolution unmanned aerial vehicle (UAV) imagery, based on Structure from Motion (SfM) point clouds. *Remote Sensing, 4*(5), 1392–1410. doi:10.3398/rs4051392

Westoby, M. J., Brasington, J., Glasser, N. F., Hambrey, M. J., & Reynolds, J. M. (2012). "Structure-from-Motion" photogrammetry: A low-cost, effective tool for geoscience applications. *Geomorphology, 179,* 300–314. doi:10.1016/j.geomorph.2012.08.021

APPENDIX A: COMPUTER CONFIGURATIONS

The Pix4D reconstructions have been performed on a single computer with the following configuration:

Table A-1. Computer Configuration for Pix4D Reconstruction

CPU	AMD Ryzen 1700X 8-core 3.4 GHz
RAM	16GB
GPU	Nvidia GTX 960 (Chipset - GM206) 4 GB GDDR5
Operating System	Windows 10 Education, 64-bit

The Agisoft reconstructions have been performed on two computers with the following configurations:

Table A-2. Desktop Computer Configuration for Agisoft Reconstruction

CPU	2 x Intel Xeon E5645 6-core 2.4GHz
RAM	16GB
GPU	Nvidia Quadro 5000 (Chipset - GF100GL) 2.5 GB GDDR5
Operating System	Windows 7 Enterprise (Version: 6.1.7601 Service Pack 1 Build 7601)

Table A-3. Laptop Computer Configuration for Agisoft Reconstruction

CPU	Intel Core i7 6567U 2-core 3.3 GHz
RAM	16GB
GPU	Intel IRIS Graphics 550
Operating System	macOS Sierra

APPENDIX B: DISTANCE MEASUREMENTS IN THE RECONSTRUCTIONS

To calculate the tire skid mark lengths in the reconstruction, we draw a line segment (a Pix4D polyline) from the T-mark at the rear car wheel to the green spray-painted box. The length of this polyline is the length of the tire mark. This is illustrated in *Figures B-1* through *B-4*. There can be measurement variations due to human subjective decisions, when manually marking the line start and end points.

Figure B-1. **Start Point of the Measurement for the Rear Right Wheel Skid Mark**

Figure B-2. **Start Point of the Measurement for the Rear Left Wheel Skid Mark**

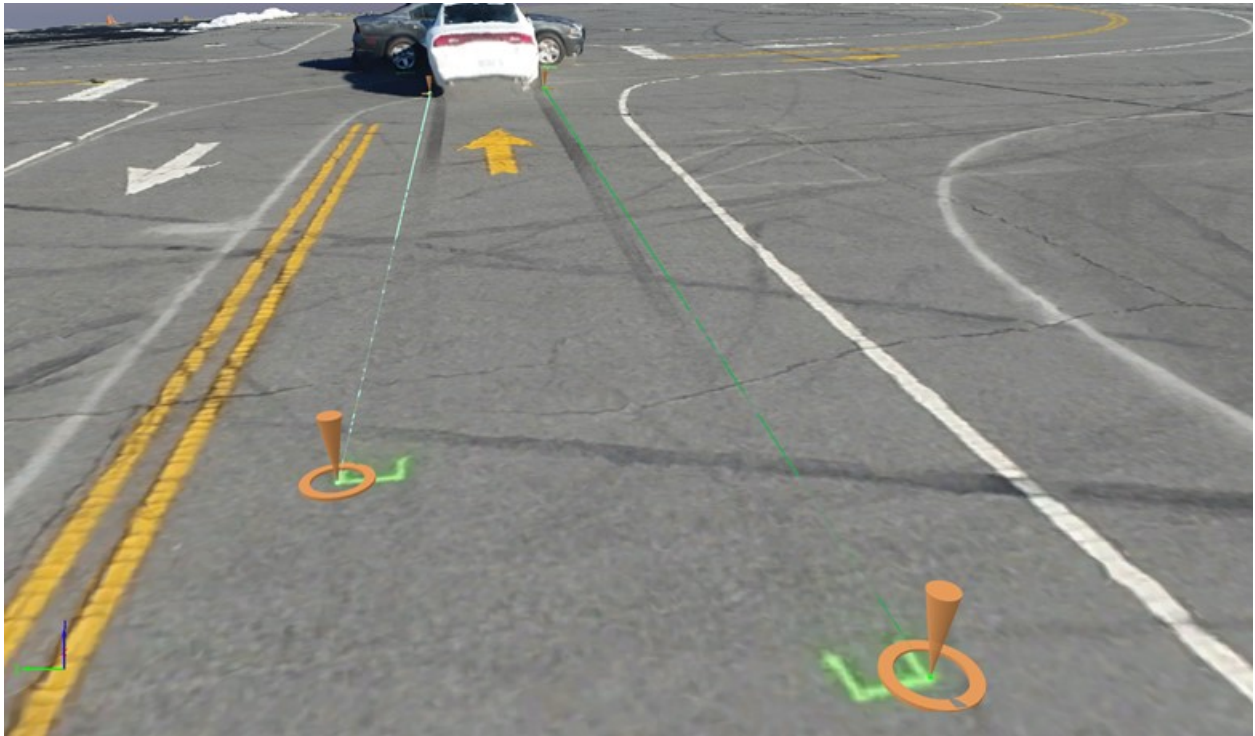**Figure B-3.** **End Point of Measurement**

Figure B-4. **Overhead View Illustrating Skid Mark Length Measurement**

The measurements of the yellow and white arrows are illustrated in *Figures B-5* and *B-6*.

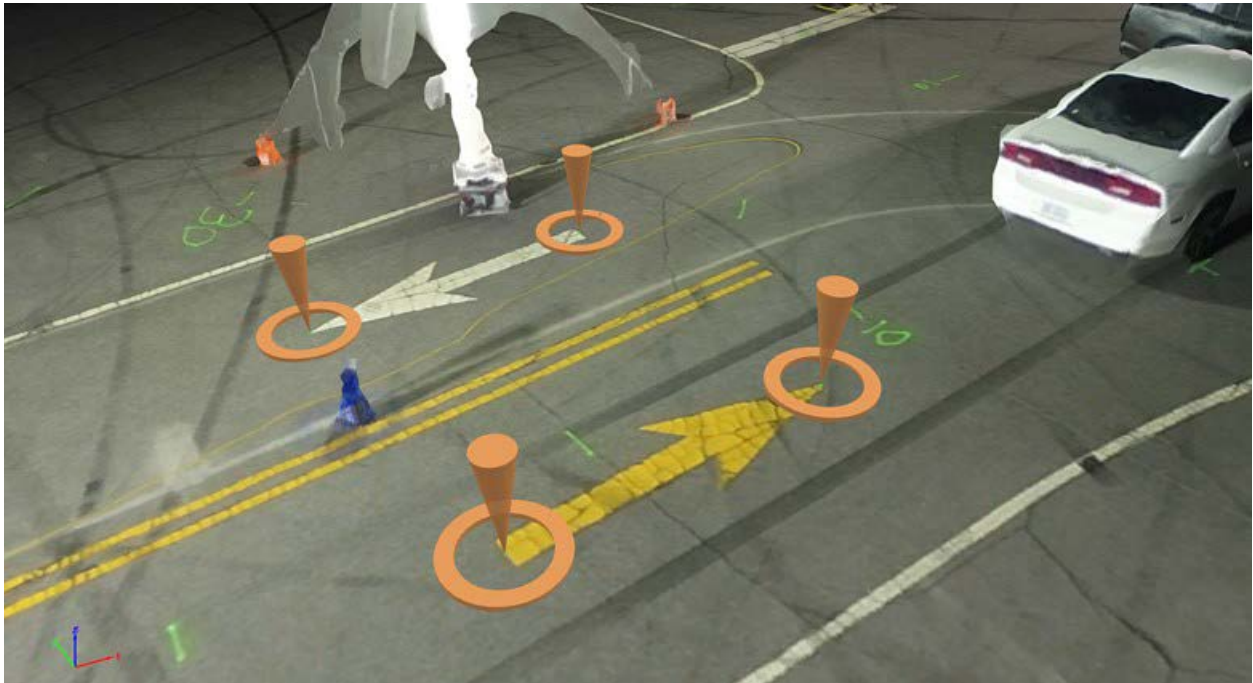**Figure B-5.**   **Yellow and White Arrow Length Measurement, Oblique View**

Figure B-6.   **Yellow and White Arrow Length Measurement, Overhead View**
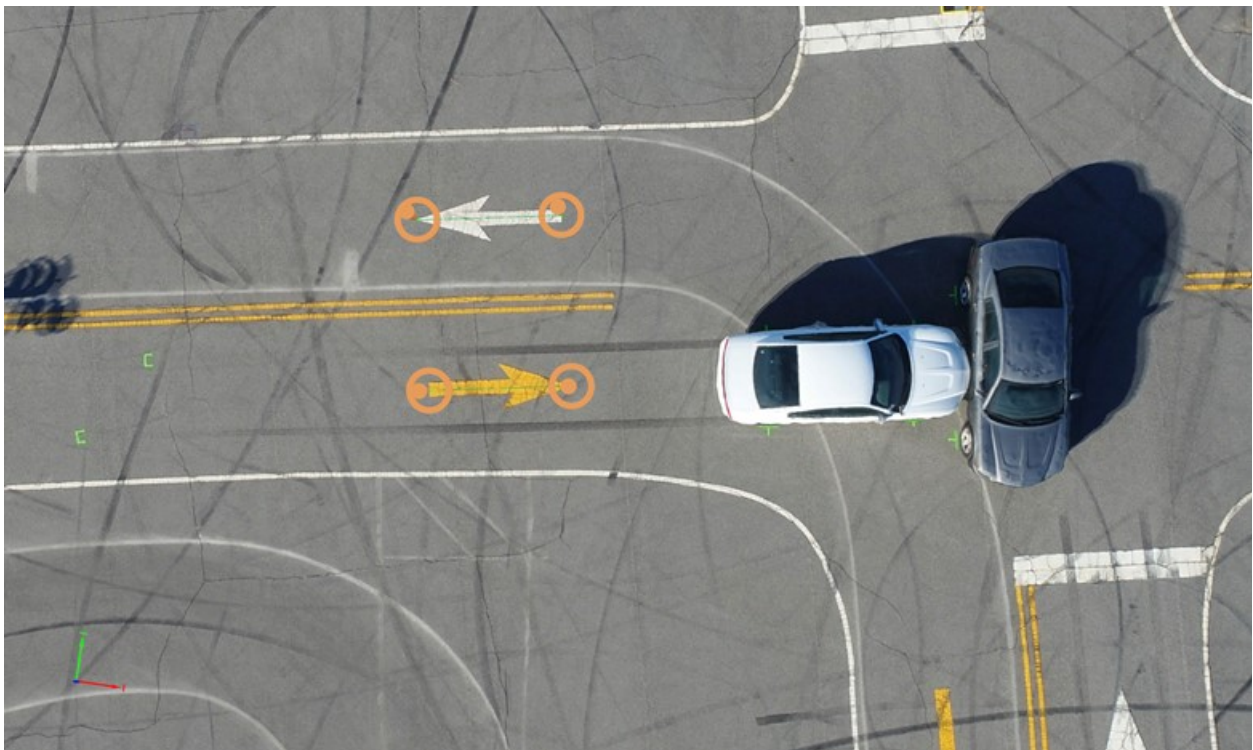
Tables B-1 through B-5 illustrates the lengths of the skid marks, and the yellow and white arrows as measured from the reconstructions. We could not measure some of the lengths, which are denoted as No Measurement. This occurred primarily because of overexposure of the scene, due to the MLTs being too close to the ground markings.

Table B-1. **Measurement of Skid Marks in Datasets Recorded on Day 1 Using DJI Phantom 4 Pro with GCPs**

			Lengths (in feet)			
			Skid Mark #1	Skid Mark #2	Yellow Arrow	White Arrow
Time	Trajectory	Lights	3-D Length (2-D Proj.)	3-D Length (2-D Proj.)	3-D Length (2-D Proj.)	3-D Length (2-D Proj.)
15:00bc	Grid	Ambient	48.04 (48.00)	43.32 (43.29)	9.96 (9.95)	10.04 (10.03)
15:00d	Orbit	Ambient	47.98 (47.94)	43.43 (43.40)	9.99 (9.98)	10.14 (10.13)
17:30b	Grid	Twilight 1 MLT	48.05 (48.01)	43.36 (43.32)	9.94 (9.93)	10.07 (10.06)
17:30c	Grid	Twilight 2 MLTs	No Measurement	43.40 (43.37)	9.93 (9.93)	10.03 (10.02)
17:30e	Grid	2 MLTs	No Measurement	43.55 (43.52)	9.96 (9.95)	10.06 (10.05)
17:30f	Grid	2 MLTs	No Measurement	43.36 (43.33)	9.96 (9.95)	10.04 (10.03)
17:30g	Orbit	2 MLTs	No Measurement	No Measurement	9.95 (9.94)	10.09 (10.09)
19:30b	Grid	1 MLT	No Measurement	No Measurement	9.92 (9.92)	10.04 (10.03)
19:30c	Grid	2 MLTs	48.04 (47.99)	43.37 (43.34)	9.97 (9.96)	10.02 (10.01)
19:30d	Orbit	2 MLTs	No Measurement	43.40 (43.36)	9.99 (9.98)	10.04 (10.04)

Table B-2. **Measurement of Skid Marks in Datasets Recorded on Day 2 Using DJI Phantom 4 Pro with GCPs**

Time	Trajectory	Lights	Lengths (in feet)			
			Skid Mark #1	Skid Mark #2	Yellow Arrow	White Arrow
			3-D Length (2-D Proj.)	3-D Length (2-D Proj.)	3-D Length (2-D Proj.)	3-D Length (2-D Proj.)
17:00a	Grid	Twilight 2 MLTs + ILT	48.04 (48.00)	43.34 (43.30)	9.92 (9.91)	10.09 (10.09)
17:00b	Grid	Twilight ILT	48.15 (47.89)	43.37 (43.34)	10.02 (10.01)	10.10 (10.09)
17:00c	Orbit	Twilight 2 MLTs + ILT	48.11 (48.07)	43.31 (43.28)	9.99 (9.98)	10.08 (10.07)
17:00d	Orbit	Twilight ILT	48.13 (48.09)	43.37 (43.34)	9.95 (9.94)	10.09 (10.08)
19:30a	Grid	2 MLTs + ILT	48.12 (48.08)	43.37 (43.34)	9.95 (9.94)	10.08 (10.08)
19:30b	Grid	ILT	No Measurement	43.40 (43.37)	9.97 (9.97)	10.09 (10.09)
19:30c	Orbit	2 MLTs + ILT	48.07 (48.03)	43.46 (43.43)	9.93 (9.93)	10.01 (10.01)
19:30d	Orbit	ILT	48.04 (48.01)	43.36 (43.33)	9.96 (9.95)	10.10 (10.09)

Table B-3. **Measurement of Skid Marks in Datasets Recorded on Day 1 Using DJI Mavic Pro with GCPs**

Time	Trajectory	Lights	Lengths (in feet)			
			Skid Mark #1	Skid Mark #2	Yellow Arrow	White Arrow
			3-D Length (2-D Proj.)	3-D Length (2-D Proj.)	3-D Length (2-D Proj.)	3-D Length (2-D Proj.)
15:00bc	Grid	Ambient	48.09 (48.04)	43.36 (43.31)	9.96 (9.95)	10.04 (10.03)
15:00d	Orbit	Ambient	48.08 (48.03)	43.44 (43.40)	9.97 (9.96)	10.05 (10.05)
17:30b	Grid	1 MLT	No Measurement	No Measurement	9.94 (9.94)	10.09 (10.09)
17:30c	Grid	2 MLTs	No Measurement	43.39 (43.36)	9.98 (9.97)	10.04 (10.04)
17:30d	Orbit	2 MLTs	No Measurement	No Measurement	9.88 (9.87)	10.06 (10.06)
19:30b	Grid	1 MLT	No Measurement	No Measurement	9.92 (9.91)	10.14 (10.13)
19:30c	Grid	2 MLTs	No Measurement	No Measurement	9.93 (9.92)	10.05 (10.05)
19:30d	Orbit	2 MLTs	No Measurement	No Measurement	9.90 (9.89)	10.08 (10.07)

Table B-4. **Measurement of Skid Marks in Datasets Recorded on Day 2 Using DJI Mavic Pro with GCPs**

Time	Trajectory	Lights	Lengths (in feet)			
			Skid Mark #1	Skid Mark #2	Yellow Arrow	White Arrow
			3-D Length (2-D Proj.)	3-D Length (2-D Proj.)	3-D Length (2-D Proj.)	3-D Length (2-D Proj.)
17:00a	Grid	Twilight 2 MLTs + ILT	48.01 (47.96)	43.40 (43.37)	9.89 (9.88)	10.03 (10.03)
17:00c	Orbit	Twilight 2 MLTs + ILT	48.09 (48.05)	43.42 (43.39)	9.89 (9.89)	10.07 (10.06)
19:30a	Grid	2 MLTs + ILT	48.09 (48.04)	43.48 (43.35)	9.96 (9.95)	10.06 (10.05)
19:30c	Orbit	2 MLTs + ILT	48.09 (48.05)	43.40 (43.37)	9.90 (9.89)	10.08 (10.08)

Table B-5. **Measurement of Skid Marks in Grid + Orbit Trajectory Datasets Recorded Using DJI Phantom 4 Pro with GCPs**

Time	Day	Lights	Lengths (in feet)			
			Skid Mark #1	Skid Mark #2	Yellow Arrow	White Arrow
			3-D Length (2-D Proj.)	3-D Length (2-D Proj.)	3-D Length (2-D Proj.)	3-D Length (2-D Proj.)
15:00bc	1	Ambient	48.02 (47.98)	43.35 (43.31)	9.87 (9.87)	10.01 (10.01)
17:30fg	1	2 MLTs	No Measurement	43.57 (43.54)	9.96 (9.95)	10.02 (10.01)
19:30cd	1	2 MLTs	No Measurement	43.35 (43.31)	10.00 (9.99)	10.04 (10.03)
17:00ac	2	Twilight 2 MLTs + ILT	48.09 (48.05)	43.31 (43.28)	9.99 (9.97)	10.02 (10.01)
17:00bd	2	Twilight ILT	48.05 (48.01)	43.40 (43.37)	9.94 (9.94)	10.01 (10.09)
19:30ac	2	2 MLTs + ILT	48.09 (48.05)	43.35 (43.32)	9.97 (9.96)	10.06 (10.05)
19:30bd	2	ILT	48.07 (48.03)	43.4 (43.37)	9.95 (9.94)	10.08 (10.08)

APPENDIX C: RECONSTRUCTION TIME DATA

Tables C-1, C-2, and ***C-3*** tabulate the reconstruction times, including the time required to generate the orthomosaic, for the datasets recorded by the DJI Phantom 4 Pro. The total time required is a sum of time required for five individual steps:

1. Initial Processing: Matching and calibrating images
2. Point Cloud Densification: Creating dense point cloud from sparse point cloud
3. 3-D Texture: Creating texture file for 3-D reconstruction
4. DSM Generation: Creating the Digital Surface Model
5. Ortho Generation: Creating the orthomosaic

Steps 1 through 3 are required for computing the 3-D reconstruction of the scene, while the next two steps are also required to compute the orthomosaic of the scene. The reconstructions were created in Pix4D, using the template of 3-D Map. This template is more suitable for generating the orthomosaic of the scene. ***Tables C-1*** and ***C-2*** tabulate grid or orbit trajectories recorded on Day 1 and Day 2 respectively. ***Table C-3*** tabulates the grid+orbit trajectories recorded on Day 1 and Day 2.

Table C-1. **Reconstruction Time Using 3-D Map Template in Pix4D. Datasets were recorded on Day 1 using DJI Phantom 4 Pro with GCPs.**

Time	Trajectory	Light	Initial Process.	Point Cloud Dense	3-D Texture	DSM Gen.	Ortho Gen.	Total
15:00d	Grid	Ambient	0:01:27	0:03:27	0:02:37	0:03:08	0:05:48	0:16:27
15:00d	Orbit	Ambient	0:07:03	0:15:35	0:05:38	0:03:09	0:18:21	0:49:46
17:30b	Grid	1 MLT	0:01:01	0:03:18	0:02:29	0:02:46	0:05:28	0:15:02
17:30c	Grid	Twilight 2 MLTs	0:00:56	0:04:47	0:02:31	0:01:48	0:05:19	0:15:21
17:30e	Grid	2 MLTs	0:01:06	0:07:37	0:03:01	0:02:04	0:06:06	0:19:54
17:30f	Grid	2 MLTs	0:00:50	0:04:58	0:02:31	0:01:50	0:05:19	0:15:28
17:30g	Orbit	2 MLTs	0:03:45	0:36:09	0:04:57	0:03:56	0:11:31	1:00:18
19:30b	Grid	1 MLT	0:00:49	0:05:25	0:02:26	0:01:57	0:04:40	0:15:17
19:30c	Grid	2 MLTs	0:00:43	0:04:28	0:02:25	0:01:44	0:05:05	0:14:25
19:30d	Orbit	2 MLTs	0:04:14	0:35:48	0:05:10	0:03:54	0:11:07	1:00:13

Table C-2. **Reconstruction Time Using 3-D Map Template in Pix4D. Datasets were recorded on Day 2 using DJI Phantom 4 Pro with GCPs.**

Time	Trajectory	Light	Initial Process.	Point Cloud Dense	3-D Texture	DSM Gen.	Ortho Gen.	Total
17:00a	Grid	Twilight 2 MLTs + ILT	0:01:27	0:03:04	0:02:24	0:02:51	0:06:02	0:15:48
17:00b	Grid	Twilight ILT	0:00:56	0:05:57	0:02:52	0:01:47	0:05:43	0:17:15
17:00c	Orbit	Twilight 2 MLTs + ILT	0:08:13	0:14:47	0:05:21	0:02:56	0:18:51	0:50:08
17:00d	Orbit	Twilight ILT	0:03:38	0:46:15	0:05:44	0:03:23	0:12:24	1:11:24
19:30a	Grid	2 MLTs + ILT	0:00:48	0:04:34	0:02:28	0:01:55	0:05:08	0:14:53
19:30b	Grid	ILT	0:00:43	0:06:19	0:02:28	0:01:52	0:04:54	0:16:16
19:30c	Orbit	2 MLTs + ILT	0:03:38	0:33:26	0:04:56	0:03:48	0:11:26	0:57:14
19:30d	Orbit	ILT	0:03:02	0:50:25	0:04:24	0:02:04	0:09:55	1:09:50

Table C-3. **Reconstruction Time Using 3-D Map Template in Pix4D. Datasets are of grid + orbit trajectory recorded using DJI Phantom 4 Pro with GCPs.**

Time	Trajectory	Light	Initial Process.	Point Cloud Dense	3-D Texture	DSM Gen.	Ortho Gen.	Total
15:00bcd (Day 1)	Grid + Orbit	Ambient	0:11:25	0:24:39	0:06:59	0:11:25	0:30:21	1:24:49
17:30fg (Day 1)	Grid + Orbit	2MLTs	0:06:24	0:59:08	0:06:40	0:05:03	0:15:59	1:33:14
19:00cd (Day 1)	Grid + Orbit	2 MLTs	0:06:15	0:59:02	0:06:01	0:05:07	0:15:24	1:31:49
17:00ac (Day 2)	Grid + Orbit	Twilight 2 MLTs + ILT	0:12:39	0:22:16	0:06:37	0:05:14	0:27:48	1:14:34
17:00bd (Day 2)	Grid + Orbit	Twilight ILT	0:07:19	1:06:49	0:06:53	0:04:06	0:24:44	1:49:51
19:30ac (Day 2)	Grid + Orbit	2 MLTs + ILT	0:06:57	0:49:30	0:05:30	0:04:46	0:15:14	1:21:57
19:30bd (Day 2)	Grid + Orbit	2 MLTs + ILT	0:05:44	1:21:22	0:06:32	0:05:01	0:15:44	1:54:23

Tables *C-4* and *C-5* tabulate the reconstruction time including the time required to generate the 3-D Model for the datasets recorded by the DJI Phantom 4 Pro. For these sets of reconstruction, as the objective was to generate the 3-D Model of the scene, the '3-D Model' template of Pix4D was used. *Table C-6* tabulates the reconstruction time for the grid + orbit trajectory datasets recorded by DJI Phantom 4 Pro using the sample reconstruction settings.

Table C-4. **Reconstruction Time Using 3-D Model Template in Pix4D. Datasets were recorded on Day 1 using DJI Phantom 4 Pro with GCPs.**

Time	Trajectory	Light	Initial Process.	Point Cloud Dense	3-D Texture	Total
15:00d	Grid	Ambient	0:02:25	0:03:59	0:02:19	0:08:43
15:00d	Orbit	Ambient	0:09:24	0:19:23	0:04:55	0:33:42
17:30b	Grid	1 MLT	0:01:52	0:03:41	0:02:08	0:07:41
17:30c	Grid	Twilight 2 MLTs	0:01:53	0:05:24	0:02:13	0:09:30
17:30e	Grid	2 MLTs	0:02:17	0:08:54	0:02:37	0:13:48
17:30f	Grid	2 MLTs	0:01:49	0:05:44	0:02:11	0:09:44
17:30g	Orbit	2 MLTs	0:05:36	0:51:24	0:04:08	1:01:08
19:30b	Grid	1 MLTs	0:01:43	0:06:21	0:02:13	0:10:17
19:30c	Grid	2 MLTs	0:01:44	0:05:14	0:02:05	0:09:03
19:30d	Orbit	2 MLTs	0:05:43	0:51:13	0:04:13	1:01:09

Table C-5. **Reconstruction Time Using 3-D Model Template in Pix4D. Datasets were recorded on Day 2 using DJI Phantom 4 Pro with GCPs.**

Time	Trajectory	Light	Initial Process.	Point Cloud Dense	3-D Texture	Total
17:00a	Grid	Twilight 2 MLTs + ILT	0:02:27	0:03:29	0:02:06	0:08:02
17:00b	Grid	Twilight ILT	0:01:58	0:07:02	0:02:32	0:11:32
17:00c	Orbit	Twilight 2 MLTs + ILT	0:10:20	0:17:05	0:04:33	0:31:58
17:00d	Orbit	Twilight ILT	0:05:40	1:04:55	0:04:22	1:14:57
19:30a	Grid	2 MLTs + ILT	0:01:47	0:05:29	0:02:12	0:09:28
19:30b	Grid	ILT	0:01:40	0:07:29	0:02:07	0:11:16
19:30c	Orbit	2 MLTs + ILT	0:05:53	0:45:48	0:04:01	0:55:42
19:30d	Orbit	ILT	0:04:56	1:12:52	0:04:04	1:21:52

Table C-6. Reconstruction Time Using 3-D Model Template in Pix4D. Datasets are of grid + orbit trajectory recorded using DJI Phantom 4 Pro with GCPs.

Time	Trajectory	Light	Initial Process.	Point Cloud Dense	3-D Texture	Total
15:00bcd (Day 1)	Grid + Orbit	Ambient	0:14:04	0:32:29	0:07:06	0:53:39
17:30fg (Day 1)	Grid + Orbit	2MLTs	0:09:38	1:23:07	0:05:37	1:38:22
19:00cd (Day 1)	Grid + Orbit	2 MLTs	0:09:23	1:23:12	0:05:17	1:37:52
17:00ac (Day 2)	Grid + Orbit	Twilight 2 MLTs + ILT	0:16:13	0:24:59	0:06:10	0:47:22
17:00bd (Day 2)	Grid + Orbit	Twilight ILT	0:09:58	1:33:22	0:05:33	1:48:53
19:30ac (Day 2)	Grid + Orbit	2 MLTs + ILT	0:09:57	1:11:09	0:05:07	1:26:13
19:30bd (Day 2)	Grid + Orbit	2 MLTs + ILT	0:08:51	2:04:17	0:05:07	2:18:15

Similarly, *Tables C-7* and *C-8* illustrate the reconstruction time for datasets recorded by the DJI Mavic Pro, on Day 1 and Day 2 respectively. These reconstructions have been done with Pix4D using the 3-D Model template.

Table C-7. Reconstruction Time Using 3-D Model Template in Pix4D. Datasets were recorded on Day 1 using DJI Mavic Pro with GCPs.

Time	Trajectory	Light	Initial Process.	Point Cloud Dense	3-D Texture	Total
15:00d	Grid	Ambient	0:02:34	0:03:10	0:01:50	0:07:34
15:00d	Orbit	Ambient	0:11:19	0:12:13	0:03:07	0:26:39
17:30b	Grid	1 MLT	0:02:27	0:04:28	0:01:49	0:08:44
17:30c	Grid	Twilight 2 MLTs	0:02:29	0:03:45	0:01:35	0:07:49
17:30d	Orbit	2 MLTs	0:05:49	0:18:22	0:02:55	0:27:06
19:30b	Grid	1 MLT	0:02:29	0:04:12	0:01:40	0:08:21
19:30c	Grid	2 MLTs	0:02:28	0:03:36	0:01:32	0:07:36
19:30d	Orbit	2 MLTs	0:05:32	0:18:37	0:02:55	0:27:04

Table C-8. **Reconstruction Time Using 3-D Model Template in Pix4D. Datasets were recorded on Day 2 using DJI Mavic Pro with GCPs.**

Time	Trajectory	Light	Initial Process.	Point Cloud Dense	3-D Texture	Total
17:00a	Grid	Twilight 2 MLTs + ILT	0:02:43	0:03:27	0:01:50	0:08:00
17:00c	Orbit	Twilight 2 MLTs + ILT	0:07:31	0:15:41	0:03:08	0:26:20
19:30a	Grid	2 MLTs + ILT	0:02:37	0:03:55	0:01:39	0:08:11
19:30c	Orbit	2 MLTs + ILT	0:05:43	0:16:55	0:02:53	0:25:31